Time-dependent density-functional description of nuclear dynamics

Takashi Nakatsukasa

Center for Computational Sciences, University of Tsukuba, Tsukuba 305-8577, Japan and RIKEN Nishina Center, 2-1 Hirosawa, Wako 351-0198, Japan

Kenichi Matsuyanagi

RIKEN Nishina Center, 2-1 Hirosawa, Wako 351-0198, Japan and Yukawa Institute for Theoretical Physics, Kyoto University, Kyoto 606-8502, Japan

Masayuki Matsuo

Department of Physics, Faculty of Science, Niigata University, Niigata 950-2181, Japan

Kazuhiro Yabana

Center for Computational Sciences, University of Tsukuba, Tsukuba 305-8577, Japan

(published 9 November 2016)

The basic concepts and recent developments in the time-dependent density-functional theory (TDDFT) for describing nuclear dynamics at low energy are presented. The symmetry breaking is inherent in nuclear energy density functionals, which provides a practical description of important correlations at the ground state. Properties of elementary modes of excitation are strongly influenced by the symmetry breaking and can be studied with TDDFT. In particular, a number of recent developments in the linear response calculation have demonstrated their usefulness in the description of collective modes of excitation in nuclei. Unrestricted real-time calculations have also become available in recent years, with new developments for quantitative description of nuclear collision phenomena. There are, however, limitations in the real-time approach; for instance, it cannot describe the many-body quantum tunneling. Thus, the quantum fluctuations associated with slow collective motions are explicitly treated assuming that time evolution of densities is determined by a few collective coordinates and momenta. The concept of collective submanifold is introduced in the phase space associated with the TDDFT and used to quantize the collective dynamics. Selected applications are presented to demonstrate the usefulness and quality of the new approaches. Finally, conceptual differences between nuclear and electronic TDDFT are discussed, with some recent applications to studies of electron dynamics in the linear response and under a strong laser field.

DOI: 10.1103/RevModPhys.88.045004

CONTENTS

I. INTRODUCTION

A. Scope of the present review

In the study of strongly correlated many-particle systems, a fundamental challenge is to find basic properties of a variety of elementary modes of excitation and to identify the degrees of freedom that are suitable for describing the collective phenomena. The collective motion in such complex systems, with an ample supply of experimental data and theoretical study, may often lead to deeper insight into the basic concepts of quantum many-body physics.

Among a variety of many-particle systems in the Universe, the nucleus provides a unique opportunity to investigate fundamental aspects of the quantum many-body problems. The nucleus is a self-bound system with finite number of fermionic particles, called nucleons, which have the isospin degrees of freedom ($t = 1/2$), in addition to the intrinsic spin ($s = 1/2$). The strong interplay between the collective and single-particle degrees of freedom plays important roles in nuclei, which produce a rich variety of unique phenomena. A prominent example of the consequence of this coupling is given by the manifestation of nuclear deformation and rotational spectra. It is also closely related to the damping and particle decay of the collective motion, the particle transfer in the heavy-ion collision, and the dissipation process in the nuclear fission. In fact, the coupling between the single-particle motion and collective motion is a key issue in nuclear structure. It is the basic idea behind the unified model of nuclei (Bohr and Mottelson, 1969, 1975), in which the collective motion is described by a shape change of the average one-body nuclear potential. It is easy to see that the basic concept of the unified model is similar to that of the mean-field theory. We therefore expect that the mean-field theory may provide a microscopic description of those phenomena, although it is limited to the one-body dynamics.

The self-consistent mean-field models for nuclei are currently a leading theory for describing properties of heavy nuclei (Bender, Heenen, and Reinhard, 2003; Lunney, Pearson, and Thibault, 2003). They self-consistently determine the nuclear one-body mean-field potential, starting from effective energy density functionals (EDFs). They are capable of describing almost all nuclei, including infinite nuclear matter, with a single universal EDF. The concept is very similar to the density-functional theory (DFT) in electronic systems, utilized in atomic, molecular, and solid state physics. A major conceptual difference is that, for the isolated finite nucleus, all the currently available nuclear DFT models are designed to reproduce the *intrinsic* ground state. The self-consistent solution produces a density distribution which spontaneously violates symmetries of the system, such as translational, rotational, and gauge symmetries. This feature

has advantages and disadvantages. The spontaneous breaking of symmetries (SSB) provides us with an intuitive explanation of a variety of nuclear phenomena. A typical example is the observed rotational spectra as a consequence of the intrinsic density deformation. On the other hand, when the symmetries are restored in finite nuclei, an additional correlation energy is generated. A question arises then, concerning whether all the correlation energy should be included in the EDF or not. We do not think this issue is completely settled yet. [Nevertheless, there are also attempts to justify the use of symmetry-violating (wave-packet) densities in a rigorous sense, which we present in Sec. II.] Perhaps, because of this unsettled problem, it is common to use terminologies of the mean-field theory, such as the time-dependent Hartree-Fock (TDHF) equations, instead of the time-dependent Kohn-Sham (TDKS) equations. In this article, we mainly use the DFT terminologies, since the naive mean-field theory is not applicable to nuclear systems, due to a strong two-body correlation (Sec. VI.A). Moreover, the mean-field calculation with a density-independent (state-independent) interaction cannot account for the nuclear saturation properties (Sec. I.B).

An extension of the DFT to the time-dependent DFT (TDDFT) provides a feasible description of many-body dynamics, which contains information on excited states in addition to the ground state. The TDDFT and its Kohn-Sham (KS) scheme are formally justified by the one-to-one correspondence between the time-dependent density and time-dependent external potential, assuming the v representability (Runge and Gross, 1984). The TDDFT has vast applications to quantum phenomena in many-body systems. In nuclear physics applications, there exist extensive studies in the simulation of the heavy-ion collision dynamics, especially of nuclear fusion and deep inelastic scattering (Negele, 1982). Ultimately, the nuclear TDDFT aims at describing nuclear excitations with different characters, such as vibration, rotation, and clustering, nuclear reactions of many kinds, such as fusion and fission, particle transfer, fragmentation, and even collective excitations in the crust and the interior of neutron stars.

One of the most extensively studied areas of the nuclear TDDFT is small-amplitude vibrations or linear response to external perturbations. This is a perturbative regime of the TDDFT, but it provides a powerful method to explore a variety of modes of excitation in nuclei. Many kinds of approaches to the linear response calculations have been developed and are presented in Sec. III. In addition to the conventional matrix formalism, we present some recent developments, such as the finite amplitude method and the Green's function method for the quasiparticle formalism with finite pair densities.

It is of significant interest and challenge to go beyond the perturbative regime. Nuclei show numerous phenomena related to the large-amplitude collective motion. In particular, nuclear reactions involving collective and noncollective dynamics of many nucleons are extensively studied using the real-time calculations in the past. In Sec. IV, we show some recent developments and applications. Recent review articles on the real-time approaches in normal (Simenel, 2012) and superfluid systems (Bulgac, 2013) may be supplementary to the present review. It is also of great interest to study the strong quantum nature of large-amplitude collective motion, such as spontaneous fission, shape transition, shape coexistence, anharmonic vibrations, and so on. For these phenomena, the real-time simulation of the TDDFT is not directly applicable to the problems. In most cases, we need requantization of the TDDFT dynamics. The requantizations of the TDHF and the imaginary-time TDHF for classically forbidden dynamics were previously discussed in another review paper in great detail (Negele, 1982). Unfortunately, the method has not been applied to realistic problems, due to a number of difficulties, such as finding suitable periodic orbits to quantize (Baranger, Strayer, and Wu, 2003). We present, in Sec. V, an alternative theory to identify an optimal collective submanifold in the TDDFT phase space. Consequently, with a small number of canonical variables, it is much more practical to quantize the collective dynamics.

Since the DFT and TDDFT are commonly adopted in many domains of quantum many-body systems, current problems and new ideas in other fields are of significant interest. Similar to nuclear physics, there are linear response TDDFT calculations and TDDFT for large-amplitude motion as an initial-value problem. However, it should be noted that there are conceptual and qualitative differences of EDFs between nuclear and electronic (TD)DFT. These issues are discussed in Sec. VI.

We tried to make the present review somewhat pedagogical and tractable for nonpractitioners and to explain essential elements of the theories. For more details, interested readers are referred to the literature.

B. Saturation and the mean-field picture

The saturation is a fundamental property of the nuclear system that is analogous to the liquid. The volume and total binding energy of observed nuclei in nature are approximately proportional to the mass number A. Extrapolating the observed property to the infinite nuclear matter with neglect of the Coulomb interaction, the nuclear matter should have an equilibrium state with $\rho_0 \approx 0.17$ fm^{-3} and $B/A \approx 16$ MeV at zero pressure and zero temperature. The empirical mass formula of Bethe and Weizsäcker (Weizsäcker, 1935; Bethe and Bacher, 1936), which is based on this liquid drop picture of nuclei, accounts well for the bulk part of the nuclear binding.

In contrast, there is much evidence pointing to the fact that the mean-free path of nucleons is larger than the size of the nucleus. The great success of the nuclear shell model (Mayer and Jensen, 1955), in which nucleons are assumed to move independently inside an average one-body potential, gives one of them. The scattering experiments with incident neutrons and protons provide more quantified information on the mean-free path. In fact, the mean-free path depends on the nucleon's energy and becomes larger for lower energy (Bohr and Mottelson, 1969). Therefore, it is natural to assume that the nucleus can be primarily approximated by the independent-particle model with an average one-body potential. For the symmetric nuclear matter, this approximation leads to the degenerate Fermi gas of the same number of protons and neutrons ($Z = N = A/2$). The observed saturation density of $\rho_0 \approx 0.17$ fm^{-3} gives the Fermi momentum $k_F \approx 1.36$ fm^{-1},

which corresponds to the Fermi energy (the maximum kinetic energy) $T_F = k_F^2/2m \approx 40$ MeV.

The justification of the independent-particle motion encourages us to investigate the mean-field models of nuclei. However, the naive mean-field models cannot properly describe the nuclear saturation property. Here the "naive" mean-field models mean those using any kind of state-independent two-body interactions. This has been known for many years (Bohr and Mottelson, 1969). Since it contains useful insight and relations to the nuclear DFT, let us explain the essential point. It is easy to consider the uniform nuclear matter with a constant attractive "mean-field" potential $V < 0$. The constancy of B/A means that it is equal to the separation energy of nucleons S. In the Fermi-gas model, it is estimated as

$$S \approx B/A \approx -(T_F + V). \tag{1}$$

Since the binding energy is $B/A \approx 16$ MeV, the potential V is about -56 MeV. Note that the relatively small separation energy is the consequence of the significant cancellation between the kinetic and the potential energies. This indicates that the nucleus has a strong quantum nature. In the mean-field theory, the total (binding) energy is given by

$$-B = \sum_{i=1}^{A} \left(T_i + \frac{V}{2} \right) = A \left(\frac{3}{5} T_F + \frac{V}{2} \right), \tag{2}$$

where we assume that the average potential results from a two-body interaction. The two kinds of expressions for B/A, Eqs. (1) and (2), lead to $T_F \approx -5V/4 \approx 70$ MeV, which is different from the previously estimated value ($\sim$40 MeV). Moreover, the negative separation energy ($T_F + V > 0$) contradicts the fact that the nucleus is bound. The presence of a three-body interaction may change this argument. However, solving the present contradiction requires an unrealistically strong three-body repulsive effect whose magnitude is comparable to that of the attractive two-body interaction.

To reconcile the independent-particle motion with the saturation property of the nucleus, the nuclear average potential must be state dependent. Allowing the potential V_i to depend on the state i, the potential V should be replaced by that for the highest occupied orbital V_F in Eq. (1), and by its average value $\langle V \rangle$ on the right-hand side of Eq. (2). Then we obtain the following relation:

$$V_F \approx \langle V \rangle + T_F/5 + B/A. \tag{3}$$

The potential V_F is shallower than its average value $\langle V \rangle$. Weisskopf (1957) suggested the momentum-dependent potential V, which can be expressed in terms of an effective mass m^*:

$$V_i = U_0 + U_1 \frac{k_i^2}{k_F^2}. \tag{4}$$

In fact, the nonlocal mean-field potential can be expressed by the momentum dependence (Ring and Schuck, 1980). Equation (4) leads to the effective mass $m^*/m = (1 + U_1/T_F)^{-1}$. Using Eqs. (1), (3), and (4), we obtain the effective mass given by

$$\frac{m^*}{m} = \left\{ \frac{3}{2} + \frac{5}{2} \frac{B}{A} \frac{1}{T_F} \right\}^{-1} \approx 0.4. \tag{5}$$

Quantitatively, this value disagrees with the experimental data. Although the empirical values of the effective mass vary according to the energy of nucleons $0.7 \lesssim m^*/m \lesssim 1$, they are almost twice larger than the value of Eq. (5). Furthermore, the total energy, Eq. (2), is written as

$$-B = \frac{1}{2} \sum_{i=1}^{A} (T_i + \epsilon_i), \tag{6}$$

where ϵ_i are single-particle energies. Within the constraint of Eq. (6), it is impossible to reproduce both the total binding energy and the single-particle spectra observed in experiments. As far as we use a normal two-body interaction, these discrepancies should be present in the mean-field calculation with any interaction, because Eqs. (5) and (6) are valid in general for a saturated self-bound system. Therefore, the naive mean-field models have a fundamental difficulty to describe the nuclear saturation.

The DFT provides a practical solution to this problem, in which we start from an EDF $E[\rho]$ instead of the interaction. The KS field is calculated as $h[\rho] = \partial E/\partial \rho$, which may contain the nontrivial density dependence different from that of the mean-field theory starting from the interaction. In nuclear physics, this additional density dependence was introduced by the density-dependent effective interaction; thus, it was called the "density-dependent Hartree-Fock" method (Negele, 1970). In this terminology, the variation of the total energy with respect to the density contains a rearrangement potential $\partial V_{\rm eff}[\rho]/\partial \rho$, which comes from the density dependence of the effective force $V_{\rm eff}[\rho]$. These terms are crucial to obtain the saturation and to provide a consistent independent-particle description of nuclei.

C. Symmetry breaking and restoration by the Anderson-Nambu-Goldstone (ANG) modes

One of the prominent features in the nuclear EDF approaches is the appearance of the SSB. For the system of a small number of particles, such as nuclei, the SSB is hidden. The experimental measurements probe the states which preserve the symmetries of the original Hamiltonian. In nuclear physics, the state with a broken symmetry is often called the "intrinsic" state. Nevertheless, we observe a number of nuclear phenomena associated with effects of the SSB, both in the ground-state properties and in excitation spectra. In nuclear physics, this was realized in the 1950s, soon after the experimental identification of the characteristic patterns of rotational spectra. Figure 1 is from a seminal review paper on the Coulomb excitation (Alder *et al.*, 1956). The nuclear potential energy function clearly indicates the nuclear deformation as the phase transition involving the SSB. The SSB in small finite-size systems has been an important concept in

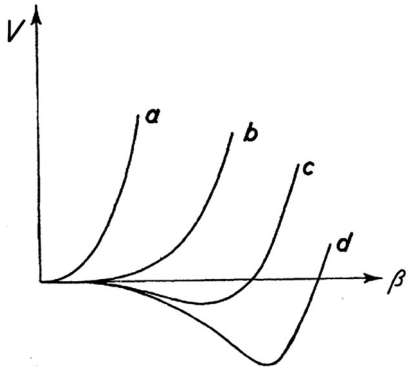

FIG. 1. Potential energy curves as functions of deformation parameter β. a corresponds to spherical nuclei, b and c correspond to transitional nuclei, and d to well-deformed nuclei. From Alder *et al.*, 1956.

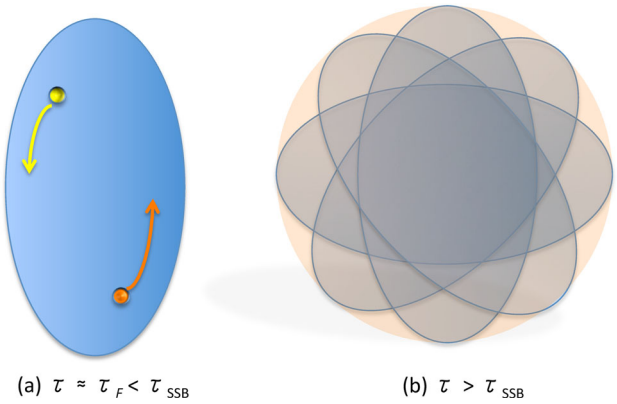

FIG. 2. Deformed nuclei in different time scales: (a) shorter than the symmetry-restoring time $\tau_{\rm SSB}$, and (b) larger than $\tau_{\rm SSB}$.

nuclear physics and chemistry for many years and has become so in fields of quantum dots and ultracold atoms (Yannouleas and Landman, 2007).

The symmetry restoration is a quantum fluctuation effect. When the spontaneous breaking of the continuous symmetry occurs, the ANG modes emerge to restore the broken symmetry (Anderson, 1958, 1963; Nambu, 1960; Goldstone, 1961). This symmetry restoration process is extremely slow for macroscopic objects, thus, the SSB is realized in a rigorous sense. In other words, the quantum fluctuation associated with the ANG mode is negligibly small in those cases. If the deformed nucleus with extremely heavy mass ($A \to \infty$) existed, the moment of inertia $\mathcal{J}$ should be macroscopically large. Then the excitation spectra of this heavy rotor would be nearly degenerate with the ground state, $E_I = I(I+1)/2\mathcal{J}$ for the state with the total angular momentum I, leading to a stable deformed wave packet. In reality, the restoration of the rotational symmetry even in heaviest nuclei takes place much faster than the shortest time resolution we can achieve with the present experimental technologies. In this sense, the SSB in nuclei is hidden. Nevertheless, the nucleonic motion is strongly influenced by the SSB, since the time scale of the symmetry restoration $\tau_{\rm SSB}$ is much longer than the periodic time of single-particle motion in the nucleus of radius R, $\tau_F = R/v_F \sim 10^{-22}$ s. This is schematically illustrated in Fig. 2. We believe that it is important to distinguish these two types of correlations in nuclei, those of relatively short time scales $\tau \sim \tau_F$ ("fast" motion), and of long time scales $\tau \sim \tau_{\rm SSB}$ ("slow" motion).

The nuclear superfluidity can be exactly understood in an analogous way as the SSB leading to the deformation in the gauge space (Brink and Broglia, 2005). The condensate of the nucleonic Cooper pairs is expressed as an intrinsic deformation in the magnitude of the pair field. The pair field creates and annihilates the pairs of nucleons giving rise to the quasiparticles that are superpositions of particles and holes, expressed by the Bogoliubov transformation. The ANG mode, called pair rotation, corresponds to the addition and removal of the nucleon pairs from the pair condensate. In this case, the "angular momentum" in the gauge space corresponds to the particle number, and the "moment of inertia" is defined by the second derivative of the ground-state energy with respect to the particle number $\mathcal{J}_{\rm pair} = (d^2E_N/dN^2)^{-1}$; see also Sec. III.B.

Since the broken symmetry is restored by the quantum fluctuation, its time scale $\tau_{\rm SSB}$ can be estimated by the uncertainty principle. The time is proportional to the moment of inertia $\mathcal{J}$ as $\tau_{\rm SSB} \sim \mathcal{J}/\hbar$, which amounts to 10^{-20}–10^{-19} s for typical deformed nuclei in the rare-earth and actinide regions. Thus, the symmetry restoration is a slow motion, compared to the nucleonic Fermi motion. Here it is important to distinguish this time scale of the "quantum" fluctuation from that of the "classical" rotation $\omega_{\rm rot}^{-1} \approx \mathcal{J}/I$. The latter could be comparable to τ_F at a very high spin (large I); however, the concept of the deformation (symmetry breaking) still holds. For the pair rotation, using an observed value of the moment of inertia in Sn isotopes (Brink and Broglia, 2005), $\tau_{\rm SSB}$ for the symmetry breaking in the gauge space can be given by $\tau_{\rm SSB} = 10^{-21}$–$10^{-20}$ s.

These concepts of SSB are invoked in the nuclear DFT and TDDFT. The symmetry restoration can be treated either by the projection method or by the (time-dependent) large-amplitude collective motion of the ANG modes (Ring and Schuck, 1980). In the present review, we mainly discuss the latter treatment with the time-dependent description.

II. BASIC FORMALISM: DFT AND TDDFT

The DFT describes a many-particle system exactly in terms of its local one-body density $\rho(\vec{r})$ alone. The DFT is based on the original theorem of Hohenberg and Kohn (1964) (HK) which was proven for the ground state of the many-particle system. Every observable can be written, in principle, as a functional of density.

In nuclear physics, as discussed in Sec. I.C, many kinds of SSB take place without an external potential. In fact, the minimization of the nuclear EDF for finite nuclei always produces a localized density profile, which spontaneously violates the translational symmetry. Furthermore, it often violates the rotational symmetry in the real space and gauge space. The SSB enables us to introduce an intrinsic (wave-packet) state. A possible justification of the DFT for the intrinsic state is presented in Sec. II.B.

For finite many-fermion systems, the shell effects associated with the quantum nature of the Fermi motion play a major

role in determining the ground state. The KS scheme (Kohn and Sham, 1965) gives a practical treatment of the shell effects in the density functional. This is presented in Sec. II.C

The DFT is designed for calculating the ground-state properties. For excited-state properties and reactions, the TDDFT is a powerful and useful tool. The basic theorem for the TDDFT was developed as an exact theorem (Runge and Gross, 1984), similar to the HK theorem in the static case. This is reviewed in Sec. II.D.

Both the DFT and TDDFT have been extended to the superconductors, introducing an external pair-removal and pair-addition potential (Oliveira, Gross, and Kohn, 1988; Wacker, Kümmel, and Gross, 1994). These extensions are relevant to nuclear physics as well, to account for various properties of heavy open-shell nuclei. In this article, we call them "superconducting nuclei" or "nuclear superfluidity." Properties of the (time-dependent) Bogoliubov–de Gennes equations will be presented in Secs. II.A and II.D.

A. Nuclear EDF models

Before presenting the theorem of DFT, we recapitulate basic equations of nuclear EDF models and their properties (Ring and Schuck, 1980; Blaizot and Ripka, 1986; Bender, Heenen, and Reinhard, 2003).

1. Basic equations

To simplify the discussion, we assume that the EDF $F[\rho]$, which represents the total energy of the nucleus, is a functional of local density $\rho(\vec{r})$ without the spin-orbit coupling. The KS equations read with the spin index $\sigma = (\uparrow, \downarrow)$,

$$\left(-\frac{1}{2m}\nabla^2 + v_s(\vec{r})\right)\varphi_i(\vec{r}\sigma) = \epsilon_i\varphi_i(\vec{r}\sigma). \tag{7}$$

Hereafter, we use the unit $\hbar = 1$. We decompose $F[\rho]$ into two parts, $F[\rho] = T_s[\rho] + E_c[\rho]$, where

$$T_s[\rho] = \sum_{i=1}^{N}\langle\varphi_i|\left(-\frac{1}{2m}\nabla^2\right)|\varphi_i\rangle$$

and the rest $E_c[\rho]$. The KS potential is defined by $v_s(\vec{r}) = \delta E_c/\delta\rho(\vec{r})$. The density is given by summing up the KS orbitals,

$$\rho(\vec{r}) = \sum_{\sigma}\sum_{i=1}^{N}|\varphi_i(\vec{r}\sigma)|^2. \tag{8}$$

When we take into account the nuclear superfluidity, we adopt an EDF which is a functional of ρ and (κ, κ^*), including the pair tensor $\kappa(\vec{r}, \vec{r}')$ whose definition (20) requires a symmetry-broken wave-packet state in Sec. II.B. If the EDF depends only on their diagonal parts [pair density $\kappa(\vec{r})$] $F[\rho, \kappa] = T_s[\rho, \kappa] + E_c[\rho, \kappa]$, Eq. (7) should be extended to the Bogoliubov–de Gennes–KS (BdGKS) equations:

$$\sum_{\sigma'}\begin{pmatrix}(h_s(\vec{r}) - \mu)\delta_{\sigma\sigma'} & \Delta_s(\vec{r})\gamma_{\sigma\sigma'} \\ -\Delta_s^*(\vec{r})\gamma_{\sigma\sigma'} & -(h_s(\vec{r}) - \mu)^*\delta_{\sigma\sigma'}\end{pmatrix}\begin{pmatrix}U_i(\vec{r}\sigma') \\ V_i(\vec{r}\sigma')\end{pmatrix} = E_i\begin{pmatrix}U_i(\vec{r}\sigma) \\ V_i(\vec{r}\sigma)\end{pmatrix}, \tag{9}$$

where $h_s(\vec{r}) \equiv -\nabla^2/(2m) + v_s(\vec{r})$, $\gamma_{\uparrow\downarrow} = -\gamma_{\downarrow\uparrow} = 1$, and $\gamma_{\uparrow\uparrow} = \gamma_{\downarrow\downarrow} = 0$. The chemical potential μ is introduced to control the total particle number. The potentials $v_s(\vec{r})$ and $\Delta_s(\vec{r})$ are, respectively, defined by

$$v_s(\vec{r}) = \frac{\delta E_c}{\delta\rho(\vec{r})}, \qquad \Delta_s(\vec{r}) = \frac{\delta E_c}{\delta\kappa^*(\vec{r})}. \tag{10}$$

The normal and pair densities are given by $\rho(\vec{r}) = \sum_\sigma\sum_i|V_i(\vec{r}\sigma)|^2$ and $\kappa(\vec{r}) = \sum_i V_i^*(\vec{r}\uparrow)U_i(\vec{r}\downarrow)$, where the summation with respect to i is taken over all the states with positive quasiparticle energies $E_i > 0$. The same convention is assumed in this article.

In nuclear physics, Eqs. (7) and (9) are often called Hartree-Fock (HF) and Hartree-Fock-Bogoliubov (HFB) equations, respectively.[1] Accordingly, the quasiparticle vacuum $|\phi_0\rangle$ is introduced and called the HFB ground state, where the Bogoliubov transformation,

$$\hat{\psi}(\vec{r}\sigma) = \sum_i\{U_i(\vec{r}\sigma)a_i + V_i^*(\vec{r}\sigma)a_i^\dagger\}, \tag{11}$$

defines the quasiparticle annihilation and creation operators $(a_i, a_i^\dagger)$ with the vacuum condition

$$a_i|\phi_0\rangle = 0. \tag{12}$$

These mean-field terminologies are due to the practical usage of the effective density-dependent interaction. The EDF is provided by the expectation value of the effective Hamiltonian at $|\phi_0\rangle$, $F[\rho, \kappa] = \langle\phi_0|\hat{H} - \mu\hat{N}|\phi_0\rangle$. The variation $\delta(F[\rho, \kappa] - \mu\int\rho(\vec{r})d\vec{r}) = 0$ leads to Eqs. (7) and (9).

2. Properties of BdGKS equations and useful notations

Solutions of the BdGKS (HFB) equation (9) are *paired* in the following sense: For each quasiparticle eigenstate Ψ_i^0 with a positive eigenvalue E_i, there exists a partner eigenstate $\tilde{\Psi}_i^0$ with the negative energy $-E_i$,

$$\Psi_i^0 = \begin{pmatrix}U_i \\ V_i\end{pmatrix}, \qquad \tilde{\Psi}_i^0 = \begin{pmatrix}V_i^* \\ U_i^*\end{pmatrix}.$$

Introducing the collective notation of the quasiparticles with positive (negative) energies at the ground state $\Psi^0 = (\Psi_1^0, \Psi_2^0, \ldots)$ $[\tilde{\Psi}^0 = (\tilde{\Psi}_1^0, \tilde{\Psi}_2^0, \ldots)]$, the orthonormal and completeness relations are equivalent to the unitarity condition $\mathcal{W}\mathcal{W}^\dagger = \mathcal{W}^\dagger\mathcal{W} = 1$ of the matrix

[1]The time-dependent equations are also called TDHF (TDHFB) in nuclear physics, instead of TDKS (TDBdGKS).

$$\mathcal{W} \equiv (\,\Psi^0 \quad \tilde{\Psi}^0\,) = \begin{pmatrix} U_1 & U_2 \cdots & V_1^* & V_2^* & \cdots \\ V_1 & V_2 \cdots & U_1^* & U_2^* & \cdots \end{pmatrix}.$$

The generalized density matrix R^0 is defined as

$$R^0 = \begin{pmatrix} \rho & \kappa \\ -\kappa^* & 1-\rho^* \end{pmatrix} = 1 - \Psi^0\Psi^{0\dagger} = \tilde{\Psi}^0\tilde{\Psi}^{0\dagger}, \quad (13)$$

which is Hermitian and idempotent $[(R^0)^2 = R^0]$. The orthonormal property immediately gives

$$R^0\Psi_i^0 = 0, \qquad R^0\tilde{\Psi}_i^0 = \tilde{\Psi}_i^0. \quad (14)$$

The BdGKS equations can be rewritten in terms of R as

$$[H_s[R^0], R^0] = 0, \quad (15)$$

where $H_s[R^0]$ is the BdGKS (or HFB) Hamiltonian on the left-hand side of Eq. (9).

Any unitary transformation among the quasiparticles $a_i' = \sum U_{ij}a_j$ keeps R^0 (ρ, κ) invariant. The quasiparticles defined by Eq. (9) give one choice of the gauge ("quasiparticle representation"). Another common choice is called "canonical representation," in which the density matrix ρ is diagonal. Note that Eqs. (13), (14), and (15) are all independent of the choice of the gauge.

In Sec. II.A.1, we used the coordinate-space representation $(\vec{r}, \sigma)$ and assumed that the density functional $E_c[\rho, \kappa]$ depends only on the diagonal densities $[\rho(\vec{r}), \kappa(\vec{r})]$ without spin dependence. It can be easily generalized to other representation $(\alpha, \beta, \ldots)$ and to functionals of density matrices in general: Hermitian $\rho_{\alpha\beta}$ and antisymmetric $\kappa_{\alpha\beta}$. The potentials are given by

$$v_s(\alpha\beta) = \left.\frac{\delta E_c}{\delta \rho_{\beta\alpha}}\right|_{R^0}, \qquad \Delta_s(\alpha\beta) = -\left.\frac{\delta E_c}{\delta \kappa^*_{\beta\alpha}}\right|_{R^0}.$$

Then the BdGKS Hamiltonian can be written as

$$H_s[R^0](\alpha'\beta') = \left.\frac{\delta F}{\delta R_{\beta'\alpha'}}\right|_{R^0}, \quad (16)$$

where $F[R] = T_s[R] + E_c[R]$. Here we introduce the *primed* indices, which are double the dimension. Let the dimension of the single-particle space be d, then the *unprimed* index runs over $\alpha = 1, \ldots, d$, while the primed one $\alpha' = 1, \ldots, 2d$.

It is not necessary, but often useful to introduce the generalized Slater determinant (quasiparticle vacuum) $|\phi_0\rangle$, defined by $a_i|\phi_0\rangle = 0$. Then we denote R^0 as

$$R^0_{\alpha'\beta'} = \langle\phi_0| \begin{pmatrix} \hat{\psi}^\dagger_\beta\hat{\psi}_\alpha & \hat{\psi}_\beta\hat{\psi}_\alpha \\ \hat{\psi}^\dagger_\beta\hat{\psi}^\dagger_\alpha & \hat{\psi}_\beta\hat{\psi}^\dagger_\alpha \end{pmatrix} |\phi_0\rangle.$$

A one-body operator $\hat{O}$ can be written in the form

$$\hat{O} = \sum_{\alpha\beta}\left[f_{\alpha\beta}\hat{\psi}^\dagger_\alpha\hat{\psi}_\beta + \frac{1}{2}\{g_{\alpha\beta}\hat{\psi}^\dagger_\alpha\hat{\psi}^\dagger_\beta + g'_{\alpha\beta}\hat{\psi}_\alpha\hat{\psi}_\beta\}\right]$$
$$= \text{const} + \frac{1}{2}(\,\hat{\psi}^\dagger \quad \hat{\psi}\,)\begin{pmatrix} f & g \\ g' & -f^T \end{pmatrix}\begin{pmatrix} \hat{\psi} \\ \hat{\psi}^\dagger \end{pmatrix}, \quad (17)$$

where g and g' are antisymmetric. If $\hat{O}$ is Hermitian, we have $f^T = f^*$ and $g^* = -g'$ $(g^\dagger = g')$.

The Bogoliubov transformation (11) is written with the unitary matrix $\mathcal{W}$ as

$$\begin{pmatrix} a \\ a^\dagger \end{pmatrix} = \mathcal{W}^\dagger\begin{pmatrix} \hat{\psi} \\ \hat{\psi}^\dagger \end{pmatrix}, \qquad \begin{pmatrix} \hat{\psi} \\ \hat{\psi}^\dagger \end{pmatrix} = \mathcal{W}\begin{pmatrix} a \\ a^\dagger \end{pmatrix}.$$

This transforms Eq. (17) into

$$\hat{O} = \sum_{ij}\left[O^{(++)}_{ij}a^\dagger_i a_j + \frac{1}{2}\{O^{(+-)}_{ij}a^\dagger_i a^\dagger_j + O^{(-+)}_{ij}a_i a_j\}\right]$$
$$= \frac{1}{2}(\,a^\dagger \quad a\,)\begin{pmatrix} O^{(++)} & O^{(+-)} \\ O^{(-+)} & O^{(--)} \end{pmatrix}\begin{pmatrix} a \\ a^\dagger \end{pmatrix}, \quad (18)$$

where $O^{(--)} = -O^{(++)T}$ and the constant shift is ignored. The matrices appearing in Eqs. (17) and (18) are essentially identical, but in different representation. We symbolically denote this as O. The superscript indices $+$ and $-$ indicate the positive- and negative-energy states; $O^{(++)}_{ij} \equiv \Psi^{0\dagger}_i O\Psi^0_j$, $O^{(+-)}_{ij} \equiv \Psi^{0\dagger}_i O\tilde{\Psi}^0_j$, $O^{(-+)}_{ij} \equiv \tilde{\Psi}^{0\dagger}_i O\Psi^0_j$, and $O^{(--)}_{ij} \equiv \tilde{\Psi}^{0\dagger}_i O\tilde{\Psi}^0_j$. The matrix elements $O^{(+-)}_{ij}$ and $O^{(-+)}_{ij}$ correspond to the two-quasiparticle creation and annihilation parts, respectively, which are occasionally denoted as O^{20}_{ij} and O^{02}_{ji} in the literature (Ring and Schuck, 1980; Avogadro and Nakatsukasa, 2011). The block elements of the density are also written as

$$R = \begin{pmatrix} R^{(++)} & R^{(+-)} \\ R^{(-+)} & R^{(--)} \end{pmatrix}.$$

For the ground-state density R^0, we have $R^{(++)} = R^{(+-)} = R^{(-+)} = 0$ and $R^{(--)} = 1$. The expectation value of $\hat{O}$ is given by $\langle\phi_0|\hat{O}|\phi_0\rangle = (1/2)\text{tr}[OR^0]$. These matrix notations are frequently used in Sec. III.

B. DFT theorem for a wave-packet state

The DFT is based on the HK theorem which guarantees a one-to-one mapping between a one-body density $\rho(\vec{r})$ for the ground state and an external potential $v_0(\vec{r})$. According to the recent progress (Barnea, 2007; Engel, 2007; Giraud, 2008; Messud, Bender, and Suraud, 2009), the theorem is extended to functionals of the localized intrinsic density of self-bound systems. Thus, it is a functional of density $\rho(\vec{r} - \vec{R})$, where $\vec{R}$ is the center of mass. In contrast to the center-of-mass motion, a strict definition of the intrinsic state is not trivial for the rotational motion of a deformed nucleus. In this section, we show a possible justification of the functional of the

wave-packet density produced by the SSB in finite systems. The arguments presented here were given by Giraud, Jennings, and Barrett (2008). The argument is exact for the SSB in the translational symmetry, while it is approximate for the SSB in the rotational symmetry.

1. Principles

A useful fact is that the SSB of the continuous symmetries produces ANG modes which are decoupled from the other degrees of freedom. It is exactly true in the case of translational symmetry. Consequently, there appear the collective variables associated with the ANG modes, which are symbolically denoted as (q, p). Here p are conserved and q are cyclic variables. The decoupling allows us to define the collective subspace $\Sigma_{\rm ANG}$ in the whole Hilbert space of many-particle systems. $\Sigma_{\rm ANG}$ is the space spanned by the collective wave functions $\{\chi(q)\}$. The subspace orthogonal to $\Sigma_{\rm ANG}$, which is denoted as $\Sigma_{\rm intr}$, describes the intrinsic motion.

In the ideal case of the SSB in the translational symmetry, the center-of-mass variables $(q, p) = (\vec{R}, \vec{P})$ and the intrinsic variables (ξ, π) are exactly decoupled. The state $|\Phi\rangle$ is rigorously given by a product wave function of $\phi(\xi)$ and $\chi(\vec{R})$,

$$|\Phi\rangle = |\phi\rangle \otimes |\chi\rangle, \qquad \hat{H} = \hat{H}_{\rm intr}(\xi, \pi) + \frac{\vec{P}^2}{2M},$$

where M is the total mass. In this case, the intrinsic subspace $\Sigma_{\rm intr}$ is defined by the space spanned by $\{\phi(\xi)\}$. The intrinsic ground state is obtained by the minimization of the intrinsic energy $\langle\phi|\hat{H}_{\rm intr}|\phi\rangle$ in the subspace $\Sigma_{\rm intr}$. The choice of the center-of-mass motion $\chi(\vec{R})$ is arbitrary for the determination of $\phi(\xi)$. Thus, we can adopt a localized form of $\chi(\vec{R})$, such as a Gaussian form $\chi(\vec{R}) \propto \exp[-(\vec{R} - \vec{R}_0)^2/2b^2]$. This leads to the wave-packet state $|\Phi\rangle$. Using the operator $\hat{P}$ which projects $\chi(q)$ onto the $\vec{P} = 0$ state, the ground-state energy can be obtained by the variation after the projection:

$$E_0 \equiv \min \left[\frac{\langle\Phi|\hat{H}\,\hat{P}\,|\Phi\rangle}{\langle\Phi|\hat{P}|\Phi\rangle} \right]_{\Sigma_{\rm intr}}, \tag{19}$$

where the variation is performed only in $\Sigma_{\rm intr}$ with a fixed $\chi(\vec{R})$.

In general, the wave-packet state is constructed in an analogous way. Choosing a localized form of $\chi(q)$, e.g., $\chi(q) \propto \exp[-(q - q_0)^2/2b^2]$, the variation after projection is performed in a restricted space $\Sigma_{\rm intr}$. The projection operator $\hat{P}$ makes the state an eigenstate of the collective momentum (symmetry operator) p; $p\hat{P}|\Phi\rangle = p_0\hat{P}|\Phi\rangle$. Then, Eq. (19) produces the ground-state energy with $p = p_0$. In nuclear physics interests, in addition to the total momentum, p may stand for either the total angular momentum J or the neutron (proton) number N (Z). The wave-packet density profile is simply given by

$$\rho(\vec{r}) \equiv \sum_{\sigma} \langle\Phi|\hat{\psi}^\dagger(\vec{r}\sigma)\hat{\psi}(\vec{r}\sigma)|\Phi\rangle$$

that depends on the choice of $\chi(q)$. In this article, we omit the isospin index $\tau = (n, p)$ for simplicity. Since we adopt a localized $\chi(q)$ which violates the symmetry, the density $\rho(\vec{r})$ is also localized, or "deformed."

In order to find the (wave-packet) density functional, we use the constrained search (Levy, 1979). The minimization in Eq. (19) is divided into two steps: the first one considers only states that produce a given wave-packet density $\rho(\vec{r})$ and the next takes the variation with respect to the density,

$$E_0 = \min_{\rho} \left\{ \min_{\Phi\to\rho} \left[\frac{\langle\Phi|\hat{H}\,\hat{P}\,|\Phi\rangle}{\langle\Phi|\hat{P}|\Phi\rangle} \right]_{\Sigma_{\rm intr}} \right\}.$$

This leads to the universal density functional

$$F[\rho] \equiv \min_{\Phi\to\rho} \left[\frac{\langle\Phi|\hat{H}\,\hat{P}\,|\Phi\rangle}{\langle\Phi|\hat{P}|\Phi\rangle} \right]_{\Sigma_{\rm intr}}.$$

Thus, the energy of the ground state with $p = p_0$ may be obtained by the minimization $E_0 = \min F[\rho]$.

The SSB of the gauge symmetry in nuclear superfluidity is caused by the pairing correlations among nucleons. Thus, in practice, it is convenient to introduce the pair tensors for the wave-packet state as

$$\kappa(\vec{r}\sigma;\vec{r}'\sigma') \equiv \langle\Phi|\hat{\psi}(\vec{r}'\sigma')\hat{\psi}(\vec{r}\sigma)|\Phi\rangle. \tag{20}$$

In other words, it is easier to construct the density functional $F[\rho, \kappa, \kappa^*]$ than $F[\rho]$, which takes into account essential aspects of the pairing correlations. Hereafter, we denote $F[\rho, \kappa]$, omitting κ^* for simplicity. Following the idea of the constrained search, it is easy to define the functional of ρ and κ,

$$F[\rho, \kappa] \equiv \min_{\Phi\to(\rho,\kappa)} \left[\frac{\langle\Phi|\hat{H}\,\hat{P}\,|\Phi\rangle}{\langle\Phi|\hat{P}|\Phi\rangle} \right]_{\Sigma_{\rm intr}}. \tag{21}$$

Instead of adopting the full pair tensors of Eq. (20), one can restrict them to their "diagonal" parts $\kappa(\vec{r}) \equiv \kappa(\vec{r}\uparrow, \vec{r}\downarrow) = -\kappa(\vec{r}\downarrow, \vec{r}\uparrow)$ in the functional. The inclusion of other forms of densities, in addition to ρ and κ, can also be achieved exactly in the same manner.

Let us make a few remarks here. First, in general, $\rho(\vec{r})$ and $\kappa(\vec{r})$ are not the exact densities in the laboratory frame (Schmid and Reinhard, 1991). Thus, $F[\rho, \kappa]$ is the functional of "localized" wave-packet densities $\rho(\vec{r})$ and $\kappa(\vec{r})$. Second, when $\Sigma_{\rm ANG}$ describes the center-of-mass motion, the decoupling is exact, and in principle, $E_0 = \min F[\rho]$ gives the exact ground-state energy. On the other hand, when the decoupling is approximate, such as the SSB in the rotational symmetry, $E_0 = \min F[\rho, \kappa]$ provides an approximate ground-state energy with the deformed densities. In the strict sense, an "infinite" system has an exact deformed ground state with an arbitrary fixed orientation $\chi(q) \sim \delta(q - q_0)$. This limit is not realized in finite nuclei. Nevertheless, we expect that the approximation becomes better for heavier nuclei. Third, in the approximate decoupling, the subspace $\Sigma_{\rm intr}$ should be chosen to be optimal for a certain eigenvalue of p_0. Therefore, $F[\rho, \kappa]$ may depend on p_0.

2. Practices

We have discussed the principles of the DFT for the wave-packet state. The universal density functional $F[\rho,\kappa]$ can be a functional of "local" densities $\rho(\vec{r})$ and $\kappa(\vec{r})$ in principle. However, even if the existence is guaranteed, it is another issue in practice whether we can construct the accurate density functional in terms of $\rho(\vec{r})$ and $\kappa(\vec{r})$ only.

For a proper account of the shell effects, the inclusion of the kinetic density is the only practical solution at present (Sec. II.C). Furthermore, for the shell structure in finite nuclei with correct magic numbers, it is indispensable to take into account the spin-orbit splitting (Mayer and Jensen, 1955). Currently, we need to adopt the spin-current densities for this purpose. In the end, the currently available EDFs for realistic applications contain several kinds of densities. The Skyrme and point-coupling covariant EDFs consist of local densities, while the Gogny and covariant (relativistic) EDFs contain nonlocal ones. Actual forms of the EDFs can be found in Bender, Heenen, and Reinhard (2003).

In Sec. II.B.1, we presented an argument in which the approximate decoupling for the rotational degrees of freedom justifies the use of the EDF of *deformed* densities. It is reliable for describing the correlations at $\tau \sim \tau_F$ in Fig. 2(a). These include the shell effects and the saturation properties. Conversely, the existing EDFs have difficulties in simultaneously reproducing binding energies of spherical and deformed nuclei. This may be due to a missing correlation associated with the quantum rotation of deformed intrinsic shapes shown in Fig. 2(b). In Sec. III.H, we show that the giant resonances (fast collective motion) are well reproduced in the linear response calculations, while the low-energy vibrations (slow collective motion) are not as good as those. In our opinion, correlations associated with large-amplitude shape fluctuations at low energy, which are in a time scale $\tau \gg \tau_F$, are missing in the available EDF. In practice, these correlations should be treated in addition to the conventional DFT and TDDFT calculations (Bender, Bertsch, and Heenen, 2006). We address this issue later in Sec. V.

The nonuniversality, p_0 dependence of $F[\rho,\kappa]$, is treated by enlarging the space $\Sigma_{\rm intr}$ to include all the p_0 states and adding an additional condition to the constrained search of Eq. (21), for the average value of p_0 (J and N) of the wave packet. This also limits the strictness of the nuclear DFT.

C. Kohn-Sham scheme

For many-fermion systems, the Fermi motion plays an important role in various quantum phenomena, such as the shell effects. This is a main source of difficulty in the local density approximation (LDA) (Ring and Schuck, 1980). At present, a scheme given by Kohn and Sham (1965) provides an only practical solution for this problem. Eventually, this leads to the self-consistent equations similar to those in the mean-field approximation.

1. Normal systems

Now we derive the KS equation (7) according to the argument by Kohn and Sham. Let us assume that the EDF is a functional of $\rho(\vec{r})$ only, $F[\rho]$. We introduce a *reference system* which is a "virtual" noninteracting system with an external potential $v_s(\vec{r})$. The ground state of the reference system is given as a Slater determinant constructed by the solution of Eq. (7). Alternatively, it is obtained by the minimization of the total energy of the reference system $E_s[\rho] = T_s[\rho] + \int v_s(\vec{r})\rho(\vec{r})d\vec{r}$. Since $E_s[\rho]$ is a functional of density, the minimization can be performed in terms of density variation with the particle-number constraint $\delta(E_s[\rho] - \mu\int\rho(\vec{r})d\vec{r}) = 0$. This leads to

$$\mu = \frac{\delta T_s[\rho]}{\delta\rho(\vec{r})} + v_s(\vec{r}). \tag{22}$$

The state determined by Eq. (22) should be identical to that of Eq. (7).

The success of the KS scheme comes from a simple idea to decompose the kinetic energy in the physical interacting system into two parts: $T_s[\rho]$ and the rest. The former is a major origin of the shell effects, and the latter is treated as a part of "correlation energy" $E_c[\rho]$. $E_c[\rho]$ corresponds to the "exchange-correlation energy" $E_{\rm xc}[\rho]$ in electronic DFT. The EDF is given by the sum $F[\rho] = T_s[\rho] + E_c[\rho]$. Then the variation $\delta(F[\rho] - \mu\int\rho(\vec{r})d\vec{r}) = 0$ leads to Eq. (22), where the potential $v_s(\vec{r})$ is defined by

$$v_s(\vec{r}) \equiv \frac{\delta E_c[\rho]}{\delta\rho(\vec{r})}.$$

Therefore, the solution of Eq. (7) provides the ground-state density of $F[\rho]$. The only practical difference between the reference system and the interacting system is that, since $v_s(\vec{r})$ is a functional of density in the latter, Eqs. (7) and (8) with v_s must be self-consistently solved. The success of the KS scheme is attributed to the goodness of the LDA for $E_c[\rho]$.

2. Superconducting systems

Next, with the density functional of Eq. (21), we introduce a noninteracting reference system under an external pair potential $\Delta_s(\vec{r})$ in addition to $v_s(\vec{r})$. The Hamiltonian with a constraint on the particle number

$$\hat{H}_s - \mu\hat{N} = \int [\Delta_s^*(\vec{r})\hat{\psi}(\vec{r}\downarrow)\hat{\psi}(\vec{r}\uparrow) + \text{H.c.}]d\vec{r} + \sum_{\sigma=\uparrow,\downarrow}\int\hat{\psi}^\dagger(\vec{r}\sigma)\left\{-\frac{\nabla^2}{2m} + v_s(\vec{r}) - \mu\right\}\hat{\psi}(\vec{r}\sigma)d\vec{r}$$

can be diagonalized by the Bogoliubov transformation (11), in which (U_i, V_i) are the solutions of Eq. (9). Alternatively, Eq. (9) can be derived by minimizing

$$F_s[\rho,\kappa] - \mu N_{\rm av} = T_s[\rho,\kappa] + \int\{v_s(\vec{r}) - \mu\}\rho(\vec{r})d\vec{r} + \int\{\Delta_s^*(\vec{r})\kappa(\vec{r}) + \Delta_s(\vec{r})\kappa^*(\vec{r})\}d\vec{r},$$

where

$$T_s[\rho,\kappa]=\sum_\sigma\sum_i\int V_i(\vec{r}\sigma)\frac{-\nabla^2}{2m}V_i^*(\vec{r}\sigma)d\vec{r}.$$

The same minimization can be done with respect to (ρ,κ,κ^*),

$$\mu=\frac{\delta T_s}{\delta\rho(\vec{r})}+v_s(\vec{r}),\qquad 0=\frac{\delta T_s}{\delta\kappa^*(\vec{r})}+\Delta_s(\vec{r}). \tag{23}$$

Equations (9) and (23) should provide the identical state.

According to the Kohn-Sham idea, we express the energy density functional of the interacting system in the form $F[\rho,\kappa]\equiv T_s[\rho,\kappa]+E_c[\rho,\kappa]$. Then the variation $\delta\big(F[\rho,\kappa]-\mu\int\rho(\vec{r})d\vec{r}\big)=0$ leads to Eq. (23), but the potentials $v_s(\vec{r})$ and $\Delta_s(\vec{r})$ are given by Eq. (10). Equation (9) with potentials (10) constitute the BdGKS scheme (Oliveira, Gross, and Kohn, 1988).

D. Time-dependent density-functional theory

1. Foundation: Runge-Gross theorem

The basic theorem of the TDDFT tells us that, starting from a common initial state $|\Phi_0\rangle$ at $t=t_0$, there is one-to-one correspondence between a pair of time-dependent densities $\big(\rho(\vec{r},t),\kappa(\vec{r},t)\big)$ and a pair of time-dependent external potentials $\big(v(\vec{r},t),\Delta(\vec{r},t)\big)$ (Runge and Gross, 1984; Wacker, Kümmel, and Gross, 1994). Here we recapitulate the proof. The external potential is required to be expandable in a Taylor series about the initial time t_0,

$$v(\vec{r},t)=\sum_{k=0}^{\infty}\frac{1}{k!}v_k(\vec{r})(t-t_0)^k, \tag{24}$$

$$\Delta(\vec{r},t)=\sum_{k=0}^{\infty}\frac{1}{k!}\Delta_k(\vec{r})(t-t_0)^k. \tag{25}$$

If two potentials (v,v') differ merely by a time-dependent function $c(t)=v(\vec{r},t)-v'(\vec{r},t)$, they should be regarded as *identical* potentials. For the different potentials, there should exist some non-negative integer n such that $\vec{\nabla}w_n(\vec{r})\neq 0$, where $w_n(\vec{r})\equiv v_n(\vec{r})-v_n'(\vec{r})$. Similarly, the pair potentials are different if $D_n(\vec{r},t)\neq 0$ at a certain n, where $D_n(\vec{r},t)\equiv\Delta_n(\vec{r},t)-\Delta_n'(\vec{r},t)$.

Let us first assume that two different external potentials $v(\vec{r},t)$ and $v'(\vec{r},t)$ produce current densities $\vec{j}(\vec{r},t)$ and $\vec{j}'(\vec{r},t)$, respectively. The pair potential is assumed to be equal, $\Delta(\vec{r},t)=\Delta'(\vec{r},t)$. In the following, we assume the Heisenberg picture, and the quantities associated with the potentials $v'(\vec{r},t)$ are denoted with primes, while those with $v(\vec{r},t)$ are without primes. The equation of motion for the current $\vec{j}(\vec{r},t)\equiv\langle\Phi_0|\hat{\vec{j}}(\vec{r},t)|\Phi_0\rangle$ is written as

$$i\frac{\partial}{\partial t}\vec{j}(\vec{r},t)=\langle\Phi_0|[\hat{\vec{j}}(\vec{r},t),\hat{H}(t)]|\Phi_0\rangle. \tag{26}$$

We have the same equation for $\vec{j}'(\vec{r},t)$, with $\hat{H}(t)$ replaced by $\hat{H}'(t)$. Since the field operators at $t=t_0$ are identical to each other, $\psi(\vec{r}\sigma,t_0)=\psi'(\vec{r}\sigma,t_0)$, they lead to

$$\begin{aligned}i\frac{\partial}{\partial t}\{\vec{j}(\vec{r},t)-\vec{j}'(\vec{r},t)\}\Big|_{t=t_0}&=\langle\Phi_0|[\hat{\vec{j}}(\vec{r},t_0),\hat{H}(t_0)-\hat{H}'(t_0)]|\Phi_0\rangle\\&=-\frac{i}{m}\rho(\vec{r},t_0)\vec{\nabla}w_0(\vec{r}).\end{aligned}$$

If $\vec{\nabla}w_0(\vec{r})\neq 0$, it is easy to see that $\vec{j}(\vec{r},t)$ and $\vec{j}'(\vec{r},t)$ are different at $t>t_0$. In case that $\vec{\nabla}w_0(\vec{r})=0$ and $\vec{\nabla}w_1(\vec{r})\neq 0$, we need to further calculate derivatives of Eq. (26) with respect to t,

$$\begin{aligned}\left(i\frac{\partial}{\partial t}\right)^2\vec{j}(\vec{r},t)\Big|_{t=t_0}&=\langle\Phi_0|[\hat{\vec{j}}(\vec{r},t),i\bar{\partial}\hat{H}/\bar{\partial}t]_{t=t_0}|\Phi_0\rangle\\&\quad+\langle\Phi_0|[[\hat{\vec{j}}(\vec{r},t_0),\hat{H}(t_0)],\hat{H}(t_0)]|\Phi_0\rangle,\end{aligned} \tag{27}$$

where $\bar{\partial}/\bar{\partial}t$ indicates the time derivative of the potentials only, not of the field operators. The second term of Eq. (27) vanishes for the difference $\partial^2/\partial t^2\{\vec{j}(\vec{r},t)-\vec{j}'(\vec{r},t)\}|_{t=t_0}$, because $\hat{H}'(t_0)=\hat{H}(t_0)+\text{const}$. Thus,

$$\frac{\partial^2}{\partial t^2}\{\vec{j}(\vec{r},t_0)-\vec{j}'(\vec{r},t)\}\big|_{t=t_0}=-\frac{1}{m}\rho(\vec{r},t_0)\vec{\nabla}w_1(\vec{r})\neq 0.$$

Again, we conclude that $\vec{j}(\vec{r},t)\neq\vec{j}'(\vec{r},t)$ at $t>t_0$. In general, if $\vec{\nabla}w_k(\vec{r})=0$ for $k<n$ and $\vec{\nabla}w_n(\vec{r})\neq 0$, we repeat the same argument to reach

$$\begin{aligned}&\frac{\partial^{n+1}}{\partial t^{n+1}}\{\vec{j}(\vec{r},t)-\vec{j}'(\vec{r},t)\}_{t=t_0}\\&\quad=-i\langle\Phi_0|[\hat{\vec{j}}(\vec{r},t_0),\bar{\partial}^n\{\hat{H}(t)-\hat{H}'(t)\}/\bar{\partial}t^n|_{t=t_0}]|\Phi_0\rangle\\&\quad=-\frac{1}{m}\rho(\vec{r},t_0)\vec{\nabla}w_n(\vec{r})\neq 0.\end{aligned}$$

Therefore, there exists a mapping from the expandable potential $v(\vec{r},t)$ and the current density $\vec{j}(\vec{r},t)$. The continuity equation relates the current density $\vec{j}(\vec{r},t)$ with the density $\rho(\vec{r},t)$. Therefore, we conclude that the densities $\rho(\vec{r},t)$ and $\rho'(\vec{r},t)$ are different at $t>t_0$.

Next let us assume the different pair potentials $\Delta(\vec{r},t)$ and $\Delta'(\vec{r},t)$. The same argument leads to

$$\frac{\partial^{n+1}}{\partial t^{n+1}}\{\kappa(\vec{r},t)-\kappa'(\vec{r},t)\}\Big|_{t=t_0}=f(\vec{r})D_n(\vec{r})\neq 0,$$

where $f(\vec{r})=i\{\rho(\vec{r},t_0)-\delta^3(0)\}$. The appearance of the delta function $\delta^3(0)$ is a consequence of the local nature of the pair potential $\Delta(\vec{r},t)$. Anyway, $f(\vec{r})$ is nonzero, and the pair densities $\kappa(\vec{r},t)$ and $\kappa'(\vec{r},t)$ become different immediately after $t=t_0$. This completes the proof of the one-to-one correspondence between the potentials $\big(v(\vec{r},t),\Delta(\vec{r},t)\big)$ and the densities $\big(\rho(\vec{r},t),\kappa(\vec{r},t)\big)$. As is obvious in the proof here, the one-to-one correspondence also holds when the density $\rho(\vec{r},t)$ is replaced by the current density $\vec{j}(\vec{r},t)$.

2. TDKS scheme: van Leeuwen theorem

In practice, the KS scheme is indispensable for quantum systems. According to the basic theorem in Sec. II.D.1 there is a one-to-one correspondence between given time-dependent densities and external potentials for any system. Let us introduce a *virtual* reference system of noninteracting particles by choosing the potentials $v_s(\vec{r},t)$ and $\Delta_s(\vec{r},t)$ in such a way that it exactly produces the densities $\rho(\vec{r},t)$ and $\kappa(\vec{r},t)$ of a *real* interacting system. This results in the time-dependent BdGKS (TDBdGKS) equations:

$$i\frac{\partial}{\partial t}\begin{pmatrix} U_i(\vec{r}\sigma;t) \\ V_i(\vec{r}\sigma;t)\end{pmatrix} = \sum_{\sigma'}\begin{pmatrix} h_s(\vec{r};t)\delta_{\sigma\sigma'} & \Delta_s(\vec{r};t)\gamma_{\sigma\sigma'} \\ -\Delta_s^*(\vec{r};t)\gamma_{\sigma\sigma'} & -h_s^*(\vec{r};t)\delta_{\sigma\sigma'}\end{pmatrix} \times \begin{pmatrix} U_i(\vec{r}\sigma';t) \\ V_i(\vec{r}\sigma';t)\end{pmatrix}. \tag{28}$$

Here $h_s(\vec{r},t) \equiv -\nabla^2/(2m) + v_s(\vec{r},t)$. With $\Delta_s = 0$, they reduce to the TDKS equations ($i = 1, \ldots, N$)

$$i\frac{\partial}{\partial t}\varphi_i(\vec{r},t) = h_s(\vec{r},t)\varphi_i(\vec{r},t). \tag{29}$$

The next obvious question is the following: Do such potentials in noninteracting systems exist to reproduce the densities in real systems? This question was answered affirmatively by van Leeuwen (1999) as follows. For simplicity, let us consider the TDKS equations without pairing. Hereafter, quantities associated with the reference system are denoted with a subscript s. First, calculating the right-hand side of Eq. (26) gives $i\partial\vec{j}(\vec{r},t)/\partial t = -\rho(\vec{r},t)\vec{\nabla}v(\vec{r},t) - \vec{f}(\vec{r},t)$. Here $\vec{f}(\vec{r},t)$ is given by the momentum-stress tensor and the interaction parts, but these details are not important in the proof. Taking the divergence of this equation and using the continuity equation, we find

$$\frac{\partial^2\rho}{\partial t^2} = \vec{\nabla}\cdot[\rho(\vec{r},t)\vec{\nabla}v(\vec{r},t)] + q(\vec{r},t), \tag{30}$$

where $q(\vec{r},t) = \vec{\nabla}\cdot\vec{f}(\vec{r},t)$. Assuming the density is identical in two systems all the time, the difference of Eq. (30) between the two leads to

$$\vec{\nabla}\cdot[\rho(\vec{r},t)\vec{\nabla}w(\vec{r},t)] = \zeta(\vec{r},t), \tag{31}$$

where $w = v - v_s$ and $\zeta = q_s - q$. This equation plays a key role in the proof. Now the question is whether we can uniquely determine $w(\vec{r},t)$ if $\rho(\vec{r},t)$ is given.

Necessary conditions for the initial state $|\Phi_s\rangle$ of the reference system are only two: (i) The two initial states $|\Phi_0\rangle$ and $|\Phi_s\rangle$ yield the same density $\rho(\vec{r},t_0) = \rho_s(\vec{r},t_0)$. (ii) Their time derivatives are identical, $\dot{\rho}(\vec{r},t_0) = \dot{\rho}_s(\vec{r},t_0)$. With $|\Phi_s\rangle$ satisfying these initial conditions, we determine the solution w of Eq. (31). We should first notice that Eq. (31) does not contain time derivatives, which means that t can be regarded as a parameter. Furthermore, Eq. (31) is of the Sturm-Liouville type; thus it has a unique solution with the boundary condition $w(\vec{r},t) = 0$ at infinity. It is now obvious that we can uniquely determine $w(\vec{r},t_0)$ at $t = t_0$ because $\zeta(\vec{r},t_0)$ is calculable with the initial states $|\Phi_0\rangle$ and $|\Phi_s\rangle$. This means in the Taylor-series expansion, Eq. (24), $w_0(\vec{r}) = v_0(\vec{r}) - v_{s0}(\vec{r})$ is solved. Taking the time derivative of Eq. (31) at $t = t_0$, we can determine $w_n(\vec{r})$ for higher-order terms in a recursive manner ($n = 1, 2, \ldots$). This procedure completely determines $v_s(\vec{r},t)$.

3. TDBdGKS equation and its properties

The key quantity in TDDFT is the time-dependent potentials $(v_s(\vec{r},t), \Delta_s(\vec{r},t))$. So far, we simply adopt the *adiabatic approximation*: We take the BdGKS potentials in Eq. (9) from static DFT and use it in the TDBdGKS equation (28), by replacing ground-state densities with the time-dependent ones:

$$v_s(t) = v_s[\rho_0]|_{\rho_0\to\rho(t)}, \qquad v_s[\rho] \equiv \delta E_c/\delta\rho \tag{32}$$

and the same prescription is applied to Δ_s. This obviously lacks the memory effect.

Properties of the static BdGKS equations shown in Sec. II.A.2 also hold for the time-dependent case, except for BdGKS equation (15) which should be replaced by

$$i\frac{\partial}{\partial t}R(t) = [H_s[R](t), R(t)]. \tag{33}$$

Here $H_s[R]$ is given by Eq. (16) with $R_0 \to R(t)$ in the adiabatic approximation. We use the same notations as those in Sec. II.A.2 with the introduction of the time dependence, such as $\Psi^0 \to \Psi(t)$, $R^0 \to R(t)$, etc.

With respect to a time-dependent unitary transformation $\Psi(t) \to \Psi(t)U(t)$, $R(t)$ and Eq. (33) are invariant, while Eq. (28) is not. Including this gauge freedom, the TDBdGKS equation (28) should be generalized to

$$i\frac{\partial}{\partial t}\Psi(t) = H_s[R](t)\Psi(t) - \Psi(t)\Xi(t), \tag{34}$$

with a Hermitian matrix $\Xi = i(dU/dt)U^\dagger = -iUdU^\dagger/dt$. The choice of $\Xi(t)$ is arbitrary and does not affect the physical contents of the calculation. The TDBdGKS equation (28) corresponds to a special gauge $\Xi(t) = 0$.

In case that the pair density and potential are absent, $\kappa(t) = \Delta(t) = 0$, Eq. (33) reduces to

$$i\frac{\partial}{\partial t}\rho(t) = [h_s[\rho](t), \rho(t)]. \tag{35}$$

This is equivalent to the TDKS equations,

$$i\frac{\partial}{\partial t}\varphi(t) = h_s[\rho](t)\varphi(t) - \varphi(t)\xi(t), \qquad \rho(t) = \varphi(t)\varphi^\dagger(t),$$

where $\varphi(t)$ is a collective notation of the nonvanishing vectors $V_i^*(t)$, $\varphi(t) = (V_1^*(t), V_2^*(t), \ldots, V_N^*(t))$ that are upper components of $\tilde{\Psi}(t)$. The quantity $\xi(t)$ is an arbitrary $N \times N$ Hermitian matrix. A choice of $\xi(t) = 0$ leads to Eq. (29).

4. Local gauge invariance

The practical success of the TDBdGKS equations relies on the availability of a good correlation functional $E_c[\rho,\kappa]$. Many applications so far employ the functional of the static potentials (10) with time-dependent densities (adiabatic approximation). Although the memory effect is missing, this simple choice guarantees exact properties of the functional, such as the harmonic potential theorem (HPT) (Dobson, 1994; Vignale, 1995). In nuclear physics applications, it is also customary to adopt a functional in the same form as the static one. Since a local density form (Skyrme type) of the nuclear correlation energy contains the kinetic and spin-current densities, to guarantee the Galilean symmetry it should include the time-odd densities, such as spin, current, and spin-tensor densities (Engel *et al.*, 1975). In fact, the nuclear EDFs usually respect an even stronger symmetry, the local gauge invariance, which is satisfied for systems with local interactions. The HPT and the Galilean invariance can be regarded as its special cases. The local gauge transformation modifies the one-body density matrix as $\rho(\vec{r},\vec{r}') \to \exp[i\{\chi(\vec{r})-\chi(\vec{r}')\}]\rho(\vec{r},\vec{r}')$. The local density $\rho(\vec{r}) = \rho(\vec{r},\vec{r})$ is apparently invariant; however, the kinetic and spin-current densities are not, because the transformation creates a flow with a velocity field $\vec{v}(\vec{r},t) = \vec{\nabla}\chi(\vec{r},t)/m$. These densities appear with characteristic combinations with the time-odd densities to satisfy the local gauge invariance (Dobaczewski and Dudek, 1995). Note that the local gauge invariance is guaranteed if the nonlocal effect is small, but it is not required by the principles. It has been utilized to restrict the functional form of nuclear EDFs (Carlsson, Dobaczewski, and Kortelainen, 2008).

The local $U(1)$ gauge transformation $\hat{\psi}(\vec{r}\sigma,t) \to e^{i\chi(\vec{r},t)}\hat{\psi}(\vec{r}\sigma,t)$ with a real function $\chi(\vec{r},t)$ changes the phase of U and V components with opposite signs [see Eq. (11)]. Thus, the transformation reads

$$\bar{\Psi}(t) = \begin{pmatrix} e^{i\chi} & 0 \\ 0 & e^{-i\chi} \end{pmatrix}\Psi(t) = \exp\{i\chi(t)\mathcal{N}\}\Psi(t), \tag{36}$$

with

$$\mathcal{N} \equiv \begin{pmatrix} 1 & 0 \\ 0 & -1 \end{pmatrix}.$$

Under this transformation, the generalized density and the Hamiltonian should be transformed as

$$\begin{pmatrix} \bar{R}(t) \\ \bar{H}_s(t) \end{pmatrix} = e^{i\chi(t)\mathcal{N}}\begin{pmatrix} R(t) \\ H_s(t) \end{pmatrix}e^{-i\chi(t)\mathcal{N}}. \tag{37}$$

The transformation (37) keeps the density $\rho(\vec{r},t)$ invariant, but multiplies $\kappa(\vec{r},t)$ by a local phase $e^{2i\chi(\vec{r},t)}$. The transformation of the kinetic term can be obtained by shifting the momentum $\vec{p}$ to $\vec{p} - m\vec{v}(\vec{r},t)$. The local gauge invariance of the density functionals guarantees that $H_s[R](\vec{r},\vec{p};t) \to \bar{H}_s[\bar{R}](\vec{r},\vec{p};t) = H_s[\bar{R}](\vec{r},\vec{p}-m\vec{v};t)$, in which the replacement of $\vec{p} \to \vec{p} - m\vec{v}$ is performed only for the kinetic energy term $|\vec{p}|^2/(2m) \to |\vec{p} - m\vec{v}(\vec{r},t)|^2/(2m)$. The transformed TDBdGKS equations for $\bar{R}$ and $\bar{\Psi}(t)$ are identical to Eqs. (33) and (34), but the Hamiltonian is replaced by $\bar{H}_s[\bar{R}](t) - \partial\chi/\partial t\cdot\mathcal{N}$. For instance, Eq. (33) now reads

$$i\frac{\partial}{\partial t}\bar{R}(t) = \left[\bar{H}_s[\bar{R}](t) - \frac{\partial\chi}{\partial t}\mathcal{N}, \bar{R}(t)\right]. \tag{38}$$

This is the TDBdGKS equation in a frame of a gauge function $\chi(\vec{r},t)$. Under the presence of the local gauge invariance in the EDF, the functional form of $\bar{H}_s$ is the same as H_s except that the momentum $\vec{p}$ is replaced by $\vec{p} - m\vec{v}$ in the kinetic term.

E. Equations for decoupled collective motion

In this section, we derive an equation for the decoupled collective motion. In order to elucidate the idea, let us start with the translational motion. In this case, the decoupling is exact. The boosted ground state with the center of mass at $\vec{R}_{\text{c.m.}}(t) = \vec{v}t$ has the density $\rho(t) = \rho(\vec{R}_{\text{c.m.}})$, which depends on time through $\vec{R}_{\text{c.m.}}(t) = \vec{v}t$. The total momentum $\vec{P}_{\text{c.m.}} = Nm\vec{v}$ is a constant of motion. The TDKS equation (35) can be written as

$$i\vec{v}\cdot\frac{\partial}{\partial\vec{R}_{\text{c.m.}}}\rho(\vec{R}_{\text{c.m.}}) = [h_s[\rho(\vec{R}_{\text{c.m.}})], \rho(\vec{R}_{\text{c.m.}})].$$

Using the expression $\rho(t) = e^{-i\vec{R}_{\text{c.m.}}(t)\cdot\vec{p}}\bar{\rho}e^{i\vec{R}_{\text{c.m.}}(t)\cdot\vec{p}}$, where $\bar{\rho}$ is time independent, it leads to

$$[h_s[\rho(t)] - \vec{v}\cdot\vec{p}, \rho(t)] = 0, \tag{39}$$

which looks like a stationary equation. In fact, since $\vec{R}_{\text{c.m.}} = \vec{v}t$ depends on time, $\rho(\vec{R}_{\text{c.m.}})$ is moving in time. We call Eq. (39) a "moving-frame" equation in the following. It should be noted that the EDFs with the Galilean symmetry are essential to reproduce the correct total mass Nm, which also influences properties of other collective motions.

1. Collective motion in general

Now let us generalize the idea and assume that there are a pair of canonical variables $(q(t), p(t))$ corresponding to a collective motion, which determine the time dependence of the generalized density $R(q(t), p(t))$. This means that the motion described by $(q(t), p(t))$ is decoupled from the other intrinsic degrees of freedom. In the TDBdGKS equation (33), the time derivative is now written in terms of the collective variables as $\dot{q}\partial/\partial q + \dot{p}\partial/\partial p$. This leads to the moving-frame equation

$$[H_s[R] - \dot{q}\mathring{P}(q,p) + \dot{p}\mathring{Q}(q,p), R(q,p)] = 0, \tag{40}$$

where $\mathring{P}(q,p)$ and $\mathring{Q}(q,p)$ are generators of the collective variables and are defined by

$$i\frac{\partial}{\partial q}R(q,p) = [\mathring{P}(q,p), R(q,p)], \tag{41}$$

$$-i\frac{\partial}{\partial p}R(q,p) = [\mathring{Q}(q,p), R(q,p)]. \tag{42}$$

Note that $\dot{q}$ and $\dot{p}$ are not constant, in general. In Sec. V, we develop this idea and derive equations of motion for a collective motion decoupled from other intrinsic degrees of freedom.

Equation (40) looks like a stationary equation with constraints $\overset{\circ}{Q}(q,p)$ and $\overset{\circ}{P}(q,p)$. However, it is important to note that the density $R(q,p)$ in Eq. (40) still varies in time because the variables (q,p) depend on time. Because of this time dependence, the "cranking terms" $-\dot{q}\overset{\circ}{P}+\dot{p}\overset{\circ}{Q}$ in Eq. (40) are not just the constraint terms in static equations, but they play a role beyond that.

To explain this point, we return again to the translational motion. Equation (39) looks identical to the static equation with a constraint operator $\vec{p}$. However, the cranking term induces the linear momentum $\mathrm{Tr}[\rho\vec{p}]=Nm\vec{v}$, and the density is never static. During the time evolution $t\to t+\delta t$, the center of mass moves as $\vec{R}_{\mathrm{c.m.}}\to\vec{R}_{\mathrm{c.m.}}+\vec{v}\delta t$. Accordingly, the density also evolves, $\rho\to\rho+\delta\rho$, $\vec{R}_{\mathrm{c.m.}}\to\vec{R}_{\mathrm{c.m.}}+\delta\vec{R}$. This density variation is described by Eq. (39),

$$[h_s-\vec{v}\cdot\vec{p},\delta\rho]+\left[\frac{\delta h_s}{\delta\rho}\delta\rho,\rho\right]=0, \tag{43}$$

in the first order in $\delta\rho$. This is nothing but the random-phase approximation (RPA) for the translational motion. If Eq. (39) is a constrained stationary equation, it does not lead to the RPA equation.

If we define the particle (unoccupied) and hole (occupied) orbitals for $h_s[\rho]-\vec{v}\cdot\vec{p}$, the particle-particle and hole-hole components $\vec{p}_{pp'}$ and $\vec{p}_{hh'}$ contribute to the determination of $\delta\rho$ in Eq. (43). In contrast, for the constrained mean-field equation (Ring and Schuck, 1980), the particle-particle and hole-hole matrix elements of the constrained operator are irrelevant. We think it is worth emphasizing that the cranking terms in Eqs. (39) and (40) are different from constraint terms in the static equation (Nakatsukasa, Walet, and Dang, 1999; Hinohara *et al.*, 2007; Nakatsukasa, 2012). The issue is addressed in Sec. V.

2. ANG modes and quasistationary solutions

The ANG modes provide examples of decoupled collective motion to which Eq. (40) is applicable. In these cases, one of the variables becomes cyclic (constant), and the generators do not depend on the variables (q,p). They are given by known one-body operators globally defined.

Translational motion: In this case, the generators $(\overset{\circ}{Q}(q,p),\overset{\circ}{P}(q,p))$ correspond to the center-of-mass coordinate and the total momentum, with $\dot{q}=\vec{v}$ and $\dot{p}=0$. Thus, we naturally derive Eq. (39) from Eq. (40). The Galilean invariance guarantees that the translational motion with a constant velocity does not influence the intrinsic state. In fact, the local gauge transformation with $\chi(\vec{r})=-m\vec{v}\cdot\vec{r}$ removes the cranking term $-\vec{v}\cdot\vec{p}$. Then using the ground-state solution ρ_0, which satisfies the static equation $[h_s[\rho_0],\rho_0]=0$ $(\vec{v}=0)$, we can construct a solution of Eq. (39), $\rho(\vec{R}_{\mathrm{c.m.}})=e^{im\vec{v}\cdot\vec{r}}\rho_0(\vec{R}_{\mathrm{c.m.}})e^{-im\vec{v}\cdot\vec{r}}$.

Rotational motion: A spatially rotating system with a constant angular velocity $\vec{\omega}$ can be described by a solution of Eq. (40) with $\dot{q}=\dot{\vec{\theta}}=\vec{\omega}$, $\dot{p}=\dot{\vec{I}}=0$. The generator $\overset{\circ}{P}(q,p)$ corresponds to the angular-momentum operator $\vec{j}$. Although we do not know the conjugate angle operator, it disappears because of the angular-momentum conservation $\dot{\vec{I}}=0$. Then it ends up as the cranking model (Inglis, 1954, 1956):

$$[h_s[\rho]-\vec{\omega}\cdot\vec{j},\rho]=0, \tag{44}$$

where the density $\rho(\vec{\theta})$ is a function of the angle $\vec{\theta}(t)=\vec{\omega}t$. Since there is no Galilean symmetry in the rotational motion, it is impossible to remove the cranking term by a gauge transformation. In this case, the decoupling is only approximate. In fact, the rotational motion influences the intrinsic state in nontrivial ways, such as the centrifugal stretching and the Coriolis coupling effects.

Pair rotation: In the superconducting phase with $\kappa(t)\neq 0$, in which the global gauge symmetry is broken, one may find another rotating solution in the gauge space with a constant angular velocity μ. The generator $\overset{\circ}{Q}(q,p)$ corresponds to the particle-number operator[2] with $q(t)=N_0$ $(\dot{q}=0)$, and $p(t)=\mu t$. Equation (40) leads to

$$[H_s[R]-\mu\mathcal{N},R]=0, \tag{45}$$

where $R(\theta)$ is a function of $\theta(t)=\mu t$. In terms of the time-dependent formalism, the appearance of the chemical potential μ in the stationary BdGKS equation (9) comes from the rotation in the gauge space.

When we study intrinsic excitations perpendicular to the ANG modes, we should extend the density $R(q,p)$ either by introducing the second set of variables $(q'(t),p'(t))$ or by allowing additional time dependence $R(q,p;t)$. The former method is adopted in Sec. V. The latter method changes the right-hand side of Eq. (40) to $i\partial R/\partial t$. For the case of the pair rotation, this leads to

$$i\frac{\partial}{\partial t}R(\theta;t)=[H_s[R]-\mu\mathcal{N},R(\theta;t)], \tag{46}$$

where μ is a function of the particle number N_0.

F. Recent development in nuclear EDF

Finding the best density functionals is always a big challenge in the DFT, not only in nuclear systems but also in electronic systems. Since we do not know the exact interaction among nucleons, even for the uniform matter at low-density and high-density limits, the exact functional is not available. Thus, strategies in nuclear DFT is somewhat different from those in electronic systems (Sec. VI). Recent developments involve the extension of the functional form and the new optimization to fit reliable calculations and

[2]Here we assume that q (p) is the time-even (time-odd) variable.

experimental data. The optimization has been performed mainly for static properties, including fission isomers and barrier heights. Here we present some efforts to improve the EDF, after those shown in Bender, Heenen, and Reinhard (2003).

The systematic optimization of the Skyrme EDF was performed to construct the functionals of UNEDF0-2 (Kortelainen *et al.*, 2010, 2012, 2014), which produce the root-mean-square deviation from the experimental binding energies of 1.5–2 MeV. These studies also show a clear deviation pattern common to all the EDFs. This indicates a necessity of novel functional forms for further improvements. The idea based on the density-matrix expansion (Negele and Vautherin, 1972; Negele, 1982) is under development to create new functionals (Carlsson, Dobaczewski, and Kortelainen, 2008; Carlsson and Dobaczewski, 2010; Stoitsov *et al.*, 2010). Other forms of EDF without the derivative terms have also been developed and produce similar accuracy (Baldo, Schuck, and Viñas, 2008; Baldo *et al.*, 2013). Although some phenomenological corrections significantly improve the reproduction of the binding energy (Goriely, Chamel, and Pearson, 2013), those corrections are not applicable to TDDFT calculations.

The Gogny EDF was also improved by fitting nuclear structure and neutron matter properties, leading to D1N (Chappert, Girod, and Hilaire, 2008) and D1M (Goriely *et al.*, 2009). A new type of the Gogny EDF was recently proposed, which extends the density-dependent term to the one with finite range (Chappert *et al.*, 2015). Another type of EDF based on the Yukawa-type potential was also proposed (Nakada, 2013; Nakada and Inakura, 2015).

The modern covariant EDFs adopt either nonlinear meson coupling or density-dependent coupling constants. In addition, there are two types of the covariant EDF: the finite-range meson field and the point-coupling models. Each EDF type had recent extensions of the functional form, such as the inclusion of the δ meson (Roca-Maza *et al.*, 2011), the cross-coupling terms (Fattoyev *et al.*, 2010), the exchange terms (Long *et al.*, 2007), and a new version of the point-coupling models (Nikšić, Vretenar, and Ring, 2008; Zhao *et al.*, 2010).

The pairing EDF responsible for the pair potential Δ is another issue. The pairing energy in the Gogny EDF is calculated with the same interaction. In contrast, most of the Skyrme and covariant EDFs independently treat the pairing EDF. Different forms of the pairing EDF were recently proposed (Yu and Bulgac, 2003; Margueron, Sagawa, and Hagino, 2008; Tian, Ma, and Ring, 2009; Yamagami, Shimizu, and Nakatsukasa, 2009; Yamagami *et al.*, 2012).

Currently, it is difficult to judge which type of nuclear EDF is the best. Their accuracy for the mass prediction is rather similar to each other among the Skyrme, the Gogny, and the covariant EDFs. Since we know none of them is perfect, the error analysis on the model is important (Erler *et al.*, 2012; Dobaczewski, Nazarewicz, and Reinhard, 2014). Furthermore, in contrast to the optimization of EDFs with respect to stationary properties, the one with respect to dynamical properties has not been performed in a systematic manner (Bender *et al.*, 2002). To our knowledge, possibilities beyond the adiabatic approximation (Sec. VI.B) have never been examined in nuclear physics.

III. LINEAR DENSITY RESPONSE

The linear density response of interacting systems can be rigorously formulated, in principle, on the basis of the TDDFT. The formulation is basically identical to the one known as the quasiparticle-random-phase approximation (QRPA) in nuclear physics (Ring and Schuck, 1980; Blaizot and Ripka, 1986).

Since the pair rotation inevitably takes place with a finite μ, the density $R(t) = R(\theta(t))$ is not stationary even for the ground state. In order to avoid complications in deriving the QRPA linear response equations, we should start either with Eq. (46) or with Eq. (38) of a gauge function $\chi(t) = \theta(t) = \mu t$, in which the time dependence through $\theta(t)$ is hidden. The following external potential, multiplied by a parameter η, is added to $H_s[R]$:

$$\eta V(t) \equiv \eta \begin{pmatrix} v_{\rm ext}(t) & \Delta_{\rm ext}(t) \\ -\Delta^*_{\rm ext}(t) & -v^*_{\rm ext}(t) \end{pmatrix}.$$

See Sec. II.A.2 for the corresponding operator form. It is convenient to introduce a small parameter η to elucidate the linearization. The time-dependent density and the Hamiltonian are linearized with respect to η as $R(t) = R_0 + \eta\delta R(t) + O(\eta^2)$ and $H_s(t) = H_s[R_0] + \eta\delta H(t) + O(\eta^2)$. The Fourier transform of Eq. (46) leads to

$$\omega\delta R(\omega) = [H_s[R_0] - \mu\mathcal{N}, \delta R(\omega)] + [V(\omega) + \delta H(\omega), R_0], \tag{47}$$

in the linear order. This equation plays a central role in this section.

A. Linear response equations and matrix representation in the quasiparticle basis

In order to evaluate Eq. (47), it is customary to adopt the quasiparticle eigenstates at the ground state in Eq. (9). Those with positive (negative) energies, Ψ^0_i [$\tilde{\Psi}^0_i$] satisfy $(H_s - \mu\mathcal{N})\Psi^0_i = E_i\Psi^0_i$ [$(H_s - \mu\mathcal{N})\tilde{\Psi}^0_i = -E_i\tilde{\Psi}^0_i$]. We may write the time-dependent quasiparticle states as $\Psi_i(t) = e^{-iE_it}[\Psi^0_i + \eta\delta\Psi_i(t)]$. Since the generalized density $R(t)$ is written in terms of the quasiparticle states $\Psi(t)$ as in Eq. (13), the fluctuating part $\delta R(t)$ in the linear order is given by

$$\begin{aligned}\delta R(t) &= -\sum_i \{\delta\Psi_i(t)\Psi^{0\dagger}_i + \Psi^0_i\delta\Psi^\dagger_i(t)\} \\ &= -\delta\Psi(t)\Psi^{0\dagger} - \Psi^0\delta\Psi^\dagger(t) = \delta\tilde{\Psi}(t)\tilde{\Psi}^{0\dagger} + \tilde{\Psi}^0\delta\tilde{\Psi}^\dagger(t).\end{aligned} \tag{48}$$

Using the notation in Sec. II.A.2, we calculate the matrix elements of Eq. (47) between these quasiparticle states. From the orthonormal relations, it is easy to see $\delta R^{(++)} = \delta R^{(--)} = 0$. Then only the matrix elements of $(+-)$ and $(-+)$

types are relevant for Eq. (47). Since these matrix are antisymmetric, the $(+-)$ and $(-+)$ matrix elements of Eq. (47) read, for $i<j$,

$$(E_i+E_j-\omega)\delta R_{ij}^{(+-)}(\omega)+\delta H_{ij}^{(+-)}(\omega)=-V_{ij}^{(+-)}(\omega),$$
$$(E_i+E_j+\omega)\delta R_{ij}^{(-+)}(\omega)+\delta H_{ij}^{(-+)}(\omega)=-V_{ij}^{(-+)}(\omega). \quad (49)$$

The residual fields $\delta H(\omega)$ are induced by the density fluctuation $\delta R(\omega)$, as $\delta H(\omega)=\partial H_s/\partial R|_{R=R_0}\cdot\delta R(\omega)$. Expanding their matrix elements as

$$\delta H_{ij}^{(+-)}(\omega)=\sum_{k<l}w_{ij,kl}\delta R_{kl}^{(+-)}(\omega)+\sum_{k<l}w'_{ij,kl}\delta R_{kl}^{(-+)}(\omega), \quad (50)$$

we obtain the QRPA linear response equations in the matrix form:

$$\left\{\begin{pmatrix}A & B\\ B^* & A^*\end{pmatrix}-\omega\begin{pmatrix}1 & 0\\ 0 & -1\end{pmatrix}\right\}\begin{pmatrix}\delta R^{(+-)}\\ \delta R^{(-+)}\end{pmatrix}=-\begin{pmatrix}V^{(+-)}\\ V^{(-+)}\end{pmatrix}, \quad (51)$$

where $A_{ij,kl}\equiv(E_i+E_j)\delta_{ik}\delta_{jl}+w_{ij,kl}$ and $B_{ij,kl}\equiv w'_{ij,kl}$. $R^\dagger=R$ and $(H_s)_{ij}^{(\pm\mp)}=\delta E/\delta R_{ji}^{(\mp\pm)}$ provide that $w_{ij,kl}$ are Hermitian and $w'_{ij,kl}$ are symmetric.

When the external potential V is identical to a one-body operator F, the strength function is given by

$$S(\omega;F)\equiv\sum_{n>0}|\langle n|F|0\rangle|^2\delta(\omega-E_n)=-\frac{1}{\pi}\mathrm{Im}R(\omega+i\eta;F), \quad (52)$$

where η is a positive infinitesimal and

$$R(\omega;F)=\sum_{i<j}\{F_{ij}^{(+-)*}\delta R_{ij}^{(+-)}(\omega)+F_{ji}^{(-+)*}\delta R_{ij}^{(-+)}(\omega)\}$$
$$=\frac{1}{2}\mathrm{Tr}[F\delta R(\omega)]. \quad (53)$$

B. Normal modes and eigenenergies

The QRPA normal modes are defined by the eigenvalue problem setting $V=0$ for Eq. (51). We denote the nth eigenvalue and eigenstate by Ω_n and a column vector Z_n of the dimension $2D$, respectively, where D is the number of independent two-quasiparticle pairs (ij) $(i<j)$. It is easy to show that there is a conjugate-partner eigenstate $\tilde{Z}_n$ with the eigenenergy $-\Omega_n$,

$$Z_n\equiv\begin{pmatrix}X_n\\ Y_n\end{pmatrix},\qquad \tilde{Z}_n\equiv\mathcal{I}Z_n^*=\begin{pmatrix}Y_n^*\\ X_n^*\end{pmatrix},$$

where

$$\mathcal{I}=\begin{pmatrix}0 & 1\\ 1 & 0\end{pmatrix}.$$

The QRPA eigenvalue equations are

$$\mathcal{N}\mathcal{H}Z_n=\Omega_nZ_n,\qquad \mathcal{N}\mathcal{H}\tilde{Z}_n=-\Omega_n\tilde{Z}_n, \quad (54)$$

with the $2D\times2D$ Hermitian matrices

$$\mathcal{H}\equiv\begin{pmatrix}A & B\\ B^* & A^*\end{pmatrix},\qquad \mathcal{N}\equiv\begin{pmatrix}1 & 0\\ 0 & -1\end{pmatrix}. \quad (55)$$

The eigenvectors are normalized as $Z_n^\dagger\mathcal{N}Z_m=-\tilde{Z}_n^\dagger\mathcal{N}\tilde{Z}_m=\delta_{nm}$.

Let us define the following $2D\times2D$ matrices:

$$\mathcal{Z}\equiv(Z,\tilde{Z})=\begin{pmatrix}X & Y^*\\ Y & X^*\end{pmatrix},\qquad \Omega\equiv\begin{pmatrix}\Omega_D & 0\\ 0 & \Omega_D\end{pmatrix}, \quad (56)$$

where Ω_D is the $D\times D$ diagonal matrix containing the eigenvalues Ω_n. Then Eq. (54) can be written as

$$\mathcal{N}\mathcal{H}\mathcal{Z}=\mathcal{Z}\Omega\mathcal{N}. \quad (57)$$

Using the Hermiticity of $\mathcal{H}$ and Eq. (57), one can prove $[\mathcal{Z}^\dagger\mathcal{N}\mathcal{Z},\Omega\mathcal{N}]=0$, which indicates that $\Omega\mathcal{N}$ and $\mathcal{Z}^\dagger\mathcal{N}\mathcal{Z}$ are both diagonal. Therefore, the normalization condition is written as $\mathcal{Z}^\dagger\mathcal{N}\mathcal{Z}=\mathcal{N}$, which we call "$\mathcal{N}$ orthonormalization." The matrix $\mathcal{N}$ plays a role of the norm matrix. Since this also means $\mathcal{N}\mathcal{Z}\mathcal{N}=(\mathcal{Z}^\dagger)^{-1}$, it leads to the completeness relation $\mathcal{Z}\mathcal{N}\mathcal{Z}^\dagger=\mathcal{N}$ (Ring and Schuck, 1980). The QRPA matrix $\mathcal{H}$ can be written as

$$\mathcal{H}=\mathcal{N}\sum_n(Z_n\Omega_nZ_n^\dagger+\tilde{Z}_n\Omega_n\tilde{Z}_n^\dagger)\mathcal{N}=\mathcal{N}\mathcal{Z}\Omega\mathcal{Z}^\dagger\mathcal{N}. \quad (58)$$

From this, it is easy to find $\mathcal{Z}^\dagger\mathcal{H}\mathcal{Z}=\Omega$.

For a given one-body Hermitian operator $\hat{F}$, we define a vector F_v by their $(+-)$-type matrix elements, $F_{ij}^{(+-)}$ with $i<j$, and its RPA conjugate partner $\tilde{F}_v=\mathcal{I}F_v^*$,

$$F_v=\begin{pmatrix}F^{(+-)}\\ 0\end{pmatrix},\qquad \tilde{F}_v=\begin{pmatrix}0\\ F^{(+-)*}\end{pmatrix}.$$

The transition amplitude of F between the ground and the nth excited state is given by

$$\langle n|\hat{F}|0\rangle=\sum_{i<j}\{F_{ij}^{(+-)}X_n(ij)+F_{ij}^{(+-)*}Y_n(ij)\}$$
$$=Z_n^\dagger(F_v+\tilde{F}_v)=(F_v+\tilde{F}_v)^TZ_n^*. \quad (59)$$

In most of the numerical applications, the QRPA eigenvalue problem is solved by constructing the QRPA matrices in the quasiparticle- or canonical-basis representations. We may transform the non-Hermitian eigenvalue problem of Eq. (54) to a Hermitian one (Ring and Schuck, 1980). For spherical nuclei, the matrix is block diagonal with respect to the angular momentum and the parity of two-quasiparticle states $[ij]_M^{J\pi}$. Thus, the numerical cost is moderate in this case and many calculations were performed; see review papers by Bender, Heenen, and Reinhard (2003) and Vretenar *et al.* (2005). In recent years, the QRPA calculations with modern EDFs have become available for deformed nuclei (Péru and Goutte, 2008;

Yoshida and Van Giai, 2008; Arteaga, Khan, and Ring, 2009; Losa *et al.*, 2010; Terasaki and Engel, 2010). The truncation of the two-quasiparticle space (ij) is usually adopted with respect to either the energy $E_i + E_j$ or the occupation of the canonical states (ρ_i, ρ_j). The calculation of the residual kernels $w_{ij,kl}$ and $w'_{ij,kl}$ is very demanding, because they have four quasiparticle indices.

If the residual kernel is written in a separable form with a Hermitian one-body operator $\hat{F}$,

$$w_{ij,kl} = \kappa F_{ij}^{(+-)} F_{lk}^{(-+)}, \qquad w'_{ij,kl} = \kappa F_{ij}^{(+-)} F_{lk}^{(+-)},$$

the computational cost may be significantly reduced because the QRPA eigenvalue problem can be cast into a dispersion equation (Ring and Schuck, 1980). For a given set of operators $\{F^{(n)}\}$, the coupling constants $\kappa^{(mn)}$ are derived from the Skyrme EDFs (Nesterenko, Kvasil, and Reinhard, 2002). This separable RPA calculation has been performed for deformed nuclei to give a reasonable description of giant resonances (Nesterenko *et al.*, 2006).

When the continuous symmetry is broken in the ground state, there is another "ground state" degenerate in energy whose density $R_0 + \delta R$ is infinitesimally deviated from R_0. Since both R_0 and $R_0 + \delta R$ satisfy the stationary equation (45), one can immediately derive Eq. (47) with $\omega = V = 0$. Therefore, the ANG modes appear as the zero-mode solution with $\Omega_{\mathrm{ANG}} = 0$. In this case, it is useful to rewrite Eq. (54) in the momentum-coordinate representation (Ring and Schuck, 1980). For the ANG mode (translation, rotation, or pair rotation), the momentum (P, J, or N) corresponds to a known operator (Sec. II.E.2). Then it ends up as the famous equation by Thouless and Valatin (1962), which determines the inertial mass and the coordinate of the ANG mode.[3] A modern technique to solve the Thouless-Valatin equation and numerical examples is presented by Hinohara (2015).

C. Finite amplitude method

Instead of explicitly calculating the residual kernels with four quasiparticle indices $w_{ij,kl}$ and $w'_{ij,kl}$, it is possible to compute them in an implicit manner. A possible approach is the finite amplitude method (Nakatsukasa, Inakura, and Yabana, 2007). The essential idea comes from the fact that the linear response equation (49), which is identical to Eq. (51), contains only the "one-body" quantities with two quasiparticle indices. The residual fields $\delta H^{(+-)}(\omega)$ and $\delta H^{(-+)}(\omega)$ can be uniquely determined for given $\delta R_{ij}^{(\pm\mp)}$. The linear expansion in Eq. (50) is achieved by a numerical finite difference method, and δH on the left-hand side is obtained without calculating $w_{ij,kl}$ and $w'_{ij,kl}$.

1. Basic idea

The Fourier component $\delta R(\omega)$ can be written in terms of their matrix elements as

$$\delta R(\omega) = \sum_{i,j} \{\Psi_i^0 \delta R_{ij}^{(+-)}(\omega) \tilde{\Psi}_j^{0\dagger} + \tilde{\Psi}_i^0 \delta R_{ij}^{(-+)}(\omega) \Psi_j^{0\dagger}\}. \quad (60)$$

Here the summation with respect to i and j is taken over all the positive-energy quasiparticles. Comparing Eqs. (48) and (60), we find $\delta\Psi_i(\omega) = -\sum_j \tilde{\Psi}_j^0 \delta R_{ji}^{(-+)}$ and $\delta\Psi_i^\dagger(\omega) = -\sum_j \delta R_{ij}^{(+-)} \tilde{\Psi}_j^{0\dagger}$. Using quasiparticle states slightly modified from Ψ_i^0,

$$\Psi_i(\omega) = \Psi_i^0 + \eta\delta\Psi_i(\omega) = \Psi_i^0 - \eta \sum_{j>0} \tilde{\Psi}_j^0 \delta R_{ji}^{(-+)}(\omega),$$
$$\Psi_i'^\dagger(\omega) = \Psi_i^{0\dagger} + \eta\delta\Psi_i^\dagger(\omega) = \Psi_i^{0\dagger} - \eta \sum_{j>0} \delta R_{ij}^{(+-)}(\omega) \tilde{\Psi}_j^{0\dagger},$$

the density $R_\eta(\omega) \equiv R_0 + \eta\delta R(\omega)$ can be written as

$$R_\eta(\omega) = 1 - \sum_i \Psi_i(\omega) \Psi_i'^\dagger(\omega) + O(\eta^2).$$

Note that, since the Fourier component $\delta R(\omega)$ is no longer Hermitian, $\Psi_i(\omega)$ and $\Psi_i'^\dagger(\omega)$ are not Hermitian conjugate to each other. The induced fields are now calculable in the following way:

$$\delta H_{ij}^{(+-)}(\omega) = \Psi_i^{0\dagger} \frac{1}{\eta} \{H_s[R_\eta(\omega)] - H_s[R_0]\} \tilde{\Psi}_j^0,$$
$$\delta H_{ij}^{(-+)}(\omega) = \tilde{\Psi}_i^{0\dagger} \frac{1}{\eta} \{H_s[R_\eta(\omega)] - H_s[R_0]\} \Psi_j^0. \quad (61)$$

Rigorously speaking, the limit of $\eta \to 0$ should be taken. However, in practice, we may use a small but finite value of η. Using Eq. (61) with a small value of η, the calculation of the induced residual fields $\delta H^{(\pm\mp)}$ can be achieved by the calculation of matrix elements of the BdGKS Hamiltonian $H_s[R]$. This is a much easier task than the calculation of the residual kernels $w_{ij,kl}$ and $w'_{ij,kl}$. Note that $H_s[R_\eta]$ should be constructed self-consistently with the quasiparticles Ψ_i and $\Psi_i'^\dagger$, namely, (U, V) with a small mixture of $\delta R^{(-+)}$ and (U^*, V^*) with a small mixture of $\delta R^{(+-)}$. In order to obtain the solution $\delta R^{(\pm\mp)}$, we solve Eq. (49) iteratively, starting from initial values for $(\delta R^{(+-)}, \delta R^{(-+)})$.

2. Strength functions

For the calculation of the strength functions, one can solve the linear response equation with a given frequency ω by choosing the external potential V identical to the operator F. Then, according to Eqs. (52) and (53), the strength function $S(\omega; F)$ with respect to F is obtained. To obtain an energy profile of $S(\omega; F)$, we need to repeat the calculation with different values of ω.

There is another approach based on the iterative construction of the subspace in which the diagonalization is performed (Olsen, Jensen, and Jørgensen, 1988; Tretiak *et al.*, 2009). The Krylov subspace generated by a pivot vector with respect to the one-body operator F preserves the energy-weighted sum rule (EWSR) values. Therefore, it is suitable for calculating a gross energy profile of the strength function by a small number of iterations. Some more details of these iterative methods are discussed in Sec. III.D. Applications of the finite

[3]Note that there have been some other attempts to explain the finite value of the moment of inertia as an analog of the Higgs mechanism with the SSB (Fujikawa and Ui, 1986).

amplitude method to the calculation of the strength functions have been performed for the Skyrme EDFs (Inakura, Nakatsukasa, and Yabana, 2009a, 2011, 2013; Nakatsukasa *et al.*, 2011; Stoitsov *et al.*, 2011; Inakura *et al.*, 2014; Mustonen *et al.*, 2014; Nakatsukasa, 2014; Pei *et al.*, 2014) and the covariant EDFs (Liang *et al.*, 2013, 2014; Nikšić *et al.*, 2013). The finite amplitude method is also applied to the calculation of the sum rules, which suggests approximate validity of the Thouless theorem for nuclear EDFs (Hinohara *et al.*, 2015).

3. Normal-mode eigenstates

It is often our interest to obtain the QRPA eigenmodes. These eigenmodes are, in principle, obtained if the matrix $\mathcal{H}$ in Eq. (57) is explicitly constructed. The finite amplitude method can also be used for this purpose to facilitate the calculation of the residual kernels (Avogadro and Nakatsukasa, 2013). Suppose we set $\delta R_{kl}^{(+-)} = 1$ for a specific pair (kl) and the rest all zero. Then the calculation of $\delta H_{ij}^{(+-)}$ using Eq. (61) provides $w_{ij,kl}$. On the other hand, setting $\delta R_{kl}^{(-+)} = 1$ and the rest zero, the calculation of $\delta H_{ij}^{(+-)}$ produces $w'_{ij,kl}$. This can be easily understood from Eq. (50). In this way, the QRPA matrix can be calculated without a complicated coding process. The usefulness of the method is demonstrated for the Skyrme (Avogadro and Nakatsukasa, 2013) and the covariant EDFs (Liang *et al.*, 2013).

When the matrix dimension becomes too large to directly handle, there are other approaches. For instance, the solution of the linear response equations (51) with complex frequencies combined with the contour integral serves for this purpose (Hinohara, Kortelainen, and Nazarewicz, 2013). This is based on the idea that the contour integral around the nth eigenenergy provides

$$(2\pi i)^{-1}\int_{C_n}\delta R_{ij}^{(+-)}(\omega)d\omega = X_n(ij)\langle n|F|0\rangle,$$
$$(2\pi i)^{-1}\int_{C_n}\delta R_{ij}^{(-+)}(\omega)d\omega = Y_n(ij)\langle n|F|0\rangle$$

for an external potential $V = F$. The contour must be chosen to enclose a single pole. This has been tested also for the charge-changing modes (Mustonen *et al.*, 2014).

The truncation of the space by an iterative procedure is another possible option; see Sec. III.D for more details.

D. Iterative methods for solutions

In the finite amplitude method, the numerical solution of the linear response equation is obtained by using an iterative algorithm. This significantly saves computational resources, especially the necessary memory size, because all we need to calculate are one-body quantities, not two-body ones.

1. Solution for fixed energy

A possible iterative procedure for the solution of Eq. (49) is given as follows: For a given external potential $V_{ij}^{(\pm\mp)}$, we assume a certain initial value for $\delta R_{ij}^{(\pm\mp)}$ for which the residual induced fields $\delta H_{ij}^{(\pm\mp)}$ are calculated according to Eq. (61). $H_s[R_\eta]$ can be calculated with the quasiparticle states Ψ_i^0 and $\Psi_i'^{0\dagger}$ replaced by $\Psi_i(\omega)$ and $\Psi_i^\dagger(\omega)$, respectively. Then, the left-hand side of Eq. (49), which is identical to that of Eq. (51), is computed. If these equations are not satisfied, we update the densities $\delta R_{ij}^{(\pm\mp)}$ according to an adopted iterative algorithm and repeat the calculation until the convergence. When the frequency ω is complex, one should adopt an iterative algorithm that can be applied to a linear algebraic equation with a non-Hermitian matrix.

2. Diagonalization in Krylov subspace

There are recent developments based on the iterative diagonalization of the Krylov space techniques. This is especially useful for calculations of the strength function, because it conserves the EWSR value of odd moments. Basically, they resort to the transformation of the matrix with dimension $2D$ into the one in the Krylov subspace with dimension $2d \ll 2D$.

Using Eq. (58), we have

$$(\mathcal{N}\mathcal{H})^L = \mathcal{Z}(\Omega\mathcal{N})^{L-1}\Omega\mathcal{Z}^\dagger\mathcal{N} = \mathcal{Z}\Omega^L\mathcal{N}^{L-1}\mathcal{Z}^\dagger\mathcal{N}. \quad (62)$$

Using the expression of transition amplitudes of Eq. (59), the EWSR value of order L is given by

$$m_L \equiv \sum_n \Omega_n^L|\langle n|F|0\rangle|^2 = \frac{1}{2}(F_v + \tilde{F}_v)^\dagger\mathcal{Z}\Omega^L\mathcal{Z}^\dagger(F_v + \tilde{F}_v).$$

For odd L, using Eq. (62), this can be written as

$$m_L = \tfrac{1}{2}(F_v + \tilde{F}_v)^\dagger(\mathcal{N}\mathcal{H})^L\mathcal{N}(F_v + \tilde{F}_v). \quad (63)$$

Therefore, starting from a pivot vector F_v and its conjugate $\tilde{F}_v$, the Krylov subspace of dimension $2d > L$,

$$\{F_v, \tilde{F}_v, (\mathcal{N}\mathcal{H})F_v, (\mathcal{N}\mathcal{H})\tilde{F}_v, \ldots, (\mathcal{N}\mathcal{H})^{d-1}F_v, (\mathcal{N}\mathcal{H})^{d-1}\tilde{F}_v\} \quad (64)$$

can span the intermediate space in Eq. (63). In Appendix A, we show that the reduction from the $2D$ into the $2d$ RPA subspace (64) conserves the sum rules m_L with odd L and $L < 2d$ (Johnson, Bertsch, and Hazelton, 1999).

To construct the subspace (64), one can adopt the Lanczos iteration algorithm. The Lanczos iteration produces an orthonormal basis set for the Krylov subspace, which makes a and b matrices tridiagonal. This works nicely for the case of a schematic separable interaction (Johnson, Bertsch, and Hazelton, 1999). However, since numerical errors are accumulated during the iterations, other algorithms, such as the non-Hermitian Arnoldi iteration, have been adopted for realistic Skyrme energy functionals (Toivanen *et al.*, 2010). Even for low-lying eigenstates, the method successfully works (Carlsson, Toivanen, and Pastore, 2012). The conjugate gradient algorithm may be another possible solver, which was used for low-lying RPA solutions in the coordinate-space representation (Imagawa and Hashimoto, 2003; Inakura *et al.*, 2005, 2006).

E. Green's function method

It becomes increasingly important to study unbound and weakly bound nuclei in physics of rare isotopes near the drip lines. There have been a number of developments for treatment of the resonance and continuum, including the continuum shell model (Okołowicz, Płoszajczak, and Rotter, 2003), the Gamow shell model (Id Betan *et al.*, 2002; Michel *et al.*, 2002), the Gamow HFB method (Michel, Matsuyanagi, and Stoitsov, 2008), the complex scaling method (Aoyama *et al.*, 2006), and the R-matrix theory (Descouvemont and Baye, 2010). In the linear response calculation based on the TDDFT, the one-body continuum (and a part of the two-body continuum) can be taken into account by the use of Green's function. In this section, we recapitulate the general formalism for superconducting cases ("continuum QRPA").

1. Response function

The QRPA linear response equation (51) can be rewritten as

$$[\Pi_0^{-1}(\omega)-\mathcal{W}]\begin{pmatrix}\delta R^{(+-)}(\omega)\\ \delta R^{(-+)}(\omega)\end{pmatrix}=\begin{pmatrix}V^{(+-)}(\omega)\\ V^{(-+)}(\omega)\end{pmatrix}, \quad (65)$$

with

$$\Pi_0^{-1}(\omega)\equiv\begin{pmatrix}\omega-A_0 & 0\\ 0 & -\omega-A_0\end{pmatrix}, \qquad \mathcal{W}\equiv\begin{pmatrix}w & w'\\ w'^* & w^*\end{pmatrix},$$

where $(A_0)_{ij,kl}=(E_i+E_j)\delta_{ik}\delta_{jl}$ in the quasiparticle representation. Equation (65) is inverted by the QRPA response function $\Pi(\omega)$ as $\delta R(\omega)=\Pi(\omega)V(\omega)$, where

$$\Pi(\omega)=[\Pi_0^{-1}(\omega)-\mathcal{W}]^{-1}=[1-\Pi_0(\omega)\mathcal{W}]^{-1}\Pi_0(\omega). \quad (66)$$

Here $\Pi_0(\omega)$ can be schematically written as

$$\Pi_0(\omega)=\sum_i\{\mathcal{G}_0(\omega-E_i)\tilde{\Psi}_i^0\tilde{\Psi}_i^{0\dagger}+\tilde{\Psi}_i^0\tilde{\Psi}_i^{0\dagger}\mathcal{G}_0(-\omega-E_i)\}, \quad (67)$$

using the Green's function $\mathcal{G}_0(E)$. Its derivation is given in Appendix B. The precise forms of Eq. (67) are given by Eqs. (B4) and (B5).

The strength function with respect to the operator F is obtained according to Eqs. (52) and (53). For $\omega\geq 0$,

$$S(\omega;F)=-\frac{1}{2\pi}\mathrm{Im}[F^\dagger\Pi(\omega+i\eta)F].$$

From Eq. (B1), one can see that, without the residual interaction $\mathcal{W}=0$, this leads to the unperturbed strength function $(1/2)\sum_{ij}|V_{ij}^{(+-)}|^2\delta(\omega-E_i-E_j)$.

Since the response function has four indices, in general, their calculation and inverse operation in Eq. (66) are very difficult tasks. It becomes practical when we need only their diagonal elements. The functional of local densities, such as the Skyrme functionals with local potentials, provides an example in which the coordinate-space representation $\{\vec{r}\}$ allows us the diagonal representation. The presence of the spin-orbit and finite-range exchange terms makes its application more difficult.

2. Boundary condition

One of the motivations of the Green's function formalism is the exact treatment of the continuum. This can be done by imposing the proper boundary condition in the Green's functions in Eq. (67). The density response in the time domain can be given by

$$\delta R(t)=\int\Pi(t-t')V(t')dt'.$$

Here $\Pi(t-t')$ should be zero for $t<t'$; $\Pi(t)=\theta(t)\Pi(t)$. This causality condition is achieved by adding a positive infinitesimal to ω in its Fourier component $\Pi(\omega)$. Thus, the replacement of $\omega\to\omega+i\eta$ leads to the retarded (outgoing) boundary condition for $\mathcal{G}_0(\omega-E_i)$ and the advanced (incoming) boundary condition for $\mathcal{G}_0(-\omega-E_i)$ in the expression of Π_0. For $\omega>E_i$, the outgoing asymptotic behavior is important for the former Green's function, which describes escaping of a particle or a Cooper pair. This provides an exact treatment of the continuum in the linear density response.

For superconducting systems with the ground-state BdGKS solution with $\kappa\neq 0$, the Green's function with the outgoing (incoming) boundary condition can be constructed for a spherical system using the partial-wave expansion (Belyaev *et al.*, 1987). The quasiparticle states Ψ_i^0, whose energy is smaller than the absolute value of the chemical potential $E_i<|\mu|$, are bound and discrete, while those with $E_i>|\mu|$ are unbound with continuum spectra. The summation over the quasiparticle states in Eq. (67) must be performed with respect to all the negative-energy states $\tilde{\Psi}_i^0$. This is not trivial because the index i is not discrete but continuous. To overcome this difficulty, the contour integral in the complex energy plane is useful (Matsuo, 2001). The spectral representation of the Green's function (B3) leads to

$$\sum_i f(-E_i)\tilde{\Psi}_i^0\tilde{\Psi}_i^{0\dagger}=(2\pi i)^{-1}\int_C f(E)\mathcal{G}_0(E), \quad (68)$$

for arbitrary function $f(E)$. Here the contour C is chosen to enclose the negative part of the real axis. Replacing the summation in Eq. (67) by the contour integral of Eq. (68), the response function is able to describe escaping of one-particle and two-particle decays from excited states. Therefore, the QRPA linear response theory with the Green's function can describe correlations among two escaping particles.

In the TDKS scheme for normal systems ($\Delta=0$), the negative-energy quasiparticles $\tilde{\Psi}_i^0$ are nothing but hole states and the summation over i runs over only the hole states. This method is known as the continuum RPA and is much easier than the continuum QRPA. The numerical applications were first achieved for spherical systems (Shlomo and Bertsch, 1975; Zangwill and Soven, 1980). The continuum RPA calculations with the Gogny EDFs have been recently achieved for spherical systems by transforming the RPA eigenvalue equation (54) into those for the channel functions (De Donno *et al.*, 2011).

For deformed systems, decomposing the BdGKS Hamiltonian into its spherical and deformed parts $H_s = H_{\rm sph} + V_{\rm def}$, we can use the identity

$$\mathcal{G}_0(E) = \mathcal{G}_{\rm sph}(E) + \mathcal{G}_{\rm sph}(E)V_{\rm def}\mathcal{G}_0(E),$$

where $\mathcal{G}_{\rm sph}(E)$ is the Green's function for the spherical Hamiltonian $H_{\rm sph}$. This method with the three-dimensional coordinate-space representation has been applied to normal systems, such as photoabsorption in molecules (Nakatsukasa and Yabana, 2001, 2003a; Yabana *et al.*, 2006) and light nuclei (Nakatsukasa and Yabana, 2005), however, not to superconducting systems. For deformed superconducting nuclei, although the full continuum linear response calculation has not been achieved yet, the construction of the Green's function has been carried out by using the coupled-channel scheme (Oba and Matsuo, 2009). A similar method was developed earlier for normal systems and applied to a linear density response in axial symmetric molecules (Levine and Soven, 1983, 1984; Levine, 1984).

F. Real-time method

Another approach to the linear response is to solve the TDBdGKS equation (28) directly in real time, with a weak perturbative external field. In the calculation, we do not linearize the equation. Thus, the same numerical code could serve for studies of the nonlinear dynamics (Sec. IV). This is particularly convenient for the calculation of the strength function $S(\omega; F)$ for a wide range of energy, associated with a one-body operator F which does not excite the ANG modes. On the contrary, the method is not suitable for obtaining information on a few excited normal modes. This is due to the uncertainty principle; the achieved energy resolution ΔE is inversely proportional to the duration of time evolution T.

A bulk property of the linear response is determined by time evolution of a short period of time. For instance, the EWSR value associated with a one-body operator F is obtained instantly as

$$m_1 = \sum_n \Omega_n |\langle n|F|0\rangle|^2 = \frac{1}{2\eta}\frac{d}{dt}{\rm Tr}[FR(t)]\bigg|_{t=0},$$

where the initial state is boosted by the operator F as

$$\Psi_i(t=0) = \begin{pmatrix} e^{i\eta F}U_i \\ e^{-i\eta F}V_i \end{pmatrix},$$

where the parameter η is a small number. This is generally true for all odd-L moments $m_L \propto d^L {\rm Tr}[FR(t)]/dt^L|_{t=0}$.

1. Strength functions

The real-time calculation of the strength function is performed in the following way. The initial state is the ground state, and an external potential $V(t) = f(t)F$, which is proportional to the operator F, is activated at time $t = 0$. In the linear regime, the function $f(t)$ should be small to validate the linear response. The strength function (52) can be obtained as

$$S(\omega; F) = \frac{-1}{2f(\omega)}{\rm Im}\int_{-\infty}^{\infty}{\rm Tr}[FR(t)]g(t)e^{i\omega t}dt, \tag{69}$$

where $f(\omega)$ is a Fourier transform of $f(t)$. If we choose $f(t) = f_0\delta(t)$, we have $f(\omega) = f_0$ which excites all the normal modes with equal strength. In the linear regime, $\int {\rm Tr}[FR(t)]e^{i\omega t}dt$ is proportional to $f(\omega)$. Thus, Eq. (69) gives a unique result.

In order to get a smooth energy profile $S(\omega; F)$, the time dependence in the integrand in Eq. (69) must vanish at $t = T$. In practice, it is customary to include the damping factor $g(t)$ in the integrand in Eq. (69), e.g., the exponential damping associated with a smearing width γ; $g(t) = \theta(t)\theta(T-t)e^{-\gamma t/2}$. The idea of the real-time method was proposed by Błocki and Flocard (1979) to calculate the energies of the giant resonances. The strength functions are calculated with modern Skyrme EDFs (Maruhn *et al.*, 2005; Nakatsukasa and Yabana, 2005; Umar and Oberacker, 2005; Fracasso, Suckling, and Stevenson, 2012), including pairing effects (Tohyama and Umar, 2002; Hashimoto and Nodeki, 2007; Ebata *et al.*, 2010; Stetcu *et al.*, 2011; Hashimoto, 2012; Ebata, Nakatsukasa, and Inakura, 2014; Scamps and Lacroix, 2014).

2. Absorbing boundary condition

In general, an external potential $V(t)$ excites the system into a superposition of many different elementary modes of excitation. Therefore, the particle decays simultaneously occur at different energies. In contrast to the linear response equation with fixed frequency ω, we do not know the asymptotic form in the real-time method. Nevertheless, in the linear regime, there is a useful method to realize an approximate outgoing boundary condition for normal systems.

A key is that the ground-state KS orbitals $\varphi_i(\vec{r})$ and the transition density in the linear response $\delta\rho(\vec{r}, t) = \sum_i \varphi_i(\vec{r})\delta\varphi_i^*(\vec{r}, t) + {\rm c.c.}$ are both localized in space. During the time evolution, we may simply *absorb* the outgoing waves from $\varphi_i(\vec{r}, t)$ in an outer region ($r > r_0$), where $\varphi_i(\vec{r})|_{r>r_0} = 0$. This can be approximately done by choosing a proper absorbing imaginary potential in the outer region. Note that, in the linear regime, the particle number is still conserved, because $\int_{\rm out}\delta\rho(\vec{r}, t)d\vec{r} = 0$. This absorbing boundary condition was adopted in nuclear TDDFT calculations (Nakatsukasa and Yabana, 2002, 2003b, 2005; Reinhard *et al.*, 2006) and treated in a rigorous manner (Pardi and Stevenson, 2013). It is also used in other fields of physical problems (Muga *et al.*, 2004; Yabana *et al.*, 2011). For the superconducting case, even at the ground state of finite localized systems, most of $U_i(\vec{r}, \sigma)$ are not localized in space. Thus, the application of the absorbing boundary condition is not trivial in this case.

G. Extension: Particle-vibration coupling

The QRPA calculation is successful in reproducing a variety of properties of nuclear excitations, especially of high-lying giant resonances. However, it has known limitations too. For instance, the widths of giant resonances in heavy nuclei are

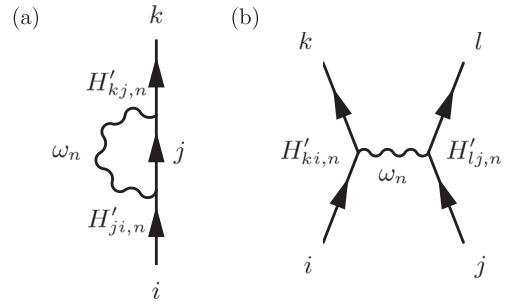

FIG. 3. Second-order diagrams for particle-vibration coupling, contributing to (a) the self-energy part $\Sigma_{ki}(E)$ and (b) effective two-particle interactions.

not well accounted for, although the peak energy and summed strength are well reproduced. The continuum QRPA is capable of calculating the escaping width of neutrons, however, it does not describe the spreading associated with coupling to complex configurations, such as many-particle–many-hole states. A possible improvement is explicit inclusion of higher-order terms and two-body correlations, which are presented in Sec. V.D.5. Another approach discussed here is the particle-vibration coupling (PVC) scheme. The PVC is also supposed to be responsible for the fact that the experimental single-particle level density near the Fermi level is higher than that in modern EDFs whose effective masses are smaller than unity.

The idea of the PVC is very old and connected to the essential concept of the Bohr-Mottelson unified model. That is to say, the single-particle motion and the vibrational (collective) motion in nuclei are coupled and influence each other. In earlier times, a phenomenological potential with a schematic separable interaction $(\kappa/2)\hat{F}\,\hat{F}$ was used in many applications, which is essentially inspired by the field coupling $H' = \kappa\alpha\hat{F}$ of Bohr and Mottelson (1975). The PVC produces dressed (renormalized) single-particle states. This affects many kinds of single-particle properties, including self-energies, single-particle moments, transfer matrix elements, and fragmentation of single-particle strengths; see Fig. 3(a). It is also expected to contribute to effective two-particle interactions, as in Fig. 3(b), which may be partially responsible for the attractive pairing interaction.

The causal single-particle Green's function obeys the Dyson equation

$$G(E) = G_0(E) + G_0(E)\Sigma(E)G(E),$$

where $G_0(E)$ is the unperturbed Green's function similar to Eq. (B3) with the causal boundary condition, and $\Sigma(E)$ is the proper self-energy part. The self-energy is alternatively denoted as $M(E)$ and called "mass operator" (Mahaux *et al.*, 1985). In the PVC, $\Sigma(E)$ takes account of coupling to collective vibrations. Normally, low-lying collective vibrational states are selectively included in $\Sigma(E)$. The lowest-order contribution to $\Sigma(E)$ is in the second-order coupling in H', as seen in Fig. 3(a). The diagonal approximation is often adopted for the Dyson equation, namely, only the diagonal matrix elements of $\Sigma(E)$ in the quasiparticle basis are taken into account.

Recently, the PVC calculation was carried out with modern EDFs (Litvinova and Ring, 2006; Colò, Sagawa, and Bortignon, 2010; Litvinova and Afanasjev, 2011; Brenna, Colò, and Bortignon, 2012; Cao *et al.*, 2014; Niu, Colò, and Vigezzi, 2014). It is extended to the quasiparticle-vibration coupling (Litvinova, Ring, and Tselyaev, 2008; Yoshida, 2009; Litvinova, 2012). They have shown successful descriptions of various kinds of nuclear phenomena, although there exist some ambiguities due to a selection of vibrational modes to be taken into account. For weakly bound systems, vibrational states as well as the single-particle states may be in the continuum. As discussed in Sec. III.E.2, this can be handled by the proper boundary condition for the Green's function. The Dyson equation in the coordinate-space representation provides a scheme to treat the continuum boundary condition, using a causal response function Π also with the continuum (Mizuyama, Colò, and Vigezzi, 2012). This was done for spherical normal systems, so far.

It is not so straightforward to formulate the PVC consistent with the principle of the DFT. A subtraction prescription is proposed (Tselyaev, 2007, 2013) and applied to the PVC (Litvinova, Ring, and Tselyaev, 2010) and the second RPA (Gambacurta, Grasso, and Engel, 2015). For the Skyrme EDF (zero-range effective interactions), some attempts have been recently made to renormalize the divergent second-order diagrams and to produce new EDFs for PVC calculations (Moghrabi *et al.*, 2012; Brenna, Colò, and Roca-Maza, 2014). To our knowledge, full respect of the Pauli principle and construction of the *DFT-based* particle-vibration coupling theory remain as challenging subjects.

H. Illustrative examples

Recent trends in the linear response studies for nuclei are calculations with all the residual fields (interactions), continuum, pairing, and deformed ground states. Let us show some examples.

1. Giant resonances and ground-state deformation

One of the successful applications of the nuclear EDF to linear response is the study of giant resonances. The giant resonances are high-frequency collective modes of excitation in nuclei, which exhaust a major part of the energy-weighted sum rule of the transition strengths. They are usually classified according to the spin S, isospin T, and multipolarity L. Their properties are supposed to reflect some basic quantities of the nuclear matter, such as the incompressibility, the symmetry energy, and the effective mass (Ring and Schuck, 1980; Harakeh and van der Woude, 2001). Among them, the isovector giant dipole resonance ($S = 0, T = 1, L = 1$), which is excited by the photoabsorption, is best known for a long time. The giant dipole resonance is simply characterized by the out-of-phase oscillations of neutrons and protons. The symmetry energy plays a major role in determination of its peak position. Figure 4 shows the photoabsorption cross section for Nd and Sm isotopes. These isotopes are classical examples in the rare-earth region exhibiting the spontaneous shape transition in the ground state from spherical to prolate-deformed shapes, with increasing the neutron number from $N = 82$ (^{142}Nd and ^{144}Sm)

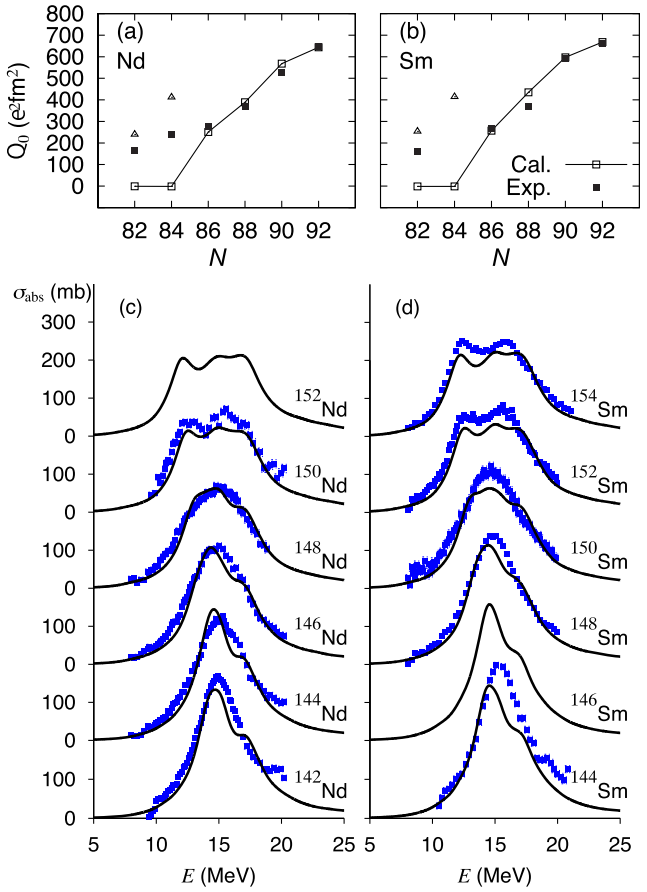

FIG. 4. Deformation and photoabsorption in Nd and Sm isotopes, calculated with the Skyrme energy functional of SkM*. Calculated and experimental intrinsic quadrupole moments are denoted by open and closed symbols, respectively, for (a) Nd and (b) Sm isotopes. For spherical nuclei with $N = 82$ and 84, we also plot the values (triangles) extracted from the QRPA calculation for $B(E2; 2^+ \to 0^+)$. Photoabsorption cross sections for (c) Nd and (d) Sm isotopes. The solid lines show the calculation and the solid (blue) symbols are experimental data (Carlos *et al.*, 1971, 1974). Adapted from Yoshida and Nakatsukasa, 2011.

to $N = 92$ (^{152}Nd and ^{144}Sm) (Bohr and Mottelson, 1975). The experimental intrinsic quadrupole moment Q_0 is estimated from $B(E2; 2_1^+ \to 0_{gs}^+)$ values, assuming the strong-coupling rotor (Bohr and Mottelson, 1975; Ring and Schuck, 1980). The self-consistent calculation with SkM* and the pairing energy functional (Yamagami, Shimizu, and Nakatsukasa, 2009) nicely reproduces these values for $N \geq 86$. The development of nuclear deformation leads to a broadening and peak splitting in the photoabsorption cross section. It is the well-known deformation splitting associated with two oscillation modes parallel to the symmetry axis ($K^\pi = 0^-$) and perpendicular to that ($K^\pi = 1^-$).

The calculation involves solving the eigenvalue problem of Eq. (57) within the space truncated with the two-quasiparticle energies $E_i + E_j \leq 60$ MeV. The photoabsorption cross section is obtained from the $E1$ transition strengths, according to Eq. (59), smeared with the Lorentzian width of 2 MeV. This smearing width is the only free parameter in the calculation, which accounts for the spreading effect beyond the present QRPA treatment; see Sec. III.G. Note that for light systems ($A \lesssim 40$) the agreement is not as good as in heavy nuclei (Erler, Klüpfel, and Reinhard, 2010). This may suggest an insufficient surface symmetry energy in current EDFs.

The isoscalar and isovector giant monopole resonances ($L = 0$) also show the deformation splitting for $N \geq 86$, which is consistent with the experimental data. The excitation energies of the split peaks are shown in Fig. 5 for Sm. This splitting is due to the coupling to the $K^\pi = 0^+$ component of the giant quadrupole resonance ($L = 2$). The monopole and quadrupole are decoupled for spherical nuclei. However, they are coupled in deformed nuclei, and the lower peak in Fig. 5 appears at the $K^\pi = 0^+$ peak of the corresponding giant quadrupole resonance.

The deformation of the momentum distribution (Fermi sphere) plays an essential role in the restoring force for the isoscalar giant resonances (Ring and Schuck, 1980). A typical well-studied example is the giant quadrupole resonance whose energy is approximately fit by $64A^{-1/3}$ MeV. The nuclear EDFs in the KS scheme nicely account for this effect of the quantum Fermi liquid, producing the correct mass number dependence. For deformed systems, in addition to this, the deformation splitting among $K^\pi = 0^+$, 1^+, and 2^+ peaks is well reproduced. The simple pairing-plus-quadrupole interaction produces the K splitting, $E_{K=2} - E_{K=0}$, of about 7 MeV for ^{154}Sm. This is too large and inconsistent with experiments (Kishimoto *et al.*, 1975). It is due to the violation of the nuclear self-consistency between the shapes of the potential and the density distribution. The calculation of the SkM* functional predicts the K splitting of 2.8 MeV (Yoshida and Nakatsukasa, 2013).

Systematic calculations with Skyrme EDFs for spherical nuclei have been performed using the canonical-basis QRPA (Paar *et al.*, 2003; Terasaki and Engel, 2006). The QRPA computer codes for deformed nuclei based on the matrix diagonalization were developed for the Skyrme EDF (Yoshida and Van Giai, 2008; Losa *et al.*, 2010; Terasaki and Engel, 2010; Yoshida and Nakatsukasa, 2011), the Gogny EDF (Péru and Goutte, 2008; Péru *et al.*, 2011), and the covariant EDF (Arteaga, Khan, and Ring, 2009). The calculations for

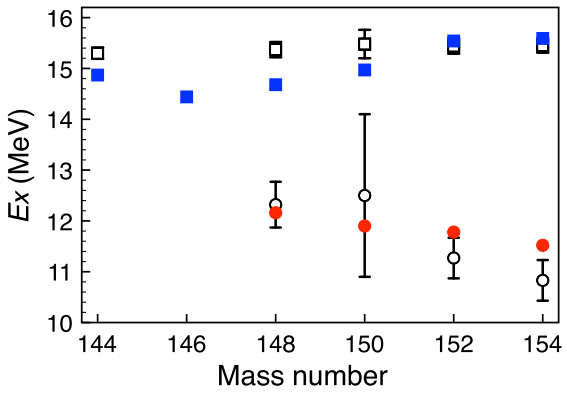

FIG. 5. The excitation energies of the isoscalar giant monopole resonances in the Sm isotopes; calculated values (solid symbols) and experimental data (open symbols) (Itoh *et al.*, 2003). From Yoshida and Nakatsukasa, 2013.

deformed systems require large computational resources for construction and storage of matrix $\mathcal{H}$ in Eq. (55). Systematic calculations for a wide range of nuclei have been performed by avoiding explicit calculations of $\mathcal{H}$, with the finite amplitude method (Inakura, Nakatsukasa, and Yabana, 2009b, 2011; Nakatsukasa *et al.*, 2011), and with the real-time method in Sec. IV.A (Scamps and Lacroix, 2013b; Ebata, Nakatsukasa, and Inakura, 2014).

2. Low-lying quadrupole states

Low-lying states associated with the quadrupole vibrations have been one of the major interests in nuclear structure problems. Systematic analysis of the QRPA calculations for the first excited $J^\pi = 2^+$ states in spherical nuclei and the gamma vibrations ($K^\pi = 2^+$) in deformed rare-earth nuclei were performed by Terasaki, Engel, and Bertsch (2008) and Terasaki and Engel (2011) using the Skyrme EDFs. They qualitatively agree with the trend of experimental data for spherical nuclei. Overall agreement of the QRPA results with experiments is better than that of the other approaches based on the generator coordinate method (GCM) (Sabbey *et al.*, 2007). However, the agreement is not quite as good for deformed nuclei. The five-dimensional collective Hamiltonian for the large-amplitude quadrupole motion may give a better description (Bertsch *et al.*, 2007; Delaroche *et al.*, 2010). The problems in the description of low-frequency quadrupole modes of excitation are discussed in Sec. V.

3. Charge-exchange modes

The isovector excitations have charge-changing ($\tau_\pm$) modes. For spherical nuclei, the calculations have been performed mostly with the Skyrme EDFs (Engel *et al.*, 1999; Bender *et al.*, 2002; Fracasso and Colò, 2005; Paar *et al.*, 2007), but also with the covariant EDFs (Paar *et al.*, 2004; Liang, Van Giai, and Meng, 2008; Niu *et al.*, 2013). The deformed QRPA calculations for the charge-exchange modes have been performed with the separable approximation (Sarriguren, de Guerra, and Escuderos, 2001; Sarriguren, 2012). Recently, the full QRPA calculations have become available too (Mustonen and Engel, 2013; Yoshida, 2013; Martini, Péru, and Goriely, 2014). The neutrino-nucleus reaction was also studied including inelastic neutral-current scattering (Dapo and Paar, 2012). The Gamow-Teller strength distribution ($S = 1, T = 1$) significantly affects the β-decay half-lives and the waiting point of the rapid neutron capture process (r process). To determine the r-process path far away from the stability line, the reliable theoretical estimates are highly desired.

4. Nuclear response in the continuum

For nuclei near the neutron drip line, weakly bound neutrons may produce large transition strength just above the threshold. Examples were observed in low-energy electric dipole ($E1$) strength in light halo nuclei, such as ^{11}Be (Nakamura *et al.*, 1994) and ^{11}Li (Ieki *et al.*, 1993; Shimoura *et al.*, 1995; Zinser *et al.*, 1997; Nakamura *et al.*, 2006). The enhancement is not associated with the collectivity, but due to the quantum mechanical "threshold effect." Whether the *collective* low-energy dipole resonances exist in heavier neutron-rich nuclei is still an open question (Hansen and Jonson, 1987; Ikeda, 1992). In order to properly address these issues in which the continuum plays an important role, the Green's function method in Sec. III.E is a powerful tool. For doubly closed spherical nuclei, we may neglect the pairing, and the continuum RPA calculations have been extensively performed to study a variety of strength functions; see Sagawa (2001) and Paar *et al.* (2007) and references therein. However, for open-shell and heavier systems, we need to treat the deformation and the paring correlations in addition to the continuum. This has been partially achieved with modern EDFs; the Green's function method for deformed systems (Nakatsukasa and Yabana, 2005) and that for superconducting systems (Mizuyama, Matsuo, and Serizawa, 2009; Serizawa and Matsuo, 2009; Daoutidis and Ring, 2011; Matsuo, 2015). The simultaneous treatment of the deformation, the pairing, and the continuum still remains as an unsolved problem.

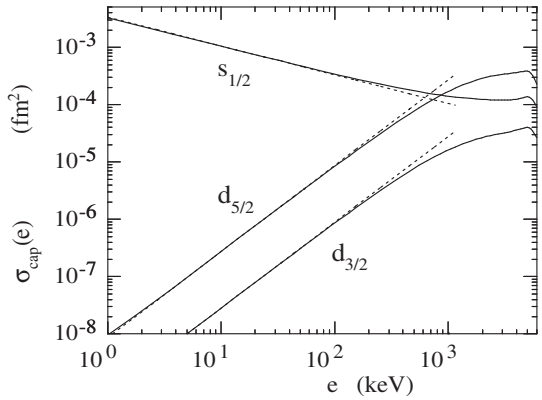

FIG. 6. Neutron capture cross sections $n + {}^{141}$Sn as functions of neutron energy e, for incident neutrons in $s_{1/2}$, $d_{3/2}$, and $d_{5/2}$ states. The Skyrme SLy4 EDF and the density-dependent pairing EDF are used. The dotted lines indicate the power-law scaling $\propto e^{l-1/2}$. From Matsuo, 2015.

The photoabsorption of neutron-rich nuclei leads to neutron decays if the excitation energy exceeds the neutron separation energy, which is very low in nuclei near the neutron drip line. It has been known that one can decompose the strength function (the photoabsorption cross section) in the continuum RPA into partial strength functions for individual channels of particle escape (Zangwill and Soven, 1980; Nakatsukasa and Yabana, 2001). Matsuo (2015) recently extended the idea to the continuum QRPA. The decomposition allows one, using the reciprocity theorem for the inverse processes, to compute the cross section of the direct neutron capture cross sections for different entrance channels separately. Figure 6 shows those for $n + {}^{141}$Sn, calculated from the $E1$ strength functions in the continuum QRPA. In this example, the cross section follows the power-law scaling rule. This would not be the case if there was a low-energy resonance.

IV. REAL-TIME CALCULATIONS BEYOND THE LINEAR REGIME

In nuclear physics, the real-time real-space calculations of the TDDFT have been explored since the 1970s, starting with

simplified energy functionals (Bonche, Koonin, and Negele, 1976). It became the primary approach for studying low-energy heavy-ion collisions. Since the Pauli blocking hinders the two-body collisions, the method was thought to work well at low energy, typically lower than the Fermi energy of about 40 MeV. There is an excellent review paper on these developments in early years, before 1982 (Negele, 1982). In recent years, we observed important progress in the real-time calculations with respect to several aspects.

(1) Realistic EDF: In earlier works, it was common to adopt simplified EDFs such that the spin-orbit term is neglected. Recent calculations remove these restrictions and incorporate the full EDF self-consistently. The adopted EDFs for time-dependent calculations have become as realistic as those for static calculations. Most time-dependent calculations beyond the linear regime have been performed with Skyrme energy functionals (Kim, Otsuka, and Bonche, 1997; Umar and Oberacker, 2006c; Simenel, 2012; Maruhn *et al.*, 2014). These changes produce even qualitative differences in nuclear dynamics. For instance, the famous fusion window anomaly was significantly hindered by the inclusion of the spin-orbit term in EDFs (Umar, Strayer, and Reinhard, 1986; Reinhard *et al.*, 1988). Extensive studies have been performed recently for studies of nuclear dynamics, such as quasifission (Oberacker, Umar, and Simenel, 2014; Scamps, Simenel, and Lacroix, 2015; Umar, Oberacker, and Simenel, 2015), charge equilibration (Iwata *et al.*, 2010a, 2010b), and high-spin rotation (Ichikawa *et al.*, 2014).

(2) TDBdGKS (TDHFB) scheme: Until recently, the dynamical pairing correlations were always neglected in real-time calculations. In the TDBdGKS scheme, the number of quasiparticle orbitals is identical to the dimension of the single-particle model space we adopt. Therefore, the real-time solution of the TDBdGKS (TDHFB) equations requires extremely heavy computational tasks.

Applications of the full TDBdGKS scheme for realistic nuclear EDF were performed with the spherical symmetry restriction (Avez, Simenel, and Chomaz, 2008). Later, it was achieved with no assumption on the spatial symmetry with the Skyrme (Stetcu *et al.*, 2011, 2015; Bulgac, 2013) and Gogny EDFs (Hashimoto, 2012). However, the applications are very limited at present, because of its high computational demands and some problems inherent in the TDBdGKS including the preparation of the initial state and treatment of the nonvanishing wave functions at the boundary. An approximate feasible approach is shown in Sec. IV.A.

(3) Nucleus-nucleus potential and friction parameters: To get insight into nuclear dynamics with energy dissipation, several ideas were proposed in the late 1970s and 1980s to extract "macroscopic" quantities, such as the nucleus-nucleus potential and the friction parameter associated with the one-body dissipation (Koonin *et al.*, 1977; Brink and Stancu, 1981; Cusson *et al.*, 1985). These ideas, which have been combined with realistic EDFs and recent computational advances, lead to further developments producing a number of new results in recent years. Two different approaches are presented in Sec. IV.B.

(4) Transfer reaction and fluctuations: The particle-number projection method in a restricted coordinate space was proposed to study the mass (charge) distribution in transfer reactions (Simenel, 2010). It is identical to the method based on the decomposition of the Slater determinant proposed by Koonin *et al.* (1977); however, the former has a significant computational advantage for heavier systems. Recent calculations with realistic EDFs show qualitative agreements with experiments; see Sec. IV.C.

The TDDFT simulations for heavy-ion collisions in early days showed that although the average values of one-body observables were well reproduced, their fluctuations were underestimated. Accordingly, for the transfer reaction, the calculated production rates are well reproduced in major channels, however, not good in rare channels. In order to overcome the difficulties, the fluctuation around the TDDFT path is taken into account; see Sec. IV.C.2.

A. Approximate schemes for TDBdGKS equations

Although the real-time calculation based on the full TDBdGKS equations in the three-dimensional space becomes available for a few cases (Stetcu *et al.*, 2011, 2015; Hashimoto, 2012), it is still a very demanding task. Thus, its approximate schemes are useful at present.

The easiest and old one is the introduction of the fixed fractional occupation numbers for KS orbitals. For the stationary Bardeen-Cooper-Schrieffer (BCS) ground state, each orbital ϕ_i has a time-reversal-conjugate partner $\phi_{\bar{i}}$ and the occupation probability $\rho_i = |v_i|^2$. Then, for the time evolution, we simply neglect the pair potential $\Delta_{ij}(t) = 0$. The TDKS equations for N_c orbitals ($N_c > N$) are solved in real time. Thus, the pairing effect is taken into account only in the fractional occupation which is completely determined at the preparation of the initial state. In this scheme, the pair potentials play no role in the time evolution.

To include the dynamical pairing in a minimum way, we may keep the diagonal form of the Hamiltonian, but with the pair potential $\Delta_{i\bar{j}}(t) = -\Delta_i(t)\delta_{ij}$. The quasiparticles are given by the canonical pair of orbitals ϕ_i and $\phi_{\bar{i}}$ multiplied by complex factors ($|u_i|^2 + |v_i|^2 = 1$):

$$\Phi_i = \begin{pmatrix} u_i\phi_i \\ -v_i^*\phi_{\bar{i}}^* \end{pmatrix}, \qquad \Phi_{\bar{i}} = \begin{pmatrix} u_i\phi_{\bar{i}} \\ v_i^*\phi_i^* \end{pmatrix}.$$

Then the TDBdGKS equation (28) is factorized into 2×2 form. Using the relation $\Delta_{\bar{i}i}\phi_{\bar{i}}^* = -\Delta_i\phi_i$, the TDBdGKS equations are split into

$$
\begin{aligned}
i\frac{\partial}{\partial t}\phi_i(t) &= \{h_s[\rho(t)] - \mu - \eta_i(t)\}\phi_i(t), \qquad i \leftrightarrow \bar{i}, \\
i\frac{d}{dt}\rho_i(t) &= \kappa_i(t)\Delta_i^*(t) - \kappa_i^*(t)\Delta_i(t), \\
i\frac{d}{dt}\kappa_i(t) &= \{\eta_i(t) + \eta_{\bar{i}}(t)\}\kappa_i(t) + \Delta_i(t)\{2\rho_i(t) - 1\},
\end{aligned}
\tag{70}
$$

where $\rho_i(t) \equiv |v_i(t)|^2$, $\kappa_i(t) \equiv u_i(t)v_i(t)$, and $\eta_i(t)$ are parameters to control the phase of the canonical orbitals $\phi_i(t)$. The $\eta_i(t)$ are arbitrary, if the diagonal form of the pair potential is consistent with the gauge invariant EDFs. When it is violated in practice, a choice of the minimal phase change was proposed (Ebata *et al.*, 2010).

When the pair potential is calculated from the antisymmetrized two-body interaction $\bar{v}$, $\Delta_i(t) = -\sum_{j>0}\kappa_j(t)\bar{v}_{i\bar{i},j\bar{j}}$. The densities are constructed as

$$
\begin{aligned}
\rho(\alpha\beta, t) &= \sum_i \rho_i(t)\phi_i(\alpha; t)\phi_i^*(\beta; t), \\
\kappa(\alpha\beta, t) &= \sum_{i>0}\kappa_i(t)\{\phi_i(\alpha; t)\phi_{\bar{i}}(\beta; t) - \phi_{\bar{i}}(\alpha; t)\phi_i(\beta; t)\}.
\end{aligned}
$$

Equations similar to Eq. (70) were derived using the time-dependent variational principle some time ago (Błocki and Flocard, 1976) and revisited in terms of the TDBdGKS equations (Ebata *et al.*, 2010). The conservation of the average particle number is guaranteed for an arbitrary choice of μ; however, the energy conservation depends on the choice of the parameter $\eta_i(t)$ (Ebata *et al.*, 2010), and the current conservation is violated in this approximation (Scamps *et al.*, 2012). The equations may describe dynamical pairing effects, coupled to motion of the canonical orbitals. The method has been applied to real-time calculations for linear response (Ebata *et al.*, 2010; Scamps and Lacroix, 2013b; Ebata, Nakatsukasa, and Inakura, 2014), neutron transfer reactions (Scamps and Lacroix, 2013a), and fusion and fission reactions (Ebata and Nakatsukasa, 2014, 2015; Scamps, Simenel, and Lacroix, 2015).

B. Heavy-ion collision: Nucleus-nucleus potential and one-body dissipation

In real-time calculation of heavy-ion collisions so far, the TDKS equations with $\kappa = \Delta = 0$ are solved in most applications. The initial state is prepared as two nuclei in their ground states, placed well separated in space. First we locate the two nuclei (N_L, Z_L) in the left and (N_R, Z_R) in the right, with respect to the z coordinate. In this initial state, each KS orbital $|\phi_i\rangle$ belongs to either "left" or "right," and those in the left nucleus are boosted toward the right by $|\phi_i(t=0)\rangle = e^{ik_L z}|\phi_i\rangle$, while those in the right by $|\phi_i(t=0)\rangle = e^{-ik_R z}|\phi_i\rangle$. Then, the time evolution of KS orbitals is computed to obtain the density $\rho(\alpha\beta; t) = \sum_i \rho_i(t)\phi_i(\alpha; t)\phi_i^*(\beta; t)$.

Recently, there are a number of works to extract the nucleus-nucleus potential and the friction from nonempirical TDDFT calculations. To achieve this, we divide the total system into two parts, one associated with a small number of collective degrees of freedom, and the rest of the Hilbert space called intrinsic space. To our understanding this division is guided by *a priori* assumptions, not by the TDDFT dynamics itself.

1. Density-constraint calculation

Among many kinds of densities, for the colliding nuclei under consideration, the normal density distribution $\rho(\vec{r}; t)$ and the current density $\vec{j}(\vec{r}; t) = (1/2i)(\vec{\nabla} - \vec{\nabla}')\rho(\vec{r}, \vec{r}'; t)|_{\vec{r}=\vec{r}'}$ are regarded as quantities associated with collective motion. Then the collective energy associated with the collisional motion is assumed to be a functional of $\rho(\vec{r})$ and $\vec{j}(\vec{r})$, which is defined as the minimization with constraints on the density and the current,

$$
E_{\rm coll}[\rho(\vec{r}, t), \vec{j}(\vec{r}, t)] = \min_{\rho \to (\rho(\vec{r}), \vec{j}(\vec{r}))} F[\rho] - E_L - E_R, \tag{71}
$$

where E_L and E_R are the ground-state energies of two nuclei. For the initial state with two nuclei far apart ($t = 0$), this approximately corresponds to the sum of the kinetic energy of the center of mass of each nucleus $P_L^2/(2A_L m) + P_R^2/(2A_R m)$ and the Coulomb energy between the two $Z_L Z_R e^2/|\vec{R}_L - \vec{R}_R|$. Since the total energy is conserved during the time evolution, we have $E_{\rm total} \approx E_L + E_R + E_{\rm coll}(t = 0)$.

The TDDFT simulation of the heavy-ion collision produces the time-dependent density $\rho(\vec{r}, t)$ and current $\vec{j}(\vec{r}, t)$. From these, the intrinsic excitation energy during the collision is given by

$$
E^*(t) = E_{\rm total} - E_{\rm coll}[\rho(\vec{r}; t), \vec{j}(\vec{r}; t)] - E_L - E_R. \tag{72}
$$

Furthermore, the collective energy is divided into two; $E_{\rm coll}[\rho(\vec{r}), \vec{j}(\vec{r})] = E_{\rm kin}[\rho(\vec{r}), \vec{j}(\vec{r})] + V_{\rm pot}[\rho(\vec{r})]$ and the nucleus-nucleus potential is defined by the latter, obtained by minimization with a constraint on $\rho(\vec{r})$,

$$
V_{\rm pot}[\rho(\vec{r})] = \min_{\rho \to \rho(\vec{r})} F[\rho] - E_L - E_R. \tag{73}
$$

This minimization automatically produces $\vec{j}(\vec{r}) = 0$ for even-even nuclei. In practice, since the density and current constraint calculation of Eq. (71) is computationally demanding, the density-constraint calculation of Eq. (73) is performed. Then, the collective kinetic energy is assumed to be

$$
E_{\rm kin}[\rho(\vec{r}), \vec{j}(\vec{r})] = \frac{1}{2m}\int \frac{|\vec{j}(\vec{r})|^2}{\rho(\vec{r})}\, d\vec{r}. \tag{74}
$$

So far all the quantities are calculated as functions of time t. A possible mapping from t to a collective coordinate $R(t)$ is given in Sec. IV.B.2.

The idea and computational algorithm of this method were proposed by Cusson *et al.* (1985). Extensive studies have been performed in recent years by Oberacker, Umar, and coworkers (Umar and Oberacker, 2006a, 2006b, 2007, 2008; Umar *et al.*, 2009, 2010, 2012; Oberacker *et al.*, 2010; Umar, Oberacker, and Horowitz, 2012; Oberacker and Umar, 2013; Simenel *et al.*, 2013). The TDDFT naturally provides a dynamical change of the nuclear structure during collisions. Therefore, the potential $V_{\rm pot}$ in Eq. (73) contains such polarization effects. However, the separation between the collective energy (71) and the dissipation energy (72) is less

reliable when two nuclei are significantly overlapped. Even without any dissipation, the current density $\vec{j}(\vec{r})$ is reduced in the overlapping region because two nuclei are moving in opposite directions. This leads to the reduction of $E_{\rm coll}$ ($E_{\rm kin}$) and to overestimation of E^*.

2. Mapping to one-dimensional Hamilton equations of motion

Another even simpler method is based on the explicit introduction of the one-dimensional (1D) collective coordinate and momentum. We recapitulate here the method presented by Washiyama and Lacroix (2008) to extract the nucleus-nucleus potential $V_{\rm pot}(R)$ and friction parameter $\gamma(R)$. Similar methods were proposed earlier (Koonin *et al.*, 1977; Brink and Stancu, 1981). We introduce the relative distance between two nuclei $R(t)$, calculated as the distance between two centers of mass in the left and right. Assuming the head-on collision on the z axis, $R(t) = (1/A_R)\int_R z\rho(\vec{r},t)d\vec{r} - (1/A_L)\int_L z\rho(\vec{r},t)d\vec{r}$. The momentum $P(t)$ is calculated as $P(t) = [A_L\int_R j_z(\vec{r},t)d\vec{r} - A_R\int_L j_z(\vec{r},t)d\vec{r}]/(A_L+A_R)$. Here the integrations $\int_{R(L)} d\vec{r}$ are defined by $\int_{R(L)} d\vec{r} f(\vec{r}) = \int d\vec{r} f(\vec{r})\theta(\pm(z-z_0))$. The $z = z_0$ plane can be chosen, for instance, as the plane of the lowest density (neck position). The TDDFT calculation produces $R(t)$ and $P(t)$ as functions of time, which are assumed to obey the 1D classical Hamilton equation of motion:

$$\frac{dR}{dt} = \frac{P}{\mu(R)}, \qquad \frac{dP}{dt} = -\frac{dV_{\rm pot}}{dR} - \gamma(R)\frac{dR}{dt}, \tag{75}$$

where the first equation provides the definition of the reduced mass $\mu(R)$. There are two unknown quantities remaining, the force $dV_{\rm pot}/dR$ and the friction parameter $\gamma(R)$. Assuming weak energy dependence of these quantities, we can estimate them by performing the TDDFT simulation with two slightly different initial energies. Note that, because of the head-on assumption, the parameter $\gamma(R)$ may represent only the radial friction, not the tangential one.

Since the density-constraint calculation at different $R(t)$ is not necessary in this approach, it is computationally easier than the previous one. Similar to the density-constrained calculation, the calculated relative momentum decreases after two nuclei touch, even if no dissipation takes place. In addition, the assumption that R and P are canonical conjugate variables becomes questionable as well.

C. Heavy-ion collision: Transfer reaction

1. Number projection

The mass number distribution after the collision was estimated for a schematic EDF (Koonin *et al.*, 1977). It is based on the decomposition of the single Slater determinant in a restricted space and has been used for electron transfer processes in atomic collisions (Ludde and Dreizler, 1983; Nagano *et al.*, 2000). Recently, an alternative expression was given using the particle-number projection (Simenel, 2010). They are identical in principle; however, the latter has a computational advantage over the previous expression.

Let us divide the space V into two regions: V_f and the rest $V_{\bar{f}} = V - V_f$. The particle number in the space V_f, N_f, is defined by $\hat{N}_f = \int_f \hat{\psi}^\dagger(\vec{r}\sigma)\hat{\psi}(\vec{r}\sigma)d\vec{r}$. The particle-number projection in the right space $\hat{P}_f(N)$ is given by

$$\hat{P}_f(N) = \frac{1}{2\pi}\int_0^{2\pi} d\theta e^{i\theta(N-\hat{N}_f)}.$$

Let us define the matrix $B_{ij}(\theta)$ as $B_{ij}(\theta) \equiv \langle\phi_i|\phi_j\rangle_{\bar{f}} + e^{-i\theta}\langle\phi_i|\phi_j\rangle_f$, with the overlap in the spaces V_f and $V_{\bar{f}}$ given by

$$\langle\phi_i|\phi_j\rangle_{f(\bar{f})} \equiv \sum_\sigma \int_{f(\bar{f})} \phi_i^*(\vec{r}\sigma)\phi_j(\vec{r}\sigma)d\vec{r}.$$

The probability that the N particles are present in V_f is given by

$$P_N = \frac{1}{2\pi}\int_0^{2\pi} d\theta e^{i\theta N}\det B(\theta). \tag{76}$$

In the real-time simulation, after the two nuclei collide and separate again, we specify the region V_f where one of the nuclei is located. Then the mass number distribution is calculated according to Eq. (76). The production cross section of the nucleus with N particles is estimated by repeating the same calculation with different impact parameter b,

$$\sigma(N) = 2\pi\int dbbP_N(b). \tag{77}$$

This is most useful for the calculations of transfer reaction cross section $\sigma_{\pm N,\pm Z}$. When the pair potential is present, the number projection is required for the initial state too.

The expectation value of the operator in each reaction product can also be evaluated with the present technique (Sekizawa and Yabana, 2014, 2015; Sonika, *et al.*, 2015). For instance, the one-body operator local in the coordinate $\hat{O} = \sum_\sigma \int O(\vec{r})\hat{\psi}^\dagger(\vec{r}\sigma)\hat{\psi}(\vec{r}\sigma)d\vec{r}$ is given by

$$O_N = \frac{1}{2\pi P_N}\int_0^{2\pi} d\theta e^{i\theta N}\det B(\theta) \times \sum_i (\langle\phi_i|O|\phi_i\rangle_L + e^{-i\theta}\langle\phi_i|O|\phi_i\rangle_R).$$

2. Fluctuations

The TDDFT provides feasible approaches to nuclear collective dynamics in a large-amplitude nature and has been successful in describing mean values of one-body observables. However, it has been known for some time that it underestimates fluctuations (Koonin *et al.*, 1977; Negele, 1982). As long as we calculate the one-body observables according to the KS orbitals, a severe limitation comes from mainly two sources: One is the missing effect of two-body collisions. The inclusion of the nucleon-nucleon collision is treated by a stochastic approach (Aichelin, 1991) or by explicit inclusion of two-body correlations (Shun-jin and Cassing, 1985). Although the two-body collision becomes less important at

lower energy, there is another well-known limitation, which we address here. The TDDFT is described by a single time-dependent mean-field (KS) potential. The collision of nuclei, in general, leads to the superposition of different final states $|\Phi^{(1)}\rangle, |\Phi^{(2)}\rangle, \ldots$ for which different mean fields should exist $v_s^{(1)}(\vec{r}), v_s^{(2)}(\vec{r}), \ldots$. Since these dynamics in multichannels are described by a single average mean field $v_s^{(\mathrm{av})}$, the TDDFT naturally hinders the fluctuation. This may be crucial at low energies, in which one-body dynamics are supposed to play a dominant role (Ikeda, Yoshida, and Yamaji, 1986).

A practical way to improve the situation is given by replacing the quantum fluctuation by a classical statistical ensemble in the initial state. Each state is evolved in time with its own mean field. This is often called "stochastic mean-field theory" (Ayik, 2008; Lacroix and Ayik, 2014).

The quantum fluctuation at the initial state is estimated by the fluctuation of the one-body operator $\hat{A}$ in a Slater determinant

$$\sigma_A^2 \equiv \langle \hat{A}^2 \rangle - \langle \hat{A} \rangle^2 = \sum_{ij} |\langle \phi_i | \hat{A} | \phi_j \rangle|^2 \rho_i (1 - \rho_j).$$

For normal systems at zero temperature, the occupation is an integer number $\rho_i = 0$ or 1. In order to describe this quantum fluctuation by the classical statistical average as $\langle \hat{A} \rangle = \mathrm{tr}[\overline{\rho^{(n)}} A]$ and $\sigma_A^2 = \overline{(\mathrm{tr}[\delta\rho^{(n)} A])^2}$, we use random Gaussian numbers for one-body density $\rho^{(n)} = \overline{\rho^{(n)}} + \delta\rho^{(n)}$, which satisfies the ensemble average values

$$\overline{\rho_{ij}^{(n)}} = \rho_i \delta_{ij}, \tag{78}$$

$$\overline{\delta\rho_{ij}^{(n)} \delta\rho_{kl}^{(n)}} = \tfrac{1}{2} \delta_{il} \delta_{jk} \{\rho_i (1 - \rho_j) + \rho_j (1 - \rho_i)\}. \tag{79}$$

Starting from each initial configuration $\rho^{(n)}$, $\rho^{(n)}(t)$ evolves in time following the TDKS equation (35), with the density given by

$$\rho^{(n)}(t) = \sum_{ij} |\phi_i^{(n)}(t)\rangle \rho_{ij}^{(n)} \langle \phi_j^{(n)}(t)|.$$

Since the off-diagonal elements of $\rho_{ij}^{(n)}$ are nonzero, we need to solve the time evolution of not only the hole states, but also the particle states.

For calculations of small fluctuations around the TDKS trajectory in the observable $\hat{A}$ at $t = t_f$, instead of performing the forward time evolution of $\delta\rho(t)$ with the initial fluctuation of Eqs. (78) and (79), we may utilize a backward time evolution. The time evolution of $\delta\rho(t)$ is described by a unitary operator $U(t)$ as $\rho(t) = U(t)\rho(t=0)U^\dagger(t)$ in general. Note that the linear approximation with respect to $\delta\rho^{(n)}$ leads to the operator $U(t)$ independent of the event label (n), Thus, the fluctuating part of the observable $\hat{A}$ can be written as

$$\delta A^{(n)}(t_f) = \mathrm{tr}[\hat{A}\delta\rho^{(n)}(t_f)] = \mathrm{tr}[\hat{B}\delta\rho^{(n)}(0)],$$

where t_f represents the final time when the observation is made and $t = 0$ is the initial time. Here the one-body Hermitian operator $\hat{B}$ is given by $B_{ij} = \{U^\dagger(t_f)\hat{A}U(t_f)\}_{ij}$. The fluctuation of $\hat{A}$ at $t = t_f$ is now given by the ensemble average at $t = 0$,

$$\sigma_A^2 = \overline{\{\delta A^{(n)}(t_f)\}^2} = \sum_{ijkl} B_{ij} B_{kl} \overline{\delta\rho_{ji}^{(n)} \delta\rho_{lk}^{(n)}} \tag{80}$$

$$= \sum_{ij} |B_{ij}|^2 \rho_i (1 - \rho_j). \tag{81}$$

In fact, Eq. (81) is the same as the one previously derived with the variational approach by Balian and Vénéroni (1985). It is easy to see that Eq. (81) can be alternatively written as $-\mathrm{tr}[[B, \rho(0)]^2]/2$ with $\rho_{ij}(0) = \rho_i \delta_{ij}$. Thus, modifying the TDDFT density $\rho(t)$ at $t = t_f$ as $\eta_\epsilon(t_f) \equiv e^{i\epsilon\hat{A}} \rho(t_f) e^{-i\epsilon\hat{A}}$, the backward evolution of $\eta_\epsilon(t)$ up to $t = 0$ gives the following expression:

$$\sigma_A^2 = \lim_{\epsilon \to 0} \frac{1}{2\epsilon^2} \mathrm{tr}[\{U^\dagger(t_f)\eta_\epsilon(t_f)U(t_f) - \rho(0)\}^2]. \tag{82}$$

This is useful for practical calculations (Simenel, 2011, 2012). The KS wave functions $|\phi_i(t_f)\rangle$ are modified to $e^{i\epsilon\hat{A}}\phi_i(t_f)$ with small ϵ, and then we calculate the backward time evolution to $t = 0$. This provides $U^\dagger(t_f)\eta_\epsilon(t_f)U(t_f)$. Several different values of ϵ may be enough to identify its quadratic dependence. More details and derivation can be found in Simenel (2012).

D. Illustrative examples

In this section, we present some examples of recent calculations in studies of nuclear collision dynamics. The full TDBdGKS calculation of collision dynamics has not been achieved, but is under progress (Stetcu *et al.*, 2015). Most of the recent calculations beyond the linear regime have been performed based on the TDKS equations with the Skyrme EDFs.

1. Internucleus potential and precompound excitation

Extensive studies using the real-time simulation have been performed for microscopic derivation of the nucleus-nucleus potential and dissipation energy at initial stages of the nuclear fusion. This can be done with the density-constraint calculation shown in Sec. IV.B. The real-time simulation for the fusion reaction produces the time evolution of the density $\rho(\vec{r}, t)$, the current $\vec{j}(\vec{r}, t)$, etc. At the beginning, the total energy is given by $E_{\mathrm{total}} = E_{\mathrm{coll}}(t = 0) + E_L + E_R$. After the two nuclei touch, E_{total} is also shared by the intrinsic excitation energy E^*.

According to Eqs. (72), (73), and (74), Umar *et al.* (2009) estimated the nucleus-nucleus potential $V(R)$ and the intrinsic excitation $E^*(R)$ for $^{40}\mathrm{Ca} + {}^{40}\mathrm{Ca}$. These are illustrated in Figs. 7 and 8. The amount of the dissipative energy E^* is roughly proportional to the bombarding energy $E_{\mathrm{c.m.}} = E_{\mathrm{coll}}(t = 0)$, while the potential V_{pot} is approximately independent of the choice of $E_{\mathrm{c.m.}}$. The excitation energy for the fused system $^{80}\mathrm{Zr}$ is expected to be $E_{\mathrm{total}} - E_{\mathrm{g.s.}}(^{80}\mathrm{Zr})$ at the

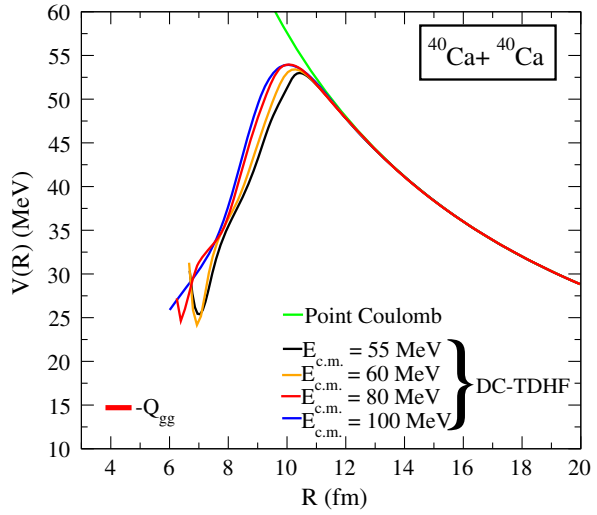

FIG. 7. Internucleus potential for $^{40}\mathrm{Ca} + {}^{40}\mathrm{Ca}$ for different energies. The horizontal axis is the distance between two ^{40}Ca nuclei. The green line indicates the Coulomb potential assuming the point charge $20e$ at the center of each nucleus. DC-TDHF is an abbreviation for the density-constrained TDHF. From Umar *et al.*, 2009.

end. The calculated E^* at the capture point near $R = 6$ fm is still lower than this value by about 20 MeV. It is confirmed that this 20 MeV is due to the difference in the density distribution between the ground state of ^{80}Zr and the capture point.

The internucleus potential obtained from the mapping to the 1D classical equation of motion (75) seems to be similar to the one of the density-constrained calculation for some light systems (Washiyama and Lacroix, 2008). However, in heavier systems where the dissipation becomes more relevant, they may produce different potentials. In fact, for the heavy systems with $Z_L Z_R \gtrsim 1600$, it is known that the fusion probability is significantly hindered. An example is given by the fact that the fusion cross section of $^{96}\mathrm{Zr} + {}^{124}\mathrm{Sn}$ ($Z_L Z_R = 2000$) is much smaller than that of $^{40}\mathrm{Ar} + {}^{180}\mathrm{Hf}$ ($Z_L Z_R = 1296$), both leading to the same fused system ^{220}Th (Sahm *et al.*, 1985). This was supposed to be due to the strong energy dissipation inside the Coulomb barrier (Swiatecki, 1982). The quasifission before the formation of a compound nucleus may play a primary role in the fusion hindrance. Although the TDDFT cannot fully take into account the collisional damping, it reproduces some features of the quasifission process (Simenel, 2012; Oberacker, Umar, and Simenel, 2014).

Figure 9 shows the calculated potential for $^{96}\mathrm{Zr} + {}^{124}\mathrm{Sn}$. The potential of the density-constrained calculation shows a maximum around $R = 13.1$ fm and decreases at $R < 13$ fm. This is very different from the one obtained by mapping to the 1D classical equations, which keeps rising even at $R < 13$ fm. This must be attributed to the difference in the decomposition of the total energy into $V(R)$, $E_{\mathrm{kin}}(R)$, and $E^*(R)$. Since we can expect the E_{kin} in these two methods are rather similar, the intrinsic excitation $E^*(R)$ should compensate the difference in $V(R)$. The relation between the two methods in Secs. IV.B.1 and IV.B.2 is not clear at present. Further studies are desired to clarify the microscopic origin of the fusion hindrance (Guo and Nakatsukasa, 2012; Simenel, 2012). It is also related to a conceptual question: What are the collective variables, the potential, and the inertial mass for proper description of many kinds of nuclear reaction? This is the main subject of Sec. V.

2. Multinucleon transfer reaction

Another example of a low-energy nuclear reaction is the multinucleon transfer reaction for heavy-ion collisions. At energies near the Coulomb barrier, this reaction involves many kinds of quantum nonequilibrium many-body dynamics, such as shell effects, neck formation, and tunneling. The GRAZING model (Winther, 1994) is frequently used to describe the multinucleon transfer reaction. This model is based on statistical treatment of the single-particle transfer processes and a semiclassical formulation of the coupled-channel method. The TDKS (TDHF) simulation may provide an

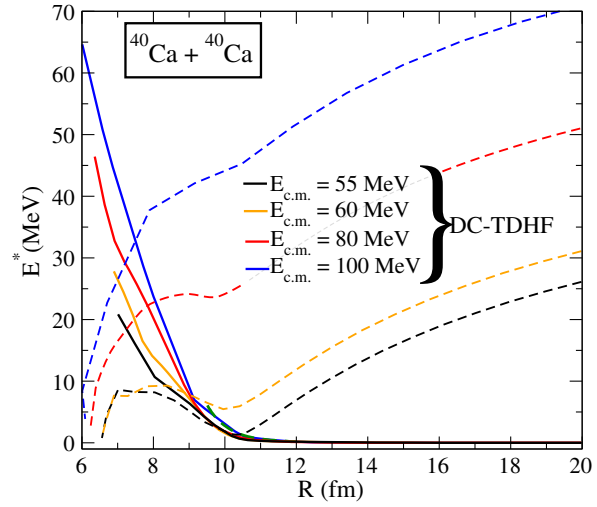

FIG. 8. Excitation energy E^* (solid lines) in Eq. (72) for $^{40}\mathrm{Ca} + {}^{40}\mathrm{Ca}$ collision at different energies. The dashed lines indicate the collective kinetic energy E_{kin} in Eq. (74). From Umar *et al.*, 2009.

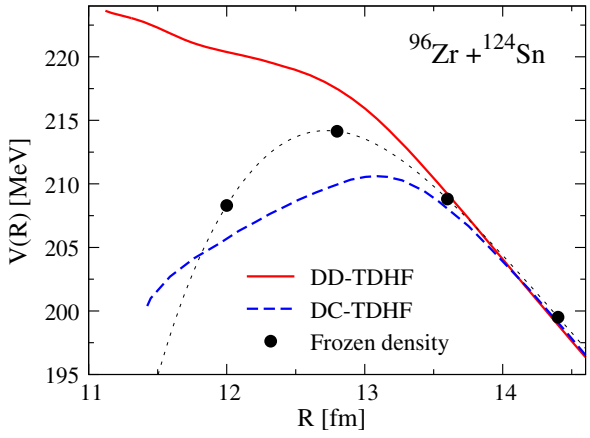

FIG. 9. Internucleus potential for $^{96}\mathrm{Zr} + {}^{124}\mathrm{Sn}$ calculated at $E_{\mathrm{c.m.}} = 230$ MeV. The solid red curve is based on Eq. (75), while the dashed blue line is the one of the density-constrained calculation of Eq. (73). The frozen density potential is plotted by the solid circles. DD-TDHF is an abbreviation for the dissipative-dynamics TDHF. From Washiyama, 2015.

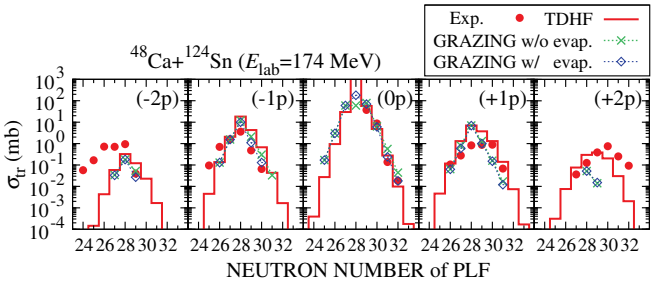

FIG. 10. Transfer cross sections for $^{48}\mathrm{Ca} + {}^{124}\mathrm{Sn}$ reaction at $E_{\mathrm{lab}} = 174$ MeV. The solid red lines show the TDDFT (TDHF) results with the particle-number projection. The experimental data and the GRAZING results are taken from Corradi *et al.* (1997). See text for details. From Sekizawa and Yabana, 2013.

alternative microscopic approach to the low-energy transfer reaction and help our fundamental understanding of the quantum dynamics.

After the real-time simulation at the impact parameter b, the transfer probability $P_{N,Z}(b)$ for each channel of (N, Z) can be calculated according to Eq. (76). Repeating the calculation with different values of b, the cross section $\sigma_{N,Z}$ is calculated as Eq. (77). An example for the $^{48}\mathrm{Ca} + {}^{124}\mathrm{Sn}$ reaction is presented in Fig. 10, showing the production cross sections of Ar $(-2p)$, K $(-1p)$, Ca $(0p)$, Sc $(+1p)$, and Ti $(+2p)$ isotopes. The horizontal axis corresponds to the neutron number of fragments. In the major channels of $0p$ and $\pm 1p$, the experimental data are well reproduced. The calculated mass distribution is rather symmetric with respect to the neutron number around $N = 28$. The experimental data seem to suggest that this symmetry is broken for the $\pm 2p$ channels. In general, the discrepancy becomes more prominent for rarer channels with a large number of exchanged nucleons (Sekizawa and Yabana, 2013). Nevertheless, the quality of the agreement is the same as the GRAZING calculation. It should be noted that the simulation was carried out using the Skyrme SLy5 EDF and there were no free parameters.

As seen in Fig. 10, in the $\pm 2p$ channels, the neutrons tend to move together with the protons, which are not reproduced in the calculation. This is due to the fact that the TDDFT calculation does not have correlations between neutron and proton distributions, namely, $P_{N,Z} = P_N P_Z$. This missing correlation and fluctuation have been studied by Simenel (2011) for $^{40}\mathrm{Ca} + {}^{40}\mathrm{Ca}$ at $E_{\mathrm{c.m.}} = 128$ MeV, using the Balian-Vénéroni formula analogous to Eq. (82). For small impact parameter b, he found a strong correlation between proton and neutron distributions. In addition, the fluctuation of the proton distribution is compared with the available experiment in Fig. 11. The conventional TDDFT simulation significantly underestimates the fluctuation. It is enhanced by Eq. (82) getting closer to the experimental data, although it is not enough for the perfect reproduction.

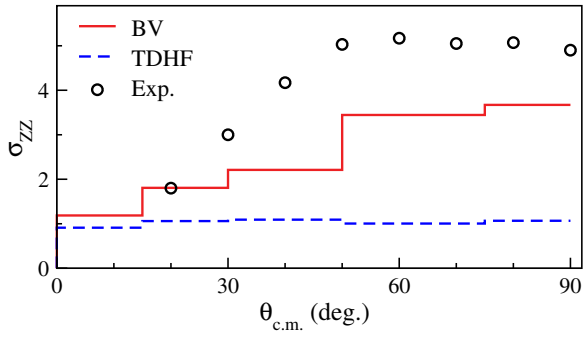

FIG. 11. The fluctuation in the proton number distribution $\sigma_{ZZ} \equiv (\langle Z^2 \rangle - \langle Z \rangle^2)^{1/2}$ for final fragments in the $^{40}\mathrm{Ca} + {}^{40}\mathrm{Ca}$ reaction. The horizontal axis corresponds to the scattering angle that is determined by the impact parameter in the TDDFT (TDHF) calculation. The solid red line shows results based on Eq. (82) to produce larger fluctuations than the dashed blue line (TDDFT). The circles show experimental data (Roynette *et al.*, 1977). From Simenel, 2011.

V. COLLECTIVE SUBMANIFOLD AND REQUANTIZATION OF TDDFT

In this section, we introduce an assumption that the time evolutions of the densities are determined by a few collective coordinates and momenta, $R(q, p)$ as done in Sec. II.E. This leads to a microscopic derivation of the collective Hamiltonian describing large-amplitude collective phenomena. We then quantize the collective variables and obtain the collective Schrödinger equation. Numerical examples are given for low-frequency quadrupole collective excitations which dominate in low-lying states in almost all nuclei. We focus on recent advances and basic ideas of the approaches based on the TDDFT but relations to other time-independent approaches are also briefly discussed.

A. Problems in large-amplitude collective motion

First let us discuss conceptual problems in TDDFT studies beyond the linear regime in nuclear physics. We have presented in Sec. III that excitation energies and transition amplitudes can be obtained in the linear response. For instance, the Fourier analysis on the time evolution of the density, such as Eq. (69), allows us to extract those quantities. In this case, when we scale the external field by a parameter f as $V \to fV$, the density fluctuation $\delta R(\omega)$ is invariant except for the same linear scaling $\delta R(\omega) \to f\delta R(\omega)$. This allows us to uniquely define the transition densities.

In principle, the TDDFT can describe exact dynamics of many-body systems (see Sec. II.D). However, in nuclear EDFs, at least, we do not know in practice how to extract information on excited states and genuine quantum phenomena which involve large-amplitude many-body dynamics. Perhaps, the most typical example is given by spontaneous fission phenomena. Even if the nucleus is energetically favored by dividing it into two fragments, the nonlinearity of the TDDFT forbids the tunneling.

Beyond the linear regime, as the oscillating amplitudes become larger, the nonlinear effects play more important roles. In fact, there are some attempts to quantify the nonlinear coupling strengths between different modes of excitation using real-time TDDFT calculations (Simenel, Chomaz, and de France, 2001, 2007; Simenel and Chomaz, 2003). In addition to the linear response, the quadratic dependence is identified to extract the coupling between dipole and quadrupole modes (Simenel and Chomaz, 2009). Nevertheless, the

practical real-time method to quantify energy spectra of anharmonic vibrations has not been established.

Our strategy for these difficulties is to adopt the "requantization" procedure. Perhaps this is not perfectly consistent with the original principle of TDDFT which should be "exact" and does not require additional quantum fluctuation in the theory. However, as noted in Secs. I.C and II.B.2, since the present nuclear EDF is reliable within a certain time scale (typically the SSB time scale), the quantum fluctuations associated with longer time scales should be addressed additionally. The TDDFT dynamics of Eq. (33) can be parametrized with classical canonical variables (ξ^α, π_α) which obey the classical Hamilton equations (Blaizot and Ripka, 1986). The space spanned by these variables is called the "TDHFB phase space," whose dimension is twice the number of two-quasiparticle pairs. Therefore, in nuclear physics, the issue has been often discussed in terms of the requantization of the TDDFT dynamics. Further arguments on the requantization are given by the stationary phase approximation to the functional integral formulation of the many-body quantum theory (Negele, 1982).

To describe long time-scale slow motion in nuclei, we introduce a small number of collective variables. In low-energy spectra in nuclei, we observe a number of states which possess properties very difficult to quantify with the real-time TDDFT simulations; for instance, states with fluctuating shapes, those with a mixture of different shapes, the anharmonic nature of many-phonon states, or quasirotational spectra which show features between vibrational and rotational excitations. Nuclear fission also provides another typical example of nuclear large-amplitude collective motion. These low-energy dynamics in nuclei requires us to develop practical theories applicable to nuclear large-amplitude collective motion (LACM).

B. Fundamental concepts for low-energy nuclear dynamics and historical remarks

In Sec. III, we present the QRPA method, as a small-amplitude approximation of the TDDFT, for microscopically describing various kinds of collective excitations around the equilibrium points, given by $[H_{\rm eff}[R_0] - \mu\mathcal{N}, R_0] = 0$. In Sec. V, we review the recent advances of the approaches aiming at microscopic description of LACM by extending the basic ideas of the QRPA to nonequilibrium states far from the local minima of the EDF. Construction of microscopic theory of LACM has been a difficult long-standing subject in nuclear structure theory. The issues in the 1980s were discussed in a proceedings (Abe and Suzuki, 1983), including the one by Villars (1983), which summarized problems and questions for theories of nuclear collective motion. Since then, we have achieved a significant progress in theoretical formulation and applications to real nuclear phenomena in recent years.

1. Basic ideas

The basic idea for constructing, on the basis of the time-dependent density-functional method, a microscopic theory of large-amplitude collective phenomena (at zero temperature) is to introduce an assumption that time evolution of the density is determined by a few collective coordinates $q(t) = \{q_1(t), q_2(t), \ldots, q_f(t)\}$ and collective momenta $p(t) = \{p_1(t), p_2(t), \ldots, p_f(t)\}$. We assume that the time-dependent density can be written as $R(t) = R(q(t), p(t))$. At this stage, p and q are introduced as parameters in place of the time t. We shall see, however, that it is possible to formulate a theory such that they are canonical variables obeying the Hamilton equations of motion, i.e., they are classical dynamical variables. Accordingly, we call them "collective variables." The great merit of this approach is that they are readily quantized, according to the standard canonical quantization. In this way, we can derive, microscopically and self-consistently, the quantum collective Hamiltonian describing LACM. Because of developments in the nuclear-theory history, we call this canonical quantization procedure a "collective quantization of time-dependent self-consistent mean field." In the TDDFT terminology, this can be regarded as the inclusion of missing correlations in long time scales. In Sec. V.C, we develop this idea in a more concrete form.

Notes on terminology and notation.—Because of these practical and historical reasons, it is customary to use the terminology and the notation of mean-field theories, such as TDHF and TDHFB instead of TDDFT (TDKS, TDBdGKS). We follow this tradition in this section. The theory presented here takes account of correlations and fluctuations beyond the mean field, which correspond to those missing in current nuclear EDFs.

In order to help comprehensibility, we introduce the TDHF(B) state $|\phi(t)\rangle$ in Sec. V.C, which is defined by the quasiparticle vacuum $a_i(t)|\phi(t)\rangle = 0$ at every time t [time-dependent version of Eq. (12)]. Accordingly, we also use the Hamiltonian $\hat{H}$ which is related to the EDF as $E[\rho] = \langle\phi(t)|\hat{H}|\phi(t)\rangle$.

2. ANG modes associated with broken symmetries and quantum fluctuations in finite systems

We discussed in Sec. II.E.2 how to treat the collective motions restoring the symmetries spontaneously broken in the mean fields for three typical examples (center-of-mass motion, pair rotation in gauge space, and three-dimensional rotation in coordinate space). Let us recall, in particular:

(1) The ANG modes restoring the gauge invariance broken in the BCS theory of superconductivity have been experimentally observed in nuclei as the pairing rotational modes (Brink and Broglia, 2005).
(2) The rotational spectra widely seen in nuclei can be regarded as ANG modes restoring the spherical symmetry spontaneously broken in the mean field (Alder *et al.*, 1956; Bohr and Mottelson, 1975; Frauendorf, 2001).
(3) We know generators of the collective variables for the ANG modes, at least for the ones of $\mathring{Q}$ and $\mathring{P}$ in Sec. II.E. Those are given by global one-body operators, such as the center-of-mass coordinate and the momentum for the translation, the angular momentum for the rotation, and the particle number for the pair rotation. However, the generators conjugate to the angular momentum and the particle number are not trivial.

On the other hand, we should keep in mind that the mean fields of finite quantum systems always accompany quantum

fluctuations. One of the most important characteristics of low-energy excitation spectra of nuclei is that the amplitudes of the quantum shape fluctuation often become very large. Among large-amplitude shape fluctuation phenomena, we should, of course, refer to the well-known spontaneous fission, which can be regarded as macroscopic quantum tunnelings through the potential barrier generated by the self-consistent mean field. To construct a microscopic theory capable of describing such large-amplitude shape fluctuations and evolutions has been a challenge in nuclear structure theory. Historically, such attempts started in the 1950s to formulate a microscopic theory of a collective model of Bohr and Mottelson. The major approach at that time is to introduce collective coordinates explicitly as functions of coordinates of individual nucleons and separate collective shape degrees of freedom from the rest [see, e.g., Tomonaga (1955)]. This turned out to fail in the description of low-energy modes of shape fluctuations. One of the important lessons we learned from these early attempts is that, in contrast to the ANG modes, it is not trivial at all to define the microscopic structure of collective coordinates appropriate for low-energy shape vibrations. The low-energy collective vibrations are associated with fluctuations of order parameters characterizing the mean field (Stringari, 1979). In this sense, it may be categorized as a kind of Higgs amplitude mode (Pekker and Varma, 2015), but we need to go beyond the small-amplitude approximation for fluctuations about the equilibrium points in order to describe them.

After the initial success of the BCS + QRPA approach for small-amplitude oscillations in the 1960s, attempts to construct a microscopic theory of LACM started in the mid-1970s. At that time, real-time TDHF (TDDFT) calculations for heavy-ion collisions also started, using semirealistic EDFs. These attempts introduced collective coordinates as parameters specifying the time evolution of the self-consistent mean field, instead of explicitly defining them as functions of coordinates of individual nucleons. This was a historical turning point in the basic concept of collective coordinate theory: In these new approaches, it is unnecessary to define *global* collective operators as functions of coordinates of individual nucleons. As we shall see in Sec. V.C, it is sufficient to determine infinitesimal generators for the time evolution of the self-consistent mean field, locally at every point of the collective variables (q, p). Note that we use, in this section, the term *local* to indicate the neighbor of a point (q, p) in the collective space, instead of the conventional coordinate $\vec{r}$ in the three-dimensional coordinate space. In general, the microscopic structures of the infinitesimal generators for shape evolution may change as functions of (q, p). From this point of view, it is not only unnecessary but also inappropriate to introduce the global operators in order to describe low-energy shape fluctuations. This is in sharp contrast with the high-frequency giant quadrupole resonances for which the small-amplitude approximation works well and the mass-quadrupole operator can be regarded as an approximate collective coordinate operator.

3. Characteristics of quadrupole excitation spectra in low-lying states

Low-frequency quadrupole vibrations of the nucleus may be regarded as collective surface excitations of a finite superfluid system. Accordingly, pairing correlations and varying shell structure of the self-consistent mean field play essential roles in their emergence (Bohr and Mottelson, 1975; Åberg, Flocard, and Nazarewicz, 1990; Bender, Heenen, and Reinhard, 2003; Rowe and Wood, 2010; Matsuyanagi, Hinohara, and Sato, 2013). For nuclei in the transitional region from spherical to deformed, amplitudes of quantum shape fluctuation remarkably increase. This corresponds to soft modes of the quantum phase transition toward symmetry-violating equilibrium deformations of the mean filed. The gain in binding energies due to the symmetry breaking is comparable in magnitude to the vibrational zero-point energies. The transitional region is prevalent in the nuclear chart, and those nuclei exhibit a rich variety of excitation spectra in systematics.

In finite quantum systems such as nuclei, the rotational ANG modes may couple rather strongly with quantum shape fluctuation modes. For instance, even when the self-consistent mean field acquires a deep local minimum at a finite value of β, the nucleus may exhibit a large-amplitude shape fluctuation in the γ degree of freedom, if the deformation potential is flat in this direction. Here, as usual, β and γ represent the magnitudes of axially symmetric and asymmetric quadrupole deformations, respectively. Such a situation is widely observed in experiments and called γ-soft nuclei. The rotational degrees of freedom about three principal axes are all activated once the axial symmetry is dynamically broken due to the quantum shape fluctuation. Consequently, rotational spectra in such γ-soft nuclei do not exhibit a simple $I(I+1)$ pattern. Such an interplay of the shape fluctuation and rotational modes may be regarded as a characteristic feature of finite quantum systems and provides an invaluable opportunity to investigate the process of the quantum phase transition through the analysis of quantum spectra.

Thus, we need to treat the two kinds of collective variables, i.e., those associated with the symmetry-restoring ANG modes and those for quantum shape fluctuations, in a unified manner to describe low-energy excitation spectra of nuclei.

C. Microscopic derivation of collective Hamiltonian

1. Extraction of collective submanifold

As mentioned in Sec. V.A, the TDHFB dynamics is represented as the classical Hamilton equations for canonical variables in the TDHFB phase space (ξ^α, π_α) (Negele, 1982; Yamamura and Kuriyama, 1987; Kuriyama *et al.*, 2001). The dimension of this phase space is large, $\alpha = 1, \ldots, D$, where D is the number of all the two-quasiparticle pairs. The TDHFB state vector $|\phi(t)\rangle = |\phi(\xi(t), \pi(t))\rangle$ is regarded as a generalized coherent state moving on a trajectory in the TDHFB phase space. For low-energy fluctuations in collective motion, however, we assume that the time evolution is governed by a few collective variables.

During the attempts to construct microscopic theory of LACM since the latter half of the 1970s, significant progress has been achieved in the fundamental concepts of collective motion. Especially important is the recognition that microscopic derivation of the collective Hamiltonian is equivalent to extraction of a collective submanifold embedded in the

TDHFB phase space, which is approximately decoupled from other "noncollective" degrees of freedom. From this point of view we can say that collective variables are nothing but local canonical variables which can be flexibly chosen on this submanifold. Here we recapitulate recent developments achieved on the basis of such concepts.

Attempts to formulate a LACM theory without assuming adiabaticity of large-amplitude collective motion were initiated by Rowe and Bassermann (1976) and Marumori (1977) and led to the formulation of the self-consistent collective coordinate (SCC) method (Marumori *et al.*, 1980). In these approaches, collective coordinates and collective momenta are treated on the same footing. In the SCC method, basic equations determining the collective submanifold are derived by requiring maximal decoupling of the collective motion of interest from other noncollective degrees of freedom. The collective submanifold is invariant with respect to the choice of the coordinate system, whereas the collective coordinates depend on it. The idea of coordinate-independent theory of collective motion was also developed by Rowe (1982) and Yamamura and Kuriyama (1987). This idea gave a significant impact on the fundamental question, "what are the collective variables?" The SCC method was first formulated for the canonical form of the TDHF without pairing. Later, it was extended to that of TDHFB for describing nuclei with superfluidity (Matsuo, 1986).

In the SCC method, the TDHFB state $|\phi(t)\rangle$ is written as $|\phi(q,p)\rangle$ under the assumption that the time evolution is governed by a few collective coordinates $q=(q^1,q^2,\ldots,q^f)$ and collective momenta $p=(p_1,p_2,\ldots,p_f)$. Note that parametrizing the TDHFB state with the $2f$ degrees of freedom (q,p) is nothing but defining a submanifold inside the TDHFB phase space (ξ^α,π_α), which we call a "collective submanifold." The time-dependent densities are readily obtained from the TDHFB state $|\phi(q,p)\rangle$ by

$$\rho(\vec{r};q,p)=\sum_\sigma\langle\phi(q,p)|\hat{\psi}^\dagger(\vec{r}\sigma)\hat{\psi}(\vec{r}\sigma)|\phi(q,p)\rangle,$$
$$\kappa(\vec{r};q,p)=\langle\phi(q,p)|\hat{\psi}(\vec{r}\downarrow)\hat{\psi}(\vec{r}\uparrow)|\phi(q,p)\rangle.$$

The following basic equations determine the TDHFB state $|\phi(q,p)\rangle$ parametrized by (q,p) and its time evolution, which gives the definition of the submanifold.

Invariance principle of the TDHFB equation: We require that the TDHFB equation of motion is invariant in the collective submanifold. This requirement can be written in a variational form as

$$\delta\langle\phi(q,p)|\left\{i\frac{\partial}{\partial t}-\hat{H}\right\}|\phi(q,p)\rangle=0. \tag{83}$$

Here the variation δ is given by $\delta|\phi(q,p)\rangle=a_i^\dagger a_j^\dagger|\phi(q,p)\rangle$ in terms of the quasiparticle operators $\{a_i^\dagger,a_j\}$, which satisfy the vacuum condition $a_i|\phi(q,p)\rangle=0$. Under the basic assumption, the time derivative is replaced by

$$\frac{\partial}{\partial t}=\sum_{i=1}^f\left(\dot{q}^i\frac{\partial}{\partial q^i}+\dot{p}_i\frac{\partial}{\partial p_i}\right)=\dot{q}^i\frac{\partial}{\partial q^i}+\dot{p}_i\frac{\partial}{\partial p_i}.$$

Hereafter, to simplify the notation, we adopt the Einstein summation convention to remove $\sum_{i=1}^f$. Accordingly, Eq. (83) is rewritten as

$$\delta\langle\phi(q,p)|\{\dot{q}^i\mathring{P}_i(q,p)-\dot{p}_i\mathring{Q}^i(q,p)-\hat{H}\}|\phi(q,p)\rangle=0 \tag{84}$$

in terms of the local infinitesimal generators defined by

$$\mathring{P}_i(q,p)|\phi(q,p)\rangle=i\frac{\partial}{\partial q^i}|\phi(q,p)\rangle, \tag{85}$$

$$\mathring{Q}^i(q,p)|\phi(q,p)\rangle=-i\frac{\partial}{\partial p_i}|\phi(q,p)\rangle. \tag{86}$$

These are one-body operators that can be written as linear combinations of bilinear products $\{a_i^\dagger a_j^\dagger,a_i^\dagger a_j,a_ja_i\}$ of the quasiparticle operators defined with respect to $|\phi(q,p)\rangle$. Equations (84), (85), and (86) correspond to Eqs. (40), (41), and (42) in Sec. II.E, respectively.

Canonicity conditions: We require q and p to be canonical variables. According to the theorem of Frobenius and Darboux (Arnold, 1989), pairs of canonical variables (q,p) exist for the TDHFB states $|\phi(q,p)\rangle$ satisfying the following *canonicity conditions*:

$$\langle\phi(q,p)|\mathring{P}_i(q,p)|\phi(q,p)\rangle=p_i+\frac{\partial S}{\partial q^i}, \tag{87}$$

$$\langle\phi(q,p)|\mathring{Q}^i(q,p)|\phi(q,p)\rangle=-\frac{\partial S}{\partial p_i}, \tag{88}$$

where S is an arbitrary differentiable function of q and p (Marumori *et al.*, 1980; Yamamura and Kuriyama, 1987). By specifying S we can fix the type of allowed canonical transformations among the collective variables (q,p). We discuss typical examples in subsequent sections and call the canonicity conditions with a specified function S *canonical-variable conditions*. Taking derivatives of Eqs. (87) and (88) with respect to p_i and q^i, respectively, we can readily confirm that the local infinitesimal generators satisfy the "weakly" canonical commutation relations,

$$\langle\phi(q,p)|[\mathring{Q}^i(q,p),\mathring{P}_j(q,p)]|\phi(q,p)\rangle=i\delta_{ij}.$$

Taking variations of Eq. (84) in the direction of the collective variables q and p, generated by $\mathring{P}_i$ and $\mathring{Q}^i$, we obtain the Hamilton equations of motion,

$$\frac{dq^i}{dt}=\frac{\partial\mathcal{H}}{\partial p_i},\qquad\frac{dp_i}{dt}=-\frac{\partial\mathcal{H}}{\partial q^i}. \tag{89}$$

Here the total energy $\mathcal{H}(q,p)\equiv\langle\phi(q,p)|\hat{H}|\phi(q,p)\rangle$ plays the role of the classical collective Hamiltonian.

Equation of collective submanifold: The invariance principle (84) and Eq. (89) lead to the following equation of collective submanifold:

$$\delta\langle\phi(q,p)|\left\{\hat{H}-\frac{\partial\mathcal{H}}{\partial p_i}\overset{\circ}{P}_i(q,p)-\frac{\partial\mathcal{H}}{\partial q^i}\overset{\circ}{Q}{}^i(q,p)\right\}|\phi(q,p)\rangle=0. \tag{90}$$

Taking variations $\delta_\perp$ in the directions orthogonal to q and p, we can immediately find $\delta_\perp\langle\phi(q,p)|\hat{H}|\phi(q,p)\rangle=0$. This implies that the energy expectation value is stationary with respect to all variations except for those along directions tangent to the collective submanifold. In other words, the large-amplitude collective motion is decoupled from other modes of excitation.

2. Solution with (η,η^*) expansion

In the original paper of the SCC method (Marumori *et al.*, 1980), the TDHFB state $|\phi(q,p)\rangle$ is written as

$$|\phi(q,p)\rangle=U(q,p)|\phi_0\rangle=e^{i\hat{G}(q,p)}|\phi_0\rangle.$$

Here $U(q,p)$ represents a time-dependent unitary transformation from the HFB ground state $|\phi_0\rangle$ taken as an initial state; $U(q,p)=1$ at $q=p=0$. It is written in terms of an Hermitian one-body operator $\hat{G}(q,p)$.

With use of complex variables $\eta=(\eta_1,\eta_2,\ldots,\eta_f)$ defined by

$$\eta_i=\frac{1}{\sqrt{2}}(q^i+ip_i),\qquad \eta_i^*=\frac{1}{\sqrt{2}}(q^i-ip_i),$$

we can rewrite the TDHFB state as

$$|\phi(\eta,\eta^*)\rangle=U(\eta,\eta^*)|\phi_0\rangle=e^{i\hat{G}(\eta,\eta^*)}|\phi_0\rangle.$$

Correspondingly, we define local infinitesimal generators $\overset{\circ}{O}{}_i^\dagger(\eta,\eta^*)$ and $\overset{\circ}{O}_i(\eta,\eta^*)$ by

$$\overset{\circ}{O}{}_i^\dagger(\eta,\eta^*)|\phi(\eta,\eta^*)\rangle=\frac{\partial}{\partial\eta_i}|\phi(\eta,\eta^*)\rangle,$$
$$\overset{\circ}{O}_i(\eta,\eta^*)|\phi(\eta,\eta^*)\rangle=-\frac{\partial}{\partial\eta_i^*}|\phi(\eta,\eta^*)\rangle.$$

Replacing (q,p) by (η,η^*), the equation of collective submanifold (90) is rewritten as

$$\delta\langle\phi_0|U^\dagger(\eta,\eta^*)\left\{\hat{H}-\frac{\partial\mathcal{H}}{\partial\eta_i^*}\overset{\circ}{O}{}_i^\dagger(\eta,\eta^*)-\frac{\partial\mathcal{H}}{\partial\eta_i}\overset{\circ}{O}_i(\eta,\eta^*)\right\}\times U(\eta,\eta^*)|\phi_0\rangle=0. \tag{91}$$

Here the variation is to be performed only for the HFB ground state $|\phi_0\rangle$.

We assume the following canonical-variable conditions:

$$\langle\phi(\eta,\eta^*)|\overset{\circ}{O}{}_i^\dagger(\eta,\eta^*)|\phi(\eta,\eta^*)\rangle=\frac{1}{2}\eta_i^*, \tag{92}$$

$$\langle\phi(\eta,\eta^*)|\overset{\circ}{O}_i(\eta,\eta^*)|\phi(\eta,\eta^*)\rangle=\frac{1}{2}\eta_i, \tag{93}$$

which are obtained by a specific choice of

$$S=-\frac{1}{2}\sum_i q^i p_i$$

in the canonicity conditions (87) and (88). From Eqs. (92) and (93), we can easily obtain the "weak" boson commutation relations,

$$\langle\phi(\eta,\eta^*)|[\overset{\circ}{O}_i(\eta,\eta^*),\overset{\circ}{O}{}_j^\dagger(\eta,\eta^*)]|\phi(\eta,\eta^*)\rangle=\delta_{ij}.$$

Because only linear canonical transformations among η and η^* keep Eqs. (92) and (93) invariant, these canonical-variable conditions are suitable for a solution of the variational equation (91) with a power-series expansion of $\hat{G}$ with respect to (η,η^*),

$$\hat{G}(\eta,\eta^*)=\hat{G}_i^{(10)}\eta_i^*+\hat{G}_i^{(01)}\eta_i+\hat{G}_{ij}^{(20)}\eta_i^*\eta_j^*+\hat{G}_{ij}^{(11)}\eta_i^*\eta_j+\hat{G}_{ij}^{(02)}\eta_i\eta_j+\cdots.$$

Requiring that the variational principle (91) holds for every power of (η,η^*), we can successively determine the one-body operator $\hat{G}^{(m,n)}$ with $m+n=1,2,3,\ldots$. This method of solution is called the "(η,η^*)-expansion method." Because (η,η^*) are complex canonical variables, they are replaced by boson operators after the canonical quantization. The lowest linear order corresponds to the QRPA. Accordingly, the collective variables (η_i,η_i^*) correspond to a specific QRPA mode in the small-amplitude limit. However, in the higher orders, the microscopic structure of $\hat{G}$ changes as a function of (η,η^*) due to the mode-mode coupling effects among different QRPA modes. In this sense, the (η,η^*)-expansion method may be regarded as a dynamical extension of the boson expansion method (Matsuo and Matsuyanagi, 1985a). Thus, the SCC method with the (η,η^*) expansion is a powerful method of treating anharmonic effects to the QRPA vibrations originating from mode-mode couplings. This is shown in its application to the two-phonon states of anharmonic γ vibration (Matsuo, Shimizu, and Matsuyanagai, 1985; Matsuo and Matsuyanagi, 1985b). The SCC method was also used for derivation of the 5D collective Hamiltonian and analysis of the quantum phase transition from spherical to deformed shapes (Yamada, 1993) and for constructing diabatic representation in the rotating shell model (Shimizu and Matsuyanagi, 2001). The validity of the canonical quantization procedure, including a treatment of the ordering ambiguity problem, was examined by Matsuo and Matsuyanagi (1985a).

3. Solution with adiabatic expansion

The (η,η^*) expansion about a single HFB equilibrium point is not suitable for treating situations where a few local minima energetically compete in the HFB potential energy surface. It is also difficult to apply the expansion method to a collective motion which goes far away from the equilibrium, such as nuclear fission. These low-energy LACMs in nuclei are often characterized by slow motion. For describing adiabatic LACM

extending over very far from the HFB equilibrium, a new method of solution was proposed (Matsuo, Nakatsukasa, and Matsuyanagi, 2000). In this method, the basic equations of the SCC method are solved by an expansion with respect to the collective momenta, keeping full orders in the collective coordinates. It is called the "adiabatic SCC (ASCC) method." Similar methods have also been developed by Klein, Walet, and Dang (1991) and Almehed and Walet (2004).

A microscopic theory for adiabatic LACM is constructed by the ASCC method in the following way. We assume that the TDHFB state $|\phi(q,p)\rangle$ can be written in the form

$$|\phi(q,p)\rangle = \exp\{ip_i\hat{Q}^i(q)\}|\phi(q)\rangle, \tag{94}$$

where $\hat{Q}^i(q)$ are one-body operators corresponding to infinitesimal generators of p_i locally defined at the state $|\phi(q)\rangle$ which represents a TDHFB state $|\phi(q,p)\rangle$ at $p\to 0$. This state $|\phi(q)\rangle$ is called a "moving-frame HFB state"; see Fig. 12 for illustrations. We use the canonical-variable conditions different from Eqs. (92) and (93),

$$\langle\phi(q,p)|\mathring{P}_i(q,p)|\phi(q,p)\rangle = p_i, \tag{95}$$

$$\langle\phi(q,p)|\mathring{Q}^i(q,p)|\phi(q,p)\rangle = 0, \tag{96}$$

which are obtained by putting $S=$ const in the canonicity conditions (87) and (88). Because Eqs. (95) and (96) are invariant only against point transformations $q\to q'(q)$ (more generally, similarity transformations), which do not mix p and q, these canonical-variable conditions are suitable for the adiabatic expansion with respect to the collective momenta p.

We insert this form of the TDHFB state (94) into the equation of collective submanifold (91) and the canonical-variable conditions (95) and (96) and make a power-series expansion in p. We can determine the microscopic structures of $\hat{Q}^i(q)$ and $|\phi(q)\rangle$ by requiring that these equations hold for every power of p. We take into account up to the second order. The canonical-variable conditions, (95) and (96), then yield the "weakly" canonical commutation relations,

$$\langle\phi(q)|[\hat{Q}^i(q),\hat{P}_j(q)]|\phi(q)\rangle = i\delta_{ij}.$$

We also obtain $\langle\phi(q)|\hat{Q}^i(q)|\phi(q)\rangle = 0$ and $\langle\phi(q)|\hat{P}_i(q)|\phi(q)\rangle = 0$, which are trivially satisfied. Here the displacement operators $\hat{P}_i(q)$ are defined by

$$\hat{P}_i(q)|\phi(q)\rangle = i\frac{\partial}{\partial q^i}|\phi(q)\rangle.$$

Note that $\hat{Q}^i(q)$ and $\hat{P}_i(q)$ operate on $|\phi(q)\rangle$, while $\mathring{Q}^i(q,p)$ and $\mathring{P}_i(q,p)$ operate on $|\phi(q,p)\rangle$. The time derivatives $\dot{q}^i$ and $\dot{p}_i$ are determined by the Hamilton equations of motion (89) with the classical collective Hamiltonian $\mathcal{H}(q,p)$ expanded with respect to p up to the second order,

$$\mathcal{H}(q,p) = V(q) + \frac{1}{2}B^{ij}(q)p_ip_j,$$
$$V(q) = \mathcal{H}(q,p=0), \qquad B^{ij}(q) = \left.\frac{\partial^2\mathcal{H}}{\partial p_i\partial p_j}\right|_{p=0}.$$

The collective inertia tensors $B_{ij}(q)$ are defined as the inverse matrix of $B^{ij}(q)$, $B^{ij}B_{jk}=\delta^i_k$. Under these preparations, the following equations, which constitute the core of the ASCC method, can be derived (Matsuo, Nakatsukasa, and Matsuyanagi, 2000). Here, to further simplify the expression, we show the case for normal systems with TDHF.

Moving-frame HF(B) equation:

$$\delta\langle\phi(q)|\hat{H}_M(q)|\phi(q)\rangle = 0, \tag{97}$$

where $\hat{H}_M(q)$ represents the Hamiltonian in the frame attached to the moving mean field,

$$\hat{H}_M(q) = \hat{H} - \frac{\partial V}{\partial q^i}\hat{Q}^i(q).$$

Moving-frame (Q)RPA equations:

$$\delta\langle\phi(q)|[\hat{H}_M(q),\hat{Q}^i(q)] - \frac{1}{i}B^{ij}(q)\hat{P}_j(q) + \frac{1}{2}\left[\frac{\partial V}{\partial q^j}\hat{Q}^j(q),\hat{Q}^i(q)\right]|\phi(q)\rangle = 0, \tag{98}$$

$$\delta\langle\phi(q)|\left[\hat{H}_M(q),\frac{1}{i}\hat{P}_i(q)\right] - C_{ij}(q)\hat{Q}^j(q) - \frac{1}{2}\left[\left[\hat{H}_M(q),\frac{\partial V}{\partial q^k}\hat{Q}^k(q)\right],B_{ij}(q)\hat{Q}^j(q)\right]|\phi(q)\rangle = 0, \tag{99}$$

where

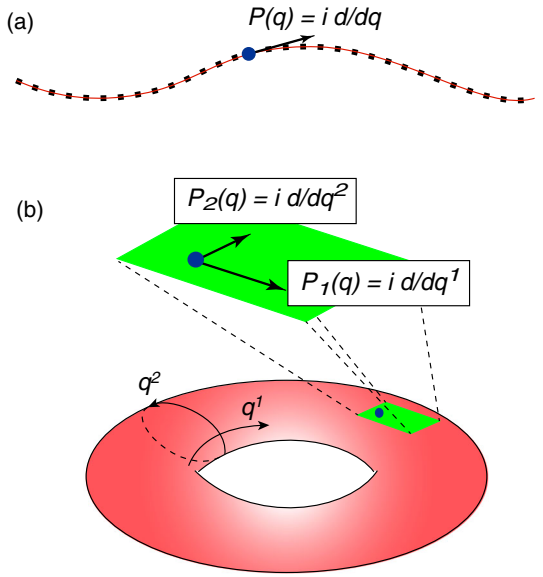

FIG. 12. Schematic illustrations of collective submanifold in the TDHFB space. (a) 1D collective path specified by a series of the states $|\phi(q)\rangle$ with a local generator $P(q)=id/dq$. (b) A section of a 2D collective hypersurface and local generators of the collective coordinate $(\hat{P}_1(q),\hat{P}_2(q))$.

$$C_{ij}(q) = \frac{\partial^2 V}{\partial q^i \partial q^j} - \Gamma^k_{ij}\frac{\partial V}{\partial q^k},$$
$$\Gamma^k_{ij}(q) = \frac{1}{2}B^{kl}\left(\frac{\partial B_{li}}{\partial q^j} + \frac{\partial B_{lj}}{\partial q^i} - \frac{\partial B_{ij}}{\partial q^l}\right).$$

The double-commutator term in Eq. (99) arises from the q derivative of the infinitesimal generators $\hat{Q}^i(q)$ and represents the curvatures of the collective submanifold. Diagonalizing the matrix $B^{ik}C_{kj}$ at each point of q, we may identify the local normal modes and eigenfrequencies $\omega_i(q)$ of the moving-frame QRPA equations.

Extension from TDHF to TDHFB for superfluid nuclei can be achieved by introducing the particle number $n \equiv N - N_0$ and their conjugate angle θ as additional collective variables; see Sec. V.C.4 and Matsuo, Nakatsukasa, and Matsuyanagi (2000) for more details.

Solving Eqs. (97), (98), and (99) self-consistently, we can determine the state $|\phi(q)\rangle$ and the microscopic expressions of the infinitesimal generators $\hat{Q}^i(q)$ and $\hat{P}_i(q)$ in bilinear forms of the quasiparticle creation and annihilation operators defined locally with respect to $|\phi(q)\rangle$; see Fig. 12. Note that these equations reduce to the HF(B) and (Q)RPA equations at the equilibrium point where $\partial V/\partial q^i = 0$. Therefore, they are natural extensions of the HFB-QRPA equations to nonequilibrium states. Here we remark on some key points of the ASCC method.

(1) Difference from the constrained HFB equations: The moving-frame HFB equation (97) resembles the constrained HFB equation. An essential difference is that the infinitesimal generators $\hat{Q}^i(q)$ here are self-consistently determined together with $\hat{P}_i(q)$ as solutions of the moving-frame QRPA equations (98) and (99) at every point of the collective coordinate q. Thus, contrary to constrained operators in the constrained HFB theory, their microscopic structure changes as functions of q. The optimal "constraining" operators are locally determined at each q. The collective submanifold embedded in the TDHFB phase space is extracted in this way.

(2) Meaning of the term "adiabatic": The word "adiabatic approximation" is frequently used with different meanings. In the present context, we use this term for the approximate solution of the variational equation (84) by taking into account up to second order in an expansion with respect to the collective momenta p. It is important to note that the effects of finite frequency of the LACM are taken into account through the moving-frame QRPA equation. No assumption is made, such as the kinetic energy of LACM is much smaller than the lowest two-quasiparticle excitation energy at every point of q.

(3) Collective inertial mass: Although the collective submanifold is invariant against coordinate transformations $q \to q'(q)$, the collective inertial tensors $B_{ij}(q)$ depend on the adopted coordinate system. The scale of the coordinates can be arbitrarily chosen as far as the canonical-variable conditions are satisfied. Note, however, that it is convenient to adopt a conventional coordinate system, such as the quadrupole (β, γ) variables, to obtain physical insights and to find the effects of time-odd components in the mean field (see Sec. V.D.1).

(4) Canonical quantization: The collective inertia tensors $B_{ij}(q)$ take a diagonal form when the classical collective Hamiltonian is represented in terms of the local normal modes of the moving-frame QRPA equations. We can then make a scale transformation of the collective coordinates q such that they become unity. The kinetic energy term in the resulting collective Hamiltonian depends only on p. Thus, there is no ordering ambiguity between q and p in the canonical quantization procedure.

4. Inclusion of the pair rotation and gauge invariance

In the QRPA at the HFB equilibrium, the ANG modes such as the number fluctuation (pairing rotational) modes are decoupled from other normal modes. Thereby, the QRPA restores the gauge invariance (number conservation) broken in the HFB mean field (Brink and Broglia, 2005). It is desirable to keep this nice property beyond the small-amplitude approximation. Otherwise, spurious number fluctuation modes would heavily mix in the LACM of interest. This can be achieved in the SCC method (Matsuo, 1986).

Introducing the number fluctuation $n = N - N_0$ and their conjugate angle θ as additional collective variables, we generalize the TDHFB state (94) to

$$|\phi(q,p,\theta,n)\rangle = e^{-i\theta\hat{N}}|\phi(q,p,n)\rangle,$$
$$|\phi(q,p,n)\rangle = e^{i[p_i\hat{Q}^i(q)+n\hat{\Theta}(q)]}|\phi(q)\rangle,$$

where $\hat{\Theta}(q)$ denotes the infinitesimal generator for the pair-rotation degree of freedom. The state vector $|\phi(q,p,n)\rangle$ may be regarded as an intrinsic state for the pair rotation. In practice, $(\hat{N}, \hat{\Theta}(q))$ should be doubled to treat both neutrons and protons. The extension of the equation for the collective submanifold (84) is straightforward:

$$\delta\langle\phi(q,p,\theta,n)|\left\{i\dot{q}^i\frac{\partial}{\partial q^i} + i\dot{p}_i\frac{\partial}{\partial p_i} + i\dot{\theta}\frac{\partial}{\partial\theta} - \hat{H}\right\}|\phi(q,p,\theta,n)\rangle = 0.$$

Note that $\dot{n} = 0$, because the Hamilton equations for the canonical conjugate pair (n, θ) are

$$\dot{\theta} = \frac{\partial\mathcal{H}}{\partial n}, \qquad \dot{n} = -\frac{\partial\mathcal{H}}{\partial\theta},$$

and the classical collective Hamiltonian $\mathcal{H}(q,p,\theta,n) \equiv \langle\phi(q,p,\theta,n)|\hat{H}|\phi(q,p,\theta,n)\rangle$ does not depend on θ.

Expanding in n as well as p up to the second order, we can determine $\hat{\Theta}(q)$ simultaneously with $\hat{Q}^i(q)$ and $\hat{P}_i(q)$ such that the moving-frame equations become invariant against the rotation of the gauge angle θ.

Hinohara *et al.* (2007) investigated the gauge-invariance properties of the ASCC equations and extended the infinitesimal generators $\hat{Q}^i(q)$ to include quasiparticle creation-annihilation parts in addition to two-quasiparticle creation and annihilation parts. This is the reason why Eqs. (98) and (99) are written in a more general form than those originally given by Matsuo, Nakatsukasa, and Matsuyanagi (2000). The gauge invariance implies that we need to fix the gauge in numerical applications. A convenient procedure of the gauge fixing is discussed by Hinohara *et al.* (2007). A more general consideration on the gauge symmetry is given from a viewpoint of constrained dynamical systems (Sato, 2015).

D. Relations to other approaches

In Sec. V.C, we reviewed the basics of a microscopic theory of LACM focusing on new developments in the ASCC method, achieved after 2000. In this section, we discuss the relations of the above formulation to other approaches to LACM. Typical approaches developed up to 1980 are described in detail in Ring and Schuck (1980), and achievements during 1980–2000 are well summarized by Dang, Klein, and Walet (2000).

1. Constrained HFB + adiabatic perturbation

This method is convenient and widely used in the microscopic description of LACM. The theory is based on the adiabatic assumption that the collective motion is much slower than the single-particle motion (see remarks in Sec. V.C.3). We first postulate a few one-body operators $\hat{F}_i$ corresponding to collective coordinates α^i. The collective potential energy is given by the constrained HFB (or constrained HF + BCS) equations

$$\delta\langle\phi_0(\alpha)|\hat{H}-\mu^i(\alpha)\hat{F}_i|\phi_0(\alpha)\rangle=0,$$
$$\alpha^i=\langle\phi_0(\alpha)|\hat{F}_i|\phi_0(\alpha)\rangle,$$

where $\mu^i(\alpha)$ are the Lagrange multipliers. Then assuming that the frequency of the collective motion is much smaller than the two-quasiparticle energies, we calculate the collective kinetic energy $T_{\rm coll}$ using the adiabatic perturbation theory; $T_{\rm coll}=(1/2)D_{ij}(\alpha)\dot{\alpha}^{i*}\dot{\alpha}^j$, where

$$D_{ij}(\alpha)=2\sum_n\frac{\langle\phi_0(\alpha)|\partial/\partial\alpha^{i*}|\phi_n(\alpha)\rangle\langle\phi_n(\alpha)|\partial/\partial\alpha^j|\phi_0(\alpha)\rangle}{E_n(\alpha)-E_0(\alpha)}$$

are called Inglis-Belyaev cranking masses (Ring and Schuck, 1980). Here $|\phi_0(\alpha)\rangle$ and $|\phi_n(\alpha)\rangle$ represent the ground and two-quasiparticle excited states for a given set of values $\alpha=\{\alpha^i\}$. In most applications, it is simplified furthermore by an assumption that the derivatives of the constrained HFB Hamiltonian with respect to α^i are proportional to $\hat{F}_i$, which leads to

$$D_{ij}(\alpha)=\frac{1}{2}[\mathcal{M}_1^{-1}(\alpha)\mathcal{M}_3(\alpha)\mathcal{M}_1^{-1}(\alpha)]_{ij},$$
$$\mathcal{M}_k(\alpha)_{ij}=\sum_n\frac{\langle\phi_0(\alpha)|\hat{F}_i{}^\dagger|\phi_n(\alpha)\rangle\langle\phi_n(\alpha)|\hat{F}_j|\phi_0(\alpha)\rangle}{[E_n(\alpha)-E_0(\alpha)]^k}.$$

These cranking masses were used in conjunction with phenomenological mean-field models in the study of fission dynamics (Brack *et al.*, 1972). In recent years, it has become possible to carry out such studies using self-consistent mean fields obtained by solving the constrained HFB equations (Baran *et al.*, 2011). The Inglis-Belyaev cranking masses have also been used for low-frequency quadrupole collective dynamics (Libert, Girod, and Delaroche, 1999; Yuldashbaeva *et al.*, 1999; Próchniak *et al.*, 2004; Delaroche *et al.*, 2010). At present, a systematic investigation on low-lying quadrupole spectra is underway in terms of the five-dimensional (5D) collective Hamiltonian (see Sec. V.E.1), which is derived from the relativistic (covariant) density functionals and by using the Inglis-Belyaev cranking formula (Li *et al.*, 2009, 2011; Nikšić *et al.*, 2009; Li, Nikšić, Vretenar, and Meng, 2010; Li, Nikšić, Vretenar, Ring, and Meng, 2010; Nikšić, Vretenar, and Ring, 2011; Fu *et al.*, 2013).

A problem of the Inglis-Belyaev cranking formula is that time-odd mean-field effects are ignored; thus, it underestimates the collective masses (inertial functions) (Dobaczewski and Dudek, 1995). Moving mean fields induce time-odd components that change sign under time reversal. However, the Inglis-Belyaev cranking formula ignores their effects on the collective masses. By taking into account such time-odd corrections to the cranking masses, one can better reproduce low-lying spectra (Hinohara *et al.*, 2012). For rotational moments of inertia, we may estimate the time-odd corrections taking the limit of $\omega_{\rm rot}\to 0$ for the quasistationary solution of Eq. (44). Since this provides about 20%–40% enhancement from the Inglis-Belyaev formula, the similar enhancement factors of 1.2–1.4 have been often utilized for vibrational inertial masses without solid justification. A better treatment of the time-odd mean-field effects is required for describing the masses of collective motion and the effective mass of single-particle motion in a self-consistent manner. For this purpose, it is highly desirable to apply the microscopic theory of LACM in Sec. V.C.3 to the TDDFT with realistic EDFs. At present, however, it remains as a challenge for the future.

2. Adiabatic TDHF theory

Attempts to derive collective Hamiltonian using adiabatic approximation to time evolution of mean fields started in the 1960s (Baranger and Kumar, 1965; Belyaev, 1965). In these pioneer works, the collective quadrupole coordinates (β,γ) were defined in terms of expectation values of the quadrupole operators and the 5D collective Hamiltonian was derived using the pairing plus quadrupole (P + Q) force model (Bes and Sorensen, 1969). During the 1970s this approach was generalized to a theory applicable to any effective interaction. This advanced approach is called the *adiabatic TDHF* (ATDHF) theory (Brink, Giannoni, and Veneroni, 1976; Baranger and Véneroni, 1978; Goeke and Reinhard, 1978).

In the ATDHF theory, the density matrix $\rho(t)$ is written in the following form and expanded as a power series with respect to the collective momentum $\chi(t)$:

$$\rho(t) = e^{i\chi(t)}\rho_0(t)e^{-i\chi(t)}$$
$$= \rho_0(t) + [i\chi, \rho_0] + \tfrac{1}{2}[i\chi, [i\chi, \rho_0]] + \cdots$$
$$= \rho_0(t) + \rho_1(t) + \rho_2(t) + \cdots.$$

Correspondingly, the time-dependent mean-field Hamiltonian $h(t)$ is also expanded with respect to a power of $\chi(t)$,

$$h[\rho(t)] = W_0(t) + W_1(t) + W_2(t) + \cdots.$$

Inserting these into the TDHF (TDKS) equation (35), we obtain for the time-odd part

$$i\dot{\rho}_0 = [W_0, \rho_1] + [W_1, \rho_0],$$

and the time-even part

$$i\dot{\rho}_1 = [W_0, \rho_0] + [W_0, \rho_2] + [W_1, \rho_1] + [W_2, \rho_0].$$

These are the basic equations of the ATDHF.

Let us introduce collective coordinates $\alpha = (\alpha^1, \ldots, \alpha^f)$ as parameters describing the time evolution of the density matrix $\rho_0(t)$ as

$$\rho_0(t) = \rho_0(\alpha(t)), \qquad \dot{\rho}_0(t) = \sum_i \frac{\partial \rho_0}{\partial \alpha^i}\dot{\alpha}^i.$$

Baranger and Vénéroni (1978) proposed iterative procedures to solve the ATDHF equations for the density matrix parametrized in this way, but this idea has not been realized until now. The ATDHF does not reduce to the RPA in the small-amplitude limit if a few collective coordinates are introduced by hand. In fact it gives a collective mass different from that of the RPA (Giannoni and Quentin, 1980a, 1980b).

The ATDHF theory developed by Villars (1977) aims at self-consistently determining optimum collective coordinates on the basis of the time-dependent variational principle. This approach, however, encountered a difficulty so that we cannot get a unique solution of its basic equations determining the collective path. This nonuniqueness problem was later solved by treating the second-order terms of the momentum expansion in a self-consistent manner (Mukherjee and Pal, 1982; Klein, Walet, and Dang, 1991). It was shown that, when the number of collective coordinates is only 1, a collective path maximally decoupled from noncollective degrees of freedom runs along a valley in the multidimensional potential energy surface associated with the TDHF states.

In order to describe low-frequency collective motions, it is necessary to take into account the pairing correlations. Thus, we need to develop the adiabatic TDHFB (ATDHFB) theory. This is one of the reasons why applications of the ATDHF theory have been restricted to collective phenomena where the pairing correlations play minor roles, such as low-energy collisions between spherical closed-shell nuclei (Goeke *et al.*, 1983). When large-amplitude shape fluctuations take place, single-particle level crossings often occur. To follow the adiabatic configuration across the level crossing points, the pairing correlation plays an essential role. Thus, an extension to ATDHFB is indispensable for the description of low-frequency collective excitations.

In the past, Dobaczewski and Skalski (1981) tried to develop the ATDHFB theory assuming the axially symmetric quadrupole deformation parameter β as the collective coordinate. Quite recently, Li *et al.* (2012) tried to derive the 5D quadrupole collective Hamiltonian on the basis of the ATDHFB. However, the extension of ATDHF to ATDHFB is not as straightforward as we naively expect. This is because, as discussed in Sec. V.C.4, we need to decouple the pair-rotational degrees of freedom (number fluctuation) from the LACM of interest.

3. Boson expansion method

The boson expansion method is an efficient microscopic method of describing anharmonic (nonlinear) vibrations going beyond the harmonic approximation of QRPA. In this approach, we first construct a collective subspace spanned by many-phonon states of vibrational quanta (determined by the QRPA) in the huge-dimensional shell-model space. These many-phonon states are mapped onto many-boson states in an ideal boson space. Anharmonic effects neglected in the QRPA are treated as higher-order terms in the power-series expansion with respect to the boson creation and annihilation operators. Starting from the QRPA about a spherical shape, one can thus derive the 5D quadrupole collective Hamiltonian in a fully quantum mechanical manner. The boson expansion method has been successfully applied to low-energy quadrupole excitation spectra in a wide range of nuclei including those lying in transitional regions of quantum phase transitions from spherical to deformed shapes (Sakamoto and Kishimoto, 1988; Klein and Marshalek, 1991).

In the time-dependent mean-field picture, state vectors in the boson expansion method are written in terms of the creation and annihilation operators $(\Gamma_i^\dagger, \Gamma_i)$ of the QRPA eigenmodes, or, equivalently, in terms of the collective coordinate and momentum operators $(\hat{Q}^i, \hat{P}_i)$,

$$|\phi(t)\rangle = e^{i\hat{G}(t)}|\phi_0\rangle,$$
$$i\hat{G}(t) = \eta_i(t)\Gamma_i^\dagger - \eta_i^*(t)\Gamma_i = ip_i(t)\hat{Q}^i - iq^i(t)\hat{P}_i.$$

With increasing amplitudes of the quadrupole shape vibration $|\eta_i(t)|$ $[|q_i(t)|]$, anharmonic (nonlinear) effects become stronger. Strong nonlinear effects may eventually change even the microscopic structure of the collective operators $(\hat{Q}_i, \hat{P}_i)$ determined by the QRPA. In such situations, it is desirable to construct a theory that allows variations of microscopic structure of collective operators as functions of $q_i(t)$. The SCC method has accomplished this task; see Sec. V.C.

4. Generator coordinate method

In the GCM, quantum eigenstates of collective motion are described as superpositions of states $|\phi(\alpha)\rangle$ labeled by the parameters $\alpha = (\alpha^1, \ldots, \alpha^f)$, which are called generator coordinates,

$$|\Psi\rangle = \int d\alpha f(\alpha)|\phi(\alpha)\rangle.$$

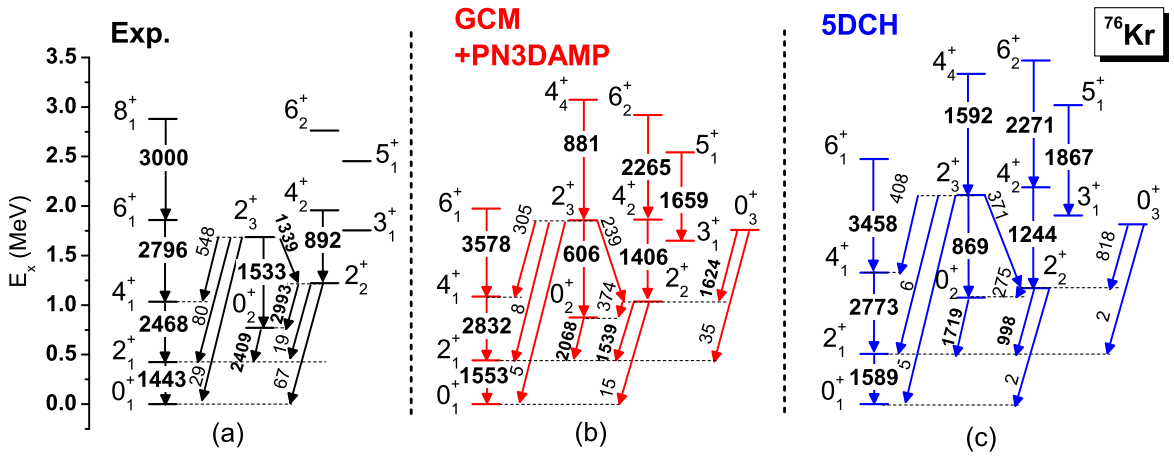

FIG. 13. Low-lying spectra and $B(E2)$ values in e^2 fm^4 for ^{76}Kr; (a) experimental data from Clément *et al.* (2007), (b) the relativistic GCM calculations in the (β,γ) plane with the particle-number and the angular-momentum projections, and (c) the calculation of the 5D collective Hamiltonian using the cranking inertial masses (Sec. V.D.1). From Yao *et al.*, 2014.

$|\phi(\alpha)\rangle$ are generating functions, normally chosen as mean-field states (Slater determinants), which provide a nonorthogonal basis for a collective subspace. The Ritz variational principle then leads to the Hill-Wheeler equation

$$\int d\alpha f^*(\alpha)\langle\phi(\alpha)|\hat{H}-E|\phi(\alpha')\rangle = 0$$

determining the weight function $f(\alpha)$. Here $\int d\alpha$ denotes multiple integration with respect to the f-dimensional generator coordinates, and volume elements of integration are absorbed in the weight function $f(\alpha)$.

The GCM has been used for a wide variety of nuclear collective phenomena (Reinhard and Goeke, 1987; Egido and Robledo, 2004; Bender, 2008; Robledo and Bertsch, 2011; Shimada, Tagami, and Shimizu, 2015). For low-frequency quadrupole collective motion in superfluid nuclei, although the proper generator coordinates are not obvious, a possible choice may be the axial and triaxial deformation parameters (β,γ), and the pairing gaps for neutrons and protons (Δ_n,Δ_p). In addition, to treat the rotational motions associated with spatial and gauge deformations, the analytic solutions of the angular-momentum eigenstates and the number eigenstates are constructed by integration over the Euler angles of rotation $\Omega=(\vartheta_1,\vartheta_2,\vartheta_3)$, and the gauge angles (φ_n,φ_p), respectively. In the major applications at the present time, however, the pairing gaps (Δ_n,Δ_p) are not treated as generator coordinates to reduce the dimensionality of integration. This leads to the following superpositions:

$$|\Psi^i_{NZIM}\rangle = \int d\beta d\gamma \sum_K f^i_{NZIK}(\beta,\gamma)\hat{P}_N\hat{P}_Z\hat{P}_{IMK}|\phi(\beta,\gamma)\rangle,$$

where $\hat{P}_{IMK}$ and $\hat{P}_N$ $(\hat{P}_Z)$ denote projection operators for the angular momentum in the three-dimensional space and the neutron (proton) number, respectively. It has been a great challenge in nuclear structure physics to carry out high-dimensional numerical integrations for solving the GCM equation using the constrained HFB states. In recent years, remarkable progress has been taking place, which makes it possible to carry out large-scale numerical computations (Bender and Heenen, 2008; Rodríguez and Egido, 2010, 2011; Yao *et al.*, 2010, 2011, 2014; Rodríguez, 2014) A recent example is shown in Fig. 13. As discussed in Sec. II, the HFB calculations using the density-dependent effective interactions are better founded by DFT. Correspondingly, the modern GCM calculation is often referred to as *multireference DFT* (Bender and Heenen, 2008).

The GCM is a useful fully quantum approach but the following problems remain to be solved.

(1) Numerical stability: In numerical calculation, one needs to find an optimum discretization (selection of basis) for the generator coordinates α, because the continuum limit of integration is not stable in general (Bonche *et al.*, 1990). It is usually determined semi-empirically but a deeper understanding of its physical basis is desirable. Another problem is a singular behavior that may occur during the symmetry projections in calculations with use of effective interactions that depend on a noninteger power of density. Currently, efforts are underway to overcome this problem (Anguiano, Egido, and Robledo, 2001; Dobaczewski *et al.*, 2007; Duguet *et al.*, 2009).

(2) Necessity of complex coordinates: It is well known that one can derive a collective Schrödinger equation by making a Gaussian overlap approximation (GOA) to the GCM equation (Griffin and Wheeler, 1957; Onishi and Une, 1975; Reinhard and Goeke, 1987; Rohoziński, 2012). There is no guarantee, however, that dynamical effects associated with time-odd components of the moving mean field are sufficiently taken into account in the collective masses (inertial functions) obtained through this procedure. In the case of center-of-mass motion, we need to use complex generator coordinates to obtain the correct mass, implying that collective momenta conjugate to collective coordinates should also be treated as generator coordinates (Peierls and Thouless, 1962; Ring and Schuck, 1980). The GOA with respect to

the momenta leads to a theory very similar to ATDHF (Goeke, Grümmer, and Reinhard, 1983). Realistic applications with complex generator coordinates are so far very few.

(3) Choice of generator coordinates: The most fundamental question is how to choose the optimum generator coordinates. It is desirable to variationally determine the generating functions $|\phi(\alpha)\rangle$ themselves. Let S denote the space spanned by $|\phi(\alpha)\rangle$. The equation determining the space S is then given by

$$\int_S d\alpha f^*(\alpha)\langle\phi(\alpha)|\hat{H}-E|\delta\phi(\alpha')\rangle_\perp = 0, \qquad (100)$$

where $|\delta\phi(\alpha')\rangle_\perp$ denotes a variation perpendicular to the space S. Let us add an adjective "optimum" to the generator coordinate determined by solving the above variational equation. It was shown that the mean-field states parametrized by a single optimum generator coordinate run along a valley of the collective potential energy surface (Holzwarth and Yukawa, 1974). This line of investigation was further developed (Reinhard and Goeke, 1979) and greatly stimulated the challenge toward constructing the microscopic theory of LACM. However, direct applications of Eq. (100) to realistic EDFs may have a problem. As discussed in Sec. V.A, the missing correlations in nuclear EDFs are those in long ranges and long time scales. The variation in Eq. (100) may take into account additional short-range correlations, which could lead to unphysical solutions (Shinohara *et al.*, 2006; Fukuoka *et al.*, 2013).

Finally, we note that conventional GCM calculations parametrized by a few real generator coordinates do not reduce to the (Q)RPA in the small-amplitude limit. It is equivalent to RPA only when all the particle-hole degrees of freedom are treated as complex generator coordinates (Jancovici and Schiff, 1964). An extension to the QRPA is not straightforward either. Thus, systematic comparison of collective inertial masses evaluated by different approximations including the ASCC, the ATDHFB, the GCM + GOA, and the adiabatic cranking methods is desirable for a better understanding of their physical implications.

5. Time-dependent density-matrix theory and higher QRPA

The TDHF theory describes the time evolution of the one-body density matrix $\rho_{ij} = \langle\phi|c_j^\dagger c_i|\phi\rangle$ on the basis of the time-dependent variational principle. To generalize this approach, one may consider, in addition to ρ_{ij}, the time evolution of the two-body correlation matrix $C_{ijkl} = \langle\phi|c_k^\dagger c_l^\dagger c_j c_i|\phi\rangle - \rho_{ik}\rho_{jl} + \rho_{il}\rho_{jk}$. This approach is called the time-dependent density-matrix (TDDM) theory (Shun-jin and Cassing, 1985). The extended RPA (Tohyama and Schuck, 2007) and the second RPA (Drozdz *et al.*, 1990; Gambacurta, Grasso, and Catara, 2011; Gambacurta *et al.*, 2012; Tohyama and Nakatsukasa, 2012) can be derived as approximations to the small-amplitude limit of the TDDM theory (Tohyama and Gong, 1989) and have been used for the analysis of damping mechanisms of giant resonances and anharmonicities of low-frequency vibrations.

In the TDDM theory, the pairing correlations are taken into account by the two-body correlations C_{ijkl}. This requires a large computational cost, however. The TDDM theory using the HFB quasiparticle representations is not available. On the other hand, the higher QRPA may provide another practical approach to its small-amplitude approximation. In the higher QRPA, in addition to the two-quasiparticle creation and annihilation operators in the conventional QRPA, $\Gamma_n^{(2)\dagger} = \sum_{i,j}(\psi_{ij}^{n(2)} a_i^\dagger a_j^\dagger + \varphi_{ij}^{n(2)} a_j a_i)$, equations of motion for four quasiparticle creation and annihilation operators,

$$\Gamma_n^{(4)\dagger} = \sum_{i,j,k,l}(\psi_{ijkl}^{n(4)} a_i^\dagger a_j^\dagger a_k^\dagger a_l^\dagger + \phi_{ijkl}^{n(4)} a_i^\dagger a_j^\dagger a_l a_k + \varphi_{ijkl}^{n(4)} a_l a_k a_j a_i),$$

are derived. This approach may be suitable for describing various mode-mode coupling effects and anharmonicities arising from Pauli-principle effects in two-phonon states where two QRPA vibrational quanta are excited. We note that the $a_i^\dagger a_j^\dagger a_l a_k$ terms in $\Gamma_n^{(4)\dagger}$ are often ignored ($\phi_{ijkl}^{n(4)} = 0$). It is known, however, that collectivities of two-phonon states cannot be well described without these terms, because they are responsible for making the ratio $B(E2; 2\,\text{phonon} \to 1\,\text{phonon})/B(E2; 1\,\text{phonon} \to \text{g.s.}) = 2$ in the harmonic limit (Tamura and Udagawa, 1964). This problem may be overcome by using the quasiparticle new Tamm-Dancoff method (Kanesaki *et al.*, 1973a, 1973b; Sakata, Marumori, and Takada, 1981). In the limit of vanishing pairing correlations, the quasiparticle-pair scattering terms $a_i^\dagger a_j^\dagger a_l a_k$ reduce to the particle-hole-pair scattering terms. Their effects are taken into account in the extended RPA, while they are ignored in the second RPA (Tohyama, 2001).

To our knowledge, no attempt has been made to introduce collective variables and derive collective Hamiltonian on the basis of the TDDM theory.

E. Application to shape coexistence and fluctuation phenomena

1. Five-dimensional quadrupole collective Hamiltonian

Vibrational and rotational motions of the nucleus can be described as the time evolution of a self-consistent mean field. This is the basic idea underlying the unified model of Bohr and Mottelson (Bohr, 1976; Mottelson, 1976). In this approach, the 5D collective Hamiltonian describing the quadrupole vibrational and rotational motions is given by (Bohr and Mottelson, 1975; Próchniak and Rohoziński, 2009)

$$H = T_{\text{rot}} + T_{\text{vib}} + V(\beta,\gamma), \qquad (101)$$

with

$$T_{\text{rot}} = \frac{1}{2}\sum_k \mathcal{J}_k \omega_k^2$$

and

$$T_{\rm vib} = \tfrac{1}{2}D_{\beta\beta}\dot{\beta}^2 + D_{\beta\gamma}\dot{\beta}\dot{\gamma} + \tfrac{1}{2}D_{\gamma\gamma}\dot{\gamma}^2,$$

where ω_k and $\mathcal{J}_k$ in the rotational energy $T_{\rm rot}$ are the three components of the angular velocities and the corresponding moments of inertia, respectively, while $(D_{\beta\beta}, D_{\beta\gamma}, D_{\gamma\gamma})$ in $T_{\rm vib}$ represent the inertial masses of the vibrational motion. Note that $\mathcal{J}_{k=1,2,3}$ and $(D_{\beta\beta}, D_{\beta\gamma}, D_{\gamma\gamma})$ are functions of β and γ. The "deformation parameters" β and γ are treated here as dynamical variables, and $\dot{\beta}$ and $\dot{\gamma}$ represent their time derivatives. They are related to the expectation values of the quadruple operators (with respect to the time-dependent mean-field states) and their variations in time. Note also that they are defined with respect to the principal axes of the body-fixed (intrinsic) frame that is attached to the instantaneous shape of the time-dependent mean field.

In the case that the potential energy $V(\beta,\gamma)$ has a deep minimum at finite value of β and $\gamma = 0°$ (or $\gamma = 60°$), a regular rotational spectrum with the $I(I+1)$ pattern may appear. In addition to the ground band, we expect the β and γ bands to appear, where vibrational quanta with respect to the β and γ degrees of freedom are excited. Detailed investigations on the γ-vibrational bands over many nuclei have revealed, however, that they usually exhibit significant anharmonicities (nonlinearities). The β-vibrational bands are even more mysterious in that they couple, sometimes very strongly, with the pairing-vibrational modes (associated with fluctuations of the pairing gap). Recent experimental data indicate the strong need for a radical review of their characters (Heyde and Wood, 2011).

2. Microscopic derivation of the 5D collective Hamiltonian

For collective submanifolds of two dimensions (2D) or higher, an enormous amount of numerical computation is necessary to find fully self-consistent solutions of the ASCC equations. To handle this problem, a practical approximation scheme, called the "local QRPA" (LQRPA) method, has been developed (Hinohara *et al.*, 2010; Sato and Hinohara, 2011; Sato *et al.*, 2012). This scheme may be regarded as a noniterative solution of Eqs. (97)–(99) without the consistency in the generator $\hat{Q}^i(q)$ between the moving-frame HFB equation and the moving-frame QRPA equations. It may also be regarded as the first step of the iterative procedure for solving the self-consistent equations. Further approximation is that, instead of treating the 5D collective coordinates simultaneously, we first derive the 2D collective Hamiltonian for vibrational motions corresponding to the (β,γ) deformations, and subsequently take into account the three-dimensional (3D) rotational motions associated with Euler angles at each point of (β,γ). With this procedure, we can easily derive the 5D collective Hamiltonian.

First, we solve the moving-frame HFB equation:

$$\delta\langle\phi(q)|\hat{H}_{\rm M}(q)|\phi(q)\rangle = 0,$$
$$\hat{H}_{\rm M}(q) = \hat{H} - \sum_\tau \lambda^{(\tau)}(q)\tilde{N}^{(\tau)} - \sum_{m=0,2}\mu_m(q)\hat{D}^{(+)}_{2m}.$$

This equation corresponds to Eq. (97) for the 2D case with $q = (q^1, q^2)$ and with $\hat{Q}^i(q)$ replaced by the mass-quadrupole operators $\hat{D}^{(+)}_{2m}$. The variables (β,γ) are defined by

$$\beta\cos\gamma = \eta D^{(+)}_{20}(q) = \eta\langle\phi(q)|\hat{D}^{(+)}_{20}|\phi(q)\rangle, \tag{102}$$

$$\frac{1}{\sqrt{2}}\beta\sin\gamma = \eta D^{(+)}_{22}(q) = \eta\langle\phi(q)|\hat{D}^{(+)}_{22}|\phi(q)\rangle, \tag{103}$$

where η is a scaling factor with the dimension of L^{-2}. These equations determine the relation between $q = (q^1, q^2)$ and (β,γ).

Next, we solve the following equations for $i = 1$ and 2:

$$\delta\langle\phi(q)|[\hat{H}_{\rm M}(q), \hat{Q}^i(q)] - \frac{1}{i}B^i(q)\hat{P}_i(q)|\phi(q)\rangle = 0,$$
$$\delta\langle\phi(q)|[\hat{H}_{\rm M}(q), \frac{1}{i}\hat{P}_i(q)] - C_i(q)\hat{Q}^i(q)|\phi(q)\rangle = 0.$$

These are the moving-frame QRPA equations without the curvature terms and are called the LQRPA equations.

Displacement of the quadrupole deformation is related to that of (q_1, q_2) by

$$dD^{(+)}_{2m} = \sum_{i=1,2}\frac{\partial D^{(+)}_{2m}}{\partial q^i}dq^i, \qquad m = 0, 2.$$

Making a scale transformation such that the inertial masses with respect to the collective coordinates (q_1, q_2) become unity and using this relation, we can write the following kinetic energy of vibrational motions in terms of time derivatives of the quadrupole deformation:

$$T_{\rm vib} = \frac{1}{2}\sum_{i=1,2}(\dot{q}^i)^2 = \frac{1}{2}\sum_{m,m'=0,2}M_{mm'}\dot{D}^{(+)}_{2m}\dot{D}^{(+)}_{2m'},$$
$$M_{mm'}(\beta,\gamma) = \sum_{i=1,2}\frac{\partial q^i}{\partial D^{(+)}_{2m}}\frac{\partial q^i}{\partial D^{(+)}_{2m'}}.$$

With Eqs. (102) and (103), it is straightforward to rewrite this expression using the time derivatives of (β,γ).

Subsequently, we solve the LQRPA equations for 3D rotational motions at every point of q. This is given by the replacement of $Q^i(q) \to \hat{\Psi}^k(q)$ and $B^i(q)\hat{P}_i(q) \to \hat{I}_k/\mathcal{J}_k(q)$, where $\hat{\Psi}^k(q)$ represents the local angle operator conjugate to the angular momentum $\hat{I}_k$. The solution provides the moments of inertia $\mathcal{J}_k(\beta,\gamma) = 4\beta^2 D_k(\beta,\gamma)\sin^2(\gamma - 2\pi k/3)$ which determine the rotational masses $D_k(\beta,\gamma)$ and the rotational energy $T_{\rm rot}$.

We can quantize the collective Hamiltonian (101) using the quantization scheme for curvilinear coordinates (the so-called Pauli prescription). The quantized rotational and vibrational Hamiltonians are given, respectively, by

$$\hat{T}_{\rm rot} = \frac{1}{2}\sum_k \hat{I}_k^2/\mathcal{J}_k$$

and

$$\hat{T}_{\rm vib} = \frac{-1}{2\sqrt{WR}}\left\{\frac{1}{\beta^4}\left[\frac{\partial}{\partial\beta}\left(\beta^2\sqrt{\frac{R}{W}}D_{\gamma\gamma}\frac{\partial}{\partial\beta}\right)\right] - \frac{\partial}{\partial\beta}\left(\beta^2\sqrt{\frac{R}{W}}D_{\beta\gamma}\frac{\partial}{\partial\gamma}\right)\right] + \frac{1}{\beta^2\sin 3\gamma}\left[-\frac{\partial}{\partial\gamma}\left(\sqrt{\frac{R}{W}}\sin 3\gamma D_{\beta\gamma}\frac{\partial}{\partial\beta}\right) + \frac{\partial}{\partial\gamma}\left(\sqrt{\frac{R}{W}}\sin 3\gamma D_{\beta\beta}\frac{\partial}{\partial\gamma}\right)\right]\right\} \tag{104}$$

with $\beta^2 W = D_{\beta\beta}D_{\gamma\gamma} - D_{\beta\gamma}^2$ and $R = D_1 D_2 D_3$.

The collective wave functions are written as

$$\Psi_{IMk}(\beta,\gamma,\Omega) = \sum_{K=0}^{I}\Phi_{IKk}(\beta,\gamma)\langle\Omega|IMK\rangle,$$

where $\Phi_{IKk}(\beta,\gamma)$ and $\langle\Omega|IMK\rangle$ represent the vibrational and rotational wave functions, respectively. Solving the collective Schrödinger equations

$$[\hat{T}_{\rm rot} + \hat{T}_{\rm vib} + V(\beta,\gamma)]\Psi_{IMk}(\beta,\gamma,\Omega) = E_{IMk}\Psi_{IMk}(\beta,\gamma,\Omega),$$

we obtain quantum spectra of quadrupole collective motion. Details of the above derivation are given by Hinohara *et al.* (2010) and Matsuyanagi *et al.* (2016).

F. Illustrative examples

The spherical shell structure gradually changes following the deformation of the mean field. If we plot single-particle level diagrams as functions of deformation parameters, significant gaps, called "deformed magic numbers," appear at the Fermi surface for certain deformations. Such deformed shell effects stabilize some deformed shapes of the mean field. Accordingly, in the HFB calculations, we may encounter multiple local minima with different shapes in similar energies. The LACM connecting multiple local minima via tunneling through potential barriers may take place to generate the shape fluctuation. These phenomena may be regarded as a kind of macroscopic quantum tunneling. Note that the barriers are not external fields but self-consistently generated as a consequence of quantum dynamics of the many-body system under consideration. Quantum spectra of low-energy excitation that involve dynamics associated with different shapes have been observed in almost all regions of the nuclear chart (Heyde and Wood, 2011). When different kinds of quantum eigenstates associated with different shapes coexist in the same energy region, we call it "shape coexistence phenomenon." This is the case when shape mixing due to tunneling motion is weak and collective wave functions retain their localization about different equilibrium shapes. On the other hand, if the shape mixing is strong, large-amplitude shape fluctuations extending to different local minima may occur. Next we illustrate these concepts with numerical applications of the LQRPA method to the oblate-prolate shape coexistence and fluctuation phenomena.

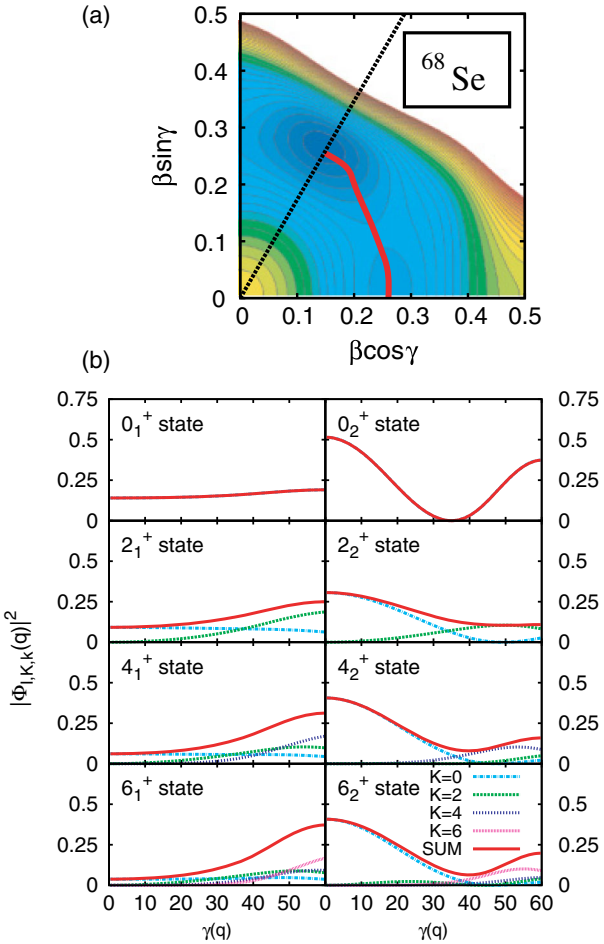

FIG. 14. Application of the ASCC method to the oblate-prolate shape coexistence phenomenon in ^{68}Se. (a) The collective path for ^{68}Se obtained by the ASCC method. The solid (red) line shows the collective path running along the valley of the potential energy surface projected on the (β,γ) deformation plane. (b) Vibrational wave functions squared of the lowest (left) and the second-lowest states (right) for each angular momentum. In each panel, different K components of the vibrational wave functions and the sum of them are plotted as functions of $\gamma(q)$. For excitation spectra, see Fig. 15. Adapted from Hinohara *et al.*, 2009.

Figures 14 and 15 show some results of the application of the ASCC and QRPA methods to the oblate-prolate shape coexistence phenomenon in ^{68}Se. It is clearly seen in Fig. 14 that the collective potential exhibits two local minima corresponding to the oblate and prolate shapes. They are associated with the deformed magic numbers at $N = Z = 34$ appearing for both shapes (Hamamoto, 2012). The valley runs in the triaxially deformed region and the barrier connecting the oblate and prolate minima is low. This is an intermediate situation between the oblate-prolate shape coexistence and the γ-unstable model of Wilets and Jean (1956). In the former, the barrier is high and the mixing of the oblate and prolate shapes is suppressed, while the collective potential is flat with respect to the γ degree of freedom in the latter. The theoretical calculation indicates that large-scale quantum shape fluctuation occurs along the triaxial valley.

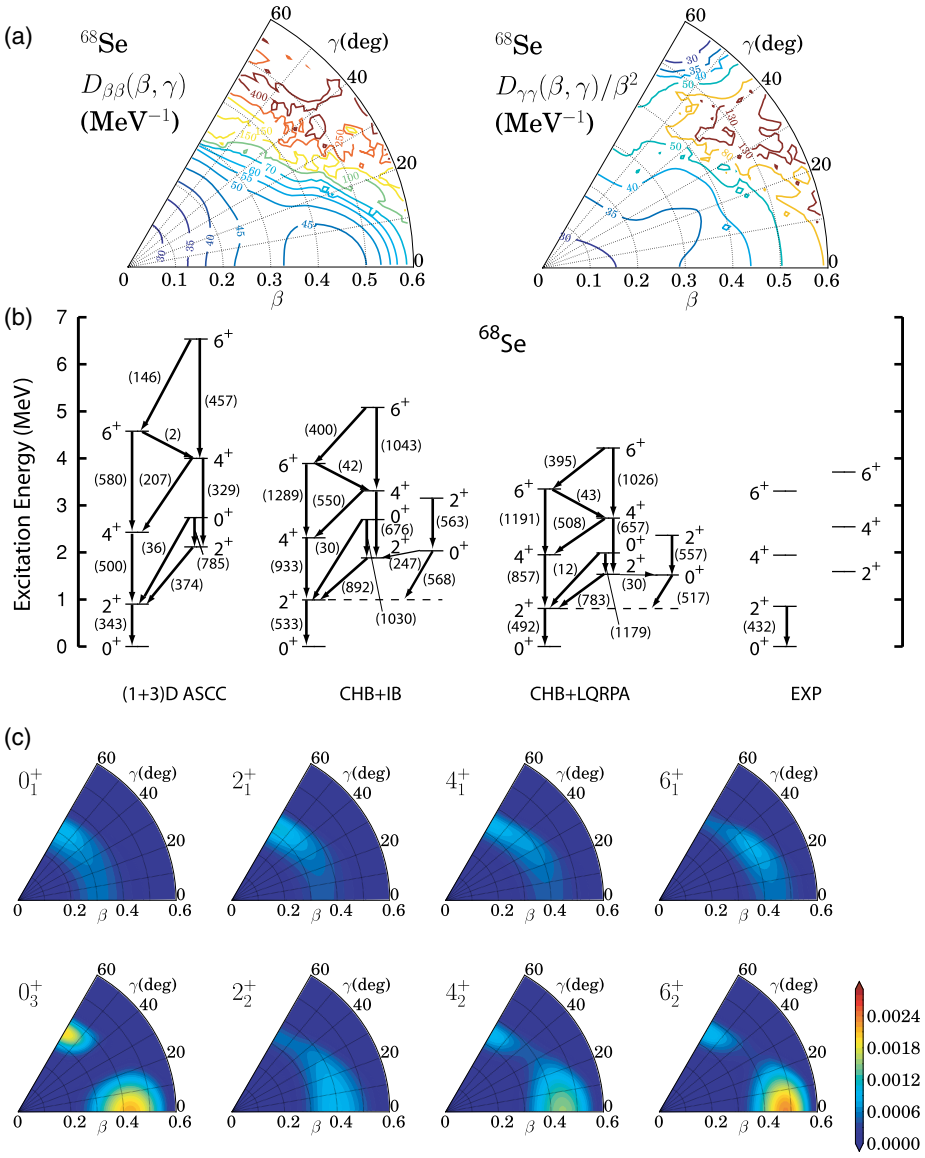

FIG. 15. Application of the LQRPA method to the oblate-prolate shape coexistence and fluctuation phenomenon in ^{68}Se. (a) Collective inertial masses $D_{\beta\beta}(\beta,\gamma)$ and $D_{\gamma\gamma}(\beta,\gamma)$, (b) excitation spectrum, and (c) vibrational wave functions $\beta^4\sum_K|\Phi_{IKk}(\beta,\gamma)|^2$. Adapted from Hinohara *et al.*, 2010.

In Fig. 14, the collective path (one-dimensional collective submanifold) self-consistently determined by solving the ASCC equations (97), (98), and (99) is indicated. The self-consistent collective path runs along the valley to connect the prolate and oblate minima. The inertial mass $B(q)$ is also determined by Eqs. (98) and (99). For the one-dimensional case, properly choosing the scale of the collective coordinate q, one can make $B(q) = B$ constant. The moments of inertia $\mathcal{J}_k(q)$ are calculated by solving the Thouless-Valatin equations at every point on the collective path.

The collective wave functions displayed in Fig. 14(b) are obtained by solving the collective Schrödinger equation for the 4D collective Hamiltonian (the 1D collective path plus 3D rotational degrees of freedom) microscopically derived with the ASCC method (Hinohara *et al.*, 2009). The ground state shows a γ-unstable feature, and accordingly the second 0^+ state also shows strong mixing between the prolate and oblate shapes. However, increasing the angular momentum, the yrast (yrare) band becomes more and more oblate (prolate) dominant. The nuclear shape is localized (stabilized) by the rotation.

In order to confirm that the one-dimensional collective coordinate is enough for the low-energy dynamics of ^{68}Se, it is desirable to find the two-dimensional collective submanifold. This is approximately done according to the LQRPA (Sec. V.E.2), in which the self-consistency between the moving-frame HFB and QRPA equations is ignored, and no iteration is performed. Figure 15 shows the result of the application of the LQRPA method for deriving the 5D collective Hamiltonian (the 2D vibrational and 3D rotational coordinates). The potential $V(\beta,\gamma)$ is shown in Fig. 15(a). The vibrational masses $D_{\beta\beta}(\beta,\gamma)$ and $D_{\gamma\gamma}(\beta,\gamma)$ significantly change as functions of (β,γ). In addition, considerable variation in the (β,γ) plane is also observed in the paring gaps (monopole and quadrupole) and the rotational moments of inertia. Because of the time-odd contributions of the moving HFB self-consistent field, the collective inertial masses (the vibrational masses and the

rotational moments of inertia) calculated with the LQRPA method are larger than those evaluated with the Inglis-Belyaev cranking formula. Their ratios also change as functions of (β, γ) (Hinohara *et al.*, 2010).

A remarkable agreement with experiment is seen in Fig. 15(b). An improvement over the 4D calculation is mostly due to the angular-momentum dependence of the optimal 1D collective path. The calculated collective wave functions in Fig. 15(c) clearly indicate the importance of the fluctuation with respect to the γ degree of freedom, which is consistent with the 1D collective path shown in Fig. 14. However, this path gradually shifts to larger β with increasing angular momentum. This stretching effect is missing in the 4D calculation.

VI. RELATION TO TDDFT IN ELECTRONIC SYSTEMS

DFT and TDDFT have been extensively applied to electronic systems, matters composed of electrons and nuclei such as atoms, molecules, nanomaterials, and solids (Parr and Yang, 1989; Dreizler and Gross, 1990; Koch and Holthausen, 2001; Martin, 2004; Sholl and Steckel, 2009; Gross and Maitra, 2012; Ullrich, 2012). Electrons in matters always need treatment by quantum mechanics, and nuclear motions can be in most cases treated by classical mechanics. In this section, we discuss DFT and TDDFT for electrons in matters, stressing similarities with and differences from nuclear DFT.

An apparent difference between electronic and nuclear systems is the interaction. The Hamiltonian of electronic systems is composed of the attractive one-body Coulomb potential between electrons and nuclei and the repulsive Coulomb interaction among electrons. Besides the difference in the interaction, the researchers in the two fields have different concepts on the DFT and TDDFT. We first discuss these conceptual differences in Sec. VI.A and describe the electronic EDFs in practical use in Sec. VI.B. We then describe applications of TDDFT in electronic systems. As in nuclear physics, there are two distinct applications: linear response TDDFT and TDDFT for large-amplitude motion as an initial-value problem. Former applications include electronic excitations and optical responses in molecules and solids, while the latter applications include electron dynamics in matters induced by strong laser pulses.

A. Conceptual difference between electronic and nuclear (TD)DFT

In electronic systems, DFT and TDDFT are considered as "self-contained" theories that can in principle be exact if accurate functionals are obtained. Improvements of the quality of the calculations should be achieved through improvement of the EDFs. There are other theoretical frameworks that can also in principle exactly describe properties of electronic many-body systems, many-body perturbation theory (MBPT) in condensed matter physics, and wave function based methods in the field of quantum chemistry. These three approaches, (TD)DFT, MBPT, and wave function based methods, are recognized as completely different theories and constitute independent, self-contained theoretical frameworks. In practical applications, DFT and MBPT are sometimes used simultaneously: for example, Green's functions that appear in the MBPT are approximately constructed from solutions of the KS equation. However, in such cases, the mixed use of different theories is clearly recognized, with some reasons such as computational conveniences.

The (TD)DFT in nuclear physics is rather different from this: for example, DFT and MBPT are often used in a mixed way. One of the reasons for this difference is probably due to different roles of the genuine HF approximation. In electronic systems, the HF approximation provides a reasonable starting point for the MBPT. The solutions of the HF and the KS equations are clearly different. In nuclear systems, on the other hand, the HF calculation using a bare nuclear force does not provide any useful result. The KS solution is the only appropriate starting point for the MBPT.

There are also qualitative differences in applications and interpretations of DFT and TDDFT between two kinds of systems. One example is the size of the system that the DFT and TDDFT are applied to: In nuclear applications, the DFT and TDDFT are usually adopted for studies of nuclei with a few tens of nucleons or more. In contrast, for electronic systems, the DFT and TDDFT are applied to as small as a few electron systems, even one electron systems. For a one electron system, of course, no potential originating from the EDF should appear. However, due to an approximate nature of the EDF in practical use, this property is often violated. The condition of a vanishing potential for a one electron system is used to improve the EDF to remove the self-interaction error, which is known as the self-interaction correction (Perdew and Zunger, 1981).

Another important difference appears in the interpretation of linear response TDDFT calculations. In nuclear TDDFT, we understand that the linear response TDDFT is accurate only for processes characterized by small-amplitude oscillation around the ground state. Low-lying excited states are characterized by large-amplitude motion and are considered to need requantization, as described in Sec. V. In electronic TDDFT, on the other hand, the linear response TDDFT has been applied to any electronic excitations no matter how the properties of the states are. The necessity of requantization has not been recognized in electronic TDDFT. The linear response TDDFT for electronic excitations and optical responses is simply called TDDFT. The *linear response* is regarded merely as a computational method, not as an approximation to the TDDFT.

We also find differences in the treatment of collision effects. In nuclear physics, theories of the two-body nucleon-nucleon collisions have been developed, so as to treat these effects in addition to the TDDFT. In contrast, efforts have been made to incorporate electron-electron collision effects within the TDKS formalism in electronic TDDFT, introducing correlation potentials with retardation. One example is an attempt to describe double ionization of atoms by strong laser pulse, discussed in Sec. VI.C. There are also attempts to treat electron-electron collisions as an extension of quantum chemistry methods such as multiconfiguration TDHF and time-dependent configuration interaction theories (Caillat *et al.*, 2005).

In electronic systems, DFT and TDDFT have been widely applied to extended systems. In describing electronic motions in infinitely periodic systems (crystalline solids), the KS

equation is solved in a unit cell of the solid, which is called "first-principles band calculations." Extended systems are classified into metallic and insulating systems, depending on the presence or absence of the band gap. Applying an external field to insulators, there appear a dielectric polarization and a surface charge. The surface charge has an influence on electrons inside the solid. Since it is the long-range effect, it cannot be incorporated in the LDA. To include the polarization effect in the DFT, density polarization functional theory (Gonze and Lee, 1997) has been developed in which the polarization is treated as an independent degree of freedom. A similar argument is applicable to electron dynamics in the TDDFT. Consider a current flowing in an extended system, or in a finite system, for example, a circular current flowing through a nanomaterial of ring shape. It is difficult to incorporate effects of the current on electron dynamics by local approximation. For such cases, time-dependent current density-functional theory (TDCDFT) treating current and vector potential as basic variables has been developed (Ullrich, 2012). The TDCDFT also attracts interest to incorporate retardation effects. It has been realized that the retardation effects cannot be introduced consistently in TDDFT, if one assumes the LDA (Dobson, 1994). In the TDCDFT, it is possible to include the retardation effect in the local approximation scheme (Vignale and Kohn, 1996).

B. Energy density functionals

In this section, we describe properties of EDFs of electronic systems in practical use, with some emphasis on differences from those in nuclear systems. As in nuclear TDDFT, the adiabatic approximation of Eq. (32) is usually adopted for most applications of electronic TDDFT; one employs the same EDF as that in the static calculation, replacing a static density with a time-dependent density without retardation. Therefore, here we mainly describe EDF for the static (ground-state) calculations. At the end of this section, we briefly mention progress beyond the adiabatic approximation.

In nuclear DFT, a general form of the EDF as a functional of density, density gradient, kinetic energy density, current density, spin density, pair density, and so on has been considered since the early stage of its progress (Engel *et al.*, 1975). In contrast, electronic DFT started with an EDF of density only in the LDA and gradually developed to include more complex elements.

The energy density of a uniform system as a function of density is the most fundamental information for the EDF. An accurate energy density of an electron gas system in the ground state was obtained around 1980 (Ceperley and Alder, 1980). It was obtained by the MBPT at high density and by numerical calculations using a quantum Monte Carlo method at medium and low density, connecting to the energy density of the Wigner crystal at very low density. Since then, a number of LDA calculations have been carried out for various systems, utilizing analytic forms of the functional which are obtained by fitting the numerical energy density. When treating systems with spin polarization such as isolated atoms and ferromagnetic materials, a local spin density approximation treating densities of spin up and spin down as basic variables was developed.

As a step toward higher accuracy from the LDA, EDFs including a gradient of electron density were developed. A group of EDFs with density gradient that are widely used today is called the generalized gradient approximation (GGA). They were constructed around 1990 and succeeded to increase the accuracy substantially from the LDA (Sousa, Fernandes, and Ramos, 2007). To further improve the accuracy, EDFs including a kinetic energy density were developed. They are called the meta-GGA (Tao *et al.*, 2003). In developing these new EDFs, exact analytical properties that should be satisfied by an EDF are respected. These attempts to increase the accuracy of the EDFs employing more and more elements were named the Jacob's ladder of the DFT by Perdew *et al.* (2005).

At present, most successful EDFs in the sense of an accurate description of measured properties are those called "hybrid functional" (Koch and Holthausen, 2001). They use a mixture of semilocal and nonlocal forms for the exchange energy. The ratio of the mixture, which is determined empirically, is chosen to be about 3:1. In molecules, the functional named B3LYP (Stephens *et al.*, 1994) is known to give good results for many systems and has quite often been used (Laurent and Jacquemin, 2013). In infinitely periodic systems, hybrid functionals have also been proposed (Heyd, Scuseria, and Ernzerhof, 2003). However, their use is somewhat limited because the calculation of the nonlocal exchange terms is computationally expensive in the plane wave basis method that is popular in solid state calculations.

In electronic systems, computational methods to solve the KS equation are classified into two. One is the local basis expansion method in which the basis functions are given with respect to atomic positions. This is adopted in most quantum chemistry codes for molecules. The other is the grid representation either in the coordinate or in the momentum space. The grid representation in momentum, which is often called the plane wave basis method, has been widely adopted in computational codes of crystalline solids. Recently, the real-space grid representation becomes more and more popular, since it is superior for calculations with massively parallel computers (Enkovaara *et al.*, 2010; Andrade *et al.*, 2012). In the grid approach, it is difficult to describe inner orbitals that are strongly bound to nuclei. The pseudopotential methods have been developed to avoid this difficulty. In the local basis expansion methods, nonlocal exchange terms can be managed with a reasonable computational cost. However, in the grid representation methods, the computational cost becomes extremely high. This situation is similar to the nuclear DFT calculations. In Skyrme HF calculations in which no nonlocal term appears, the real-space grid representation is a popular computational method, while in the HF calculations with Gogny interaction, the basis expansion method such as the harmonic oscillator basis is used to handle the nonlocal Fock terms.

Even with hybrid functionals it is not possible to incorporate long-range electron correlations that are responsible for the van der Waals forces which are important between two neutral molecules. For this problem, one practical and successful approach is to add a long-range potential energy $-C/R^6$ to every pair of atoms, on top of the DFT (Grimme, 2006). Microscopic approaches to construct EDFs

incorporating the long-range electron correlations have also been actively pursued (Berland *et al.*, 2015).

While accurate calculation of the ground-state energy is the principal goal of the DFT calculations, orbital energies, in particular, the energy gap between occupied and unoccupied orbitals, is important to describe electronic excitations and dynamics in TDDFT. Comparing energy gaps of insulators obtained from eigenvalues of the KS equation with measured energy gaps, the KS energy gaps are systematically too small. For a better description of energy gaps, potentials as functionals of the density gradient and of the kinetic energy density have been developed. For atoms and molecules, a potential named LB94 (van Leeuwen and Baerends, 1994), which includes the density gradient, has been successfully used for optical response calculations. The potential is constructed so that it has the correct asymptotic form $-e^2/r$, which should be satisfied in electrically neutral systems. For extended systems, the meta-GGA potential that includes kinetic energy density was proposed by Tran and Blaha (2009), which has attracted recent interest. These potentials are directly given as a functional of density, gradient of the density, and kinetic energy density. The EDFs that provide these potentials are not constructed. We do not know even whether such EDFs exist or not.

Beyond the adiabatic approximation is certainly an important issue. In the linear response TDDFT, the number of excited states is equal to the number of $1\mathrm{p}-1\mathrm{h}$ configurations. If one would hope to describe many-particle–many-hole-like configurations within the linear response TDDFT, the frequency dependence of the exchange-correlation kernel, the second derivative of the energy density functional with respect to densities, should be crucial. Inclusion of electron-electron collision effects through the energy density functional will also require the frequency dependence. Although extensive efforts have been made to construct nonadiabatic functionals, the functionals which are useful for wide purposes have not yet been obtained. A nonadiabatic energy functional in TDCDFT proposed by Vignale and Kohn (1996) has been tested for several problems. In that functional, the nonadiabaticity has been discussed making relations to the viscoelastic stresses of electronic quantum liquid.

C. Applications

1. Linear response

Among applications of electronic TDDFT, the linear response TDDFT in the adiabatic approximation has been widely used and highly successful to describe electronic excitations and optical responses of molecules. As in nuclear TDDFT, the basic idea is to extract excitation energies and response functions from the density change induced by a weak external field applied to molecules.

Historically, optical responses of spherical systems have been investigated first. Using a similar approach to that in nuclear theory employing the continuum Green's function, optical responses of rare gas atoms have been investigated by Zangwill and Soven (1980) and of metallic clusters by Ekardt (1984); see Sec. III.E.

In the middle 1990s and later, efficient computational methods have been developed for linear response TDDFT calculations of molecules without any spatial symmetries. A matrix diagonalization method preparing occupied and unoccupied orbitals was developed by Casida *et al.* (1998) and named the "Casida method" (Sec. III.B). A method solving the linear Schrödinger-like equation for a given external field with a fixed frequency is known as the Sternheimer method (Nakatsukasa and Yabana, 2001). A real-time method was also developed (Yabana and Bertsch, 1996; Yabana *et al.*, 2006), solving the TDKS equation in real time after an impulsive external field applied to the system (Sec. III.F). The matrix diagonalization method is the most widely used in practical purposes. The real-time method is superior to calculate collective excitations to which a large number of electron-hole pairs contribute. After the middle 1990s, linear response TDDFT was implemented in many quantum chemistry codes as a tool to calculate electronically excited states of molecules with reasonable accuracy and cost. Using these codes, researchers who do not have much knowledge and experience with TDDFT, including experimentalists, can easily perform the linear response TDDFT calculations of molecules. After 2011, the number of papers that include TDDFT as keywords exceeded 1000 per year.

As the method was applied to a wide variety of molecules, it was realized that linear response TDDFT with local or semilocal approximation fails systematically (Ullrich, 2012). For example, electronic excitation energies of long-chain molecules are systematically underestimated. Excitation energies of charge-transfer excitations, in which the electron and the hole are spatially remote, are also underestimated. These failures are attributed to the incomplete cancellation of the electron self-energy.

Linear responses of extended systems are characterized by dielectric functions $\epsilon(\vec{q},\omega)$. The dielectric functions of metallic systems that are dominated by plasmon are reasonably described by the adiabatic TDDFT. In contrast, it does not give satisfactory results for semiconductors and insulators. In these solids, optical responses around the band gap energy are characterized by excitons, bound excited states of electrons and holes. It was realized that the excitons cannot be described in the adiabatic TDDFT with local approximations (Onida, Reining, and Rubio, 2002). For optical responses in semiconductors and insulators, the GW-plus-Bethe-Salpeter approach, solving the Bethe-Salpeter equation with the Green's functions containing self-energy given by the GW approximation, was quite successful (Rohlfing and Louie, 2000).

2. Electron dynamics under strong field

In nuclear physics, TDDFT calculations as initial-value problems have been developed in the studies of heavy-ion collisions. In electronic systems, similar initial-value approaches have been widely applied to interactions of a strong laser pulse with matters.

One of the active frontiers of laser science is to produce strong and ultrashort light pulses and to explore their interaction with matter. At an extremely intense limit, high energy phenomena such as vacuum breakdown and nuclear reactions induced by strong laser pulses have been actively

investigated (Di Piazza *et al.*, 2012). In material sciences, interactions of light pulses whose scales are approaching atomic units have attracted significant interest. When the magnitude of the laser electric field approaches those of binding electrons to ions, the electron dynamics induced by the laser pulse will become extremely nonlinear (Brabec and Krausz, 2000). The shortest light pulse available today is comparable to the period of a hydrogen atom. Using such an ultrashort laser pulse as a flash light, there have been intense attempts to take snapshots of electron dynamics in atoms, molecules, and solids (Krausz and Ivanov, 2009). To theoretically investigate extremely nonlinear and ultrafast electron dynamics in matter, computational approaches solving the time-dependent Schrödinger equation for one-electron systems and the TDKS equation for many-electron systems have been extensively developed.

In strong laser pulse irradiation on atoms and molecules, various phenomena such as tunnel and multiphoton ionizations, above threshold ionization, high harmonic generation, and Coulomb explosion have been described using the real-time TDDFT (Chu and Telnov, 2004; Marques and Gross, 2004; Ullrich, 2012). In the interaction of strong laser pulses with metallic clusters, nonlinear interactions between a strong laser pulse and the plasmon, collective electronic excitation, play an important role (Calvayrac *et al.*, 2000; Wopperer *et al.*, 2015). In the multiple ionization of atoms at relatively low laser intensities, it is known that the secondary ionization proceeds mainly through the rescattering process: an ionized electron is accelerated by the applied laser pulse and collides with the atom from which the electron was first emitted. This collision process has been regarded as a test case to develop EDFs that could describe collision effects. However, it turned out that finding such a functional is, as anticipated, not an easy task (Ullrich, 2012).

Recently, interactions of strong laser pulses with solids have attracted interest, aiming at exploring new phenomena that could bring innovative optical devices. The TDDFT calculations have been carried out to analyze nonlinear electron dynamics in solids, including ultrafast current generation in transparent material (Wachter *et al.*, 2014), and coupled dynamics of electrons and macroscopic electromagnetic fields (Yabana *et al.*, 2012).

Real-time TDDFT calculations have been applied to fields other than laser sciences. One example is electron transfer dynamics in ion collisions. Electronic TDHF calculations have also been applied to nuclear fusion reactions in astrophysical environments to investigate electronic screening effects (Shoppa *et al.*, 1993). The collision of energetic ions impinging on a graphene sheet has been explored (Bubin *et al.*, 2012; Zhang, Miyamoto, and Rubio, 2012). Collisions between multiply ionized and neutral atoms have been investigated (Nagano *et al.*, 2000).

3. Coupled dynamics of electrons and atoms

Before ending this section, we present a simultaneous description of electronic and atomic motions. In nuclear physics, there is no degree of freedom corresponding to atomic motion. However, coupling of a slow collective motion with fast internal motions as in nuclear fusion and fission dynamics may have some similarities.

If the material has an energy gap and electrons always stay in their ground state, we assume the adiabatic, Born-Oppenheimer approximation. In such cases, we separate the problem into two steps: For a given atomic configuration, we first solve the static KS equation to obtain the electronic ground state. Then the forces acting on atoms are calculated using the Feynman-Hellman theorem. Finally the atomic motions are calculated solving the Newton equation. This is the so-called *ab initio* molecular dynamics calculation, initiated with a slightly different implementation by Car and Parrinello (1985).

Simultaneous descriptions of electronic excitation and atomic motion, which are often termed nonadiabatic molecular dynamics, are much more involved. We first consider a simple molecule where one or at most a few electronic states are important. When the electronic levels are well separated, we assume Newtonian motion for atoms on the adiabatic potential energy surface. When the two electronic states come close in energy at a certain atomic configuration, quantum transitions between different potential energy surfaces need to be treated. The potential energy surfaces may be efficiently calculated with the linear response TDDFT. Such simulations were widely applied to photomolecule reactions (Persico and Granucci, 2014). We note that in such simulations the TDKS equation needs not to be solved in real time.

How can we treat cases in which a number of electronic levels are close in energy and transitions frequently take place? The electronic excitation spectra can even form the continuum in solids. There is an alternative method called the Ehrenfest dynamics. In this method, the TDKS equations for electrons and Newtonian equations for atoms are solved simultaneously in real time, as coupled equations. At each time, the force acting on each atom is calculated from the electron density (Shinohara *et al.*, 2010; Tavernelli, 2015).

These two methods are conceptually very different. The former method utilizes the linear response TDDFT to prepare potential energy surfaces, while the latter utilizes a solution of real-time TDKS equation as an initial-value problem. At present, it is empirically decided which method to use for a given problem. Accumulation of results will eventually make it possible to assess the quality of approximation of the two approaches.

VII. SUMMARY AND FUTURE OUTLOOK

The TDDFT using modern nuclear EDFs provides a unified, systematic, and quantitative description of nuclear structure and reaction. Thanks to its nontrivial density dependence, these EDFs are capable of simultaneously reproducing the bulk properties of nuclei (saturation, equation of state, etc.) and properties of individual nucleus (shell effects, deformation, etc.). The nuclear EDF also shows various kinds of spontaneous breaking of the symmetry (SSB). Especially, the translational symmetry is always violated for finite nuclei. The SSB can be incorporated in a stringent manner by the DFT theorems for the wave-packet states. Nevertheless, there remain several open questions for rigorous justification of the DFT in nuclear physics (Giraud, 2010). Because of a significant increase in

computational resources and development in parallelized computer programs, the TDDFT serves as modern approaches to a variety of nuclear phenomena which were addressed only with phenomenological models. Since all the parameters in nuclear EDFs are basically fixed, it can provide nonempirical predictions. In the present review, we summarize recent developments in the three categories: linear density response, real-time method, and requantization of TDDFT collective submanifold.

The linear density response around the ground state is known as (Q)RPA in nuclear physics. Recent calculations treat all the residual fields induced by the density variations in the EDF. This is particularly important for the separation of ANG modes associated with the SSB. The program coding and numerical computation have been facilitated by the finite amplitude method and other iterative methods to the linear response. These developments significantly reduce the computational costs and necessary memory capacity for deformed heavy nuclei.

The treatment of the continuum is another issue which has been extensively studied in recent years to explore unique properties of weakly bound nuclei near the drip lines. The most complete formalism is the continuum QRPA simultaneously treating the continuum in the particle-hole and particle-particle (hole-hole) channels with the Green's function method. However, so far the numerical calculation has been achieved only for spherical systems.

The real-time TDDFT calculation provides useful insight into nuclear many-body dynamics, such as microscopic understanding of nuclear reaction and energy dissipation. One of the recent major achievements is the large-scale 3D calculation in the TDBdGKS (TDHFB) scheme (Sec. IV). Although the full calculations for nuclear dynamics in this scheme are so far limited to the linear response, one can expect further applications to large-amplitude dynamics in the near future. In the meantime, the approximate treatment of the BCS-like pairing may provide a useful guidance for that (Sec. IV.A).

A microscopic derivation of the internucleus potential and the dissipation was recently developed by several authors and applied to many systems (Sec. IV.B). This provides a connection between the microscopic TDDFT simulation and the phenomenological potential approaches to nuclear fusion. The method even quantitatively describes the sub-barrier fusion reaction for some cases, by extracting the potential from the TDDFT calculation (Umar and Oberacker, 2007, 2008). These methods may be justifiable before two nuclei overlap substantially in the fusion process. However, it requires further development and studies in clarifying the entire dynamics in the fusion process. The real-time TDDFT studies of quasifission are in progress too (Sec. IV).

Recent studies on the multinucleon transfer reaction show reasonable agreement with experimental mass distribution (Sec. IV.C). The fluctuations in major channels seem to be taken into account by the TDDFT simulation with the particle-number projection. However, some discrepancies were also identified, especially in minor channels. For the improvement, the stochastic mean-field and Baranger-Véneroni variational approaches may provide a tool to correct these missing fluctuations and correlations (IV.C.2). It was partially successful but further studies are desired.

At present, all the available nuclear EDFs seem to be unable to express, in the KS scheme, correlations associated with low-energy modes of (slow) collective motion. They have been addressed by additional correlations beyond the KS scheme, which includes the particle-vibration coupling, the higher random-phase approximation, the time-dependent density-matrix method, the generator coordinate method, and so on. In this review, we put some emphasis on the requantization of the TDDFT collective submanifold to take into account the missing correlations (Sec. V). The self-consistent derivation of a collective Hamiltonian (submanifold) suitable for description of low-energy large-amplitude motion can be achieved by solving the ASCC equations. The inertial masses include time-odd effects and are guaranteed to produce the correct total mass for the translation. The method also overcomes known difficulties in the adiabatic TDHF method. It has been applied to studies of nuclear quadrupole dynamics in the pairing-plus-quadrupole model. For the aim of deriving a collective Hamiltonian for various kinds of LACM on the basis of the modern EDFs, the finite amplitude method and new iterative solvers in Sec. III.D may be utilized to numerically solve the moving-frame QRPA equations in an efficient way.

The collective inertial masses should be studied furthermore. The collective inertial mass, which is locally defined, represents the inertia of the many-body system against an infinitesimal change of the collective coordinate. As the single-particle-energy spectrum in the mean field changes during the LACM, the level crossing at the Fermi energy successively occurs. We expect that the configuration rearrangement at the level crossing is essential to keep the system at low energy. Thus, for low-energy nuclear dynamics, the pairing correlation plays an essential role in determination of the collective mass parameters (Barranco *et al.*, 1990). It remains as an interesting subject to investigate how the self-consistent determination of the optimal directions of collective motion and the finite frequency $\omega(q)$ of the moving-frame QRPA modes affect the level crossing dynamics of the superfluid nuclear systems.

In addition to the quadrupole collective motions, large-amplitude collective phenomena associated with instability toward octupole deformations of the mean field as well as interplay of the quadrupole and octupole modes of excitations have been widely observed in low-lying states of nuclei (Butler and Nazarewicz, 1996). In the high-spin yrast region where the nucleus is highly excited but cold (zero temperature), new types of rotations and vibrations may emerge (Satuła and Wyss, 2005), such as wobbling motions (Hamamoto and Hagemann, 2003; Shoji and Shimizu, 2009; Frauendorf and Dönau, 2014) and superdeformed shape vibrations (Nakatsukasa *et al.*, 1996). It is quite interesting to apply the microscopic theory of LACM to these new collective phenomena (Matsuyanagi *et al.*, 2010). Macroscopic quantum tunnelings through self-consistently generated barriers, such as spontaneous fissions and deep sub-barrier fusions, are, needless to say, great challenges of nuclear structure physics.

In electronic TDDFT, the linear response is considered to be exact, and the anharmonic large-amplitude nature should not matter (Sec. VI.A). The failures in describing a certain class of excited states are due to incomplete EDFs, not to the limited applicability of the linear response. This makes a striking contrast to the concept of nuclear DFT and TDDFT. Because of these conceptual differences, major efforts in the electronic DFT and TDDFT are devoted to the improvement in the quality of EDFs. Construction of a practical and accurate EDF including the retardation effects beyond the adiabatic local density approximation is currently under investigation. This is a challenging subject in the electronic TDDFT. Nevertheless, using the adiabatic EDFs, there have been numerous successful applications in both the linear response and the initial-value TDDFT for molecules and solids (Sec. VI.C).

The nuclear many-body dynamics in the large-amplitude collective motion is still a big challenge for nuclear physics. This review has described theoretical and computational progress in the nuclear TDDFT studies, which we think is significant in the last decades. We hope it provides stimulus to researchers in the field.

ACKNOWLEDGMENTS

We are grateful to many collaborators and colleagues, including P. Avogadro, S. Ebata, N. Hinohara, T. Inakura, H. Z. Liang, K. Mizuyama, K. Sato, K. Sekizawa, K. Washiyama. and K. Yoshida. This work was supported in part by the JSPS KAKENHI Grants No. 24105006, No. 25287065, No. 26400268, and No. 15H03674.

APPENDIX A: KRYLOV REDUCTION OF THE RPA SPACE

It is easy to see that the $2d$ Krylov subspace (64) contains the RPA-conjugate partners. In fact, $(\mathcal{N}\mathcal{H})^m F_v$ and $(\mathcal{N}\mathcal{H})^m \tilde{F}_v$ are RPA conjugate to each other $[(\mathcal{N}\mathcal{H})^m \tilde{F}_v = (-1)^m \mathcal{I}\{(\mathcal{N}\mathcal{H})^m F_v\}^*]$. We can show this using $\mathcal{H}\mathcal{I} = \mathcal{I}\mathcal{H}^*$ and $\mathcal{N}\mathcal{I} = -\mathcal{I}\mathcal{N}$.

Next let us map the RPA equation in the $2D$ space to that in the $2d$ space. Suppose that we construct the $\mathcal{N}$-orthonormalized basis $\{Q_1, \ldots, Q_d; \tilde{Q}_1, \ldots, \tilde{Q}_d\}$ from Eq. (64). Let us define the $2D \times 2d$ rectangular matrix $\mathcal{Q} \equiv (Q, \tilde{Q})$, which is a projection from the $2D$ full space into the $2d$ subspace. For instance, the Hamiltonian and the norm matrix in Eq. (55) are transformed into $2d \times 2d$ Hermitian matrices as

$$h \equiv \mathcal{Q}^\dagger \mathcal{H} \mathcal{Q} = \begin{pmatrix} a & b \\ b^* & a^* \end{pmatrix}, \qquad n \equiv \mathcal{Q}^\dagger \mathcal{N} \mathcal{Q} = \begin{pmatrix} 1 & 0 \\ 0 & -1 \end{pmatrix}.$$

Here a and b are $d \times d$ matrices given by $a_{ij} \equiv Q_i^\dagger \mathcal{N}\mathcal{H} Q_j = -(\tilde{Q}_i^\dagger \mathcal{N}\mathcal{H}\tilde{Q}_j)^*$ and $b_{ij} \equiv Q_i^\dagger \mathcal{N}\mathcal{H}\tilde{Q}_j = -(\tilde{Q}_i^\dagger \mathcal{N}\mathcal{H} Q_j)^*$. The eigenvectors

$$z_n \equiv \begin{pmatrix} x_n \\ y_n \end{pmatrix}, \qquad \tilde{z}_n \equiv \begin{pmatrix} y_n^* \\ x_n^* \end{pmatrix}$$

are obtained by diagonalizing the $2d \times 2d$ matrix nh. In analogy to Eq. (56), we define the matrix notation

$$z \equiv (z, \tilde{z}) = \begin{pmatrix} x & y^* \\ y & x^* \end{pmatrix}, \qquad \omega \equiv \begin{pmatrix} \omega_d & 0 \\ 0 & \omega_d \end{pmatrix}.$$

The eigenvalue equation (57) is mapped to

$$nhz = z\omega n. \tag{A1}$$

It is easy to show that the reduction (A1) preserves the sum rules m_L with odd L. Since the subspace (64) is complete for intermediate states ($L < 2d$) in Eq. (63), we can replace the norm matrix $\mathcal{N}$ by $\mathcal{Q}n\mathcal{Q}^\dagger$. Then, Eq. (63) can be rewritten as

$$\begin{aligned} m_L &= \frac{1}{2}(F_v + \tilde{F}_v)^\dagger \mathcal{Q}(nh)^L n \mathcal{Q}^\dagger (F_v + \tilde{F}_v) \\ &= \frac{1}{2}(F_v + \tilde{F}_v)^\dagger \mathcal{Q} z \omega^L z^\dagger \mathcal{Q}^\dagger (F_v + \tilde{F}_v) \\ &= \sum_{n=1}^{d} \omega_n^L |\langle n|F|0\rangle|^2, \end{aligned}$$

where we used the relation $z^\dagger h z = \omega$ which is derived from Eq. (A1). Here $z^\dagger \mathcal{Q}^\dagger (F_v + \tilde{F}_v)$ is nothing but the transition strength $\langle n|F|0\rangle$ calculated with the approximate eigenvectors

$$Z' = \mathcal{Q} z = \begin{pmatrix} X' & Y'^* \\ Y' & X'^* \end{pmatrix}.$$

APPENDIX B: RESPONSE FUNCTION WITH THE GREEN'S FUNCTION

In this Appendix, we show the derivation of Eq. (67). The unperturbed (independent-particle) density response $\delta R^0(\omega)$ is defined by the limit of the vanishing residual kernels $w = w' = 0$. Since the response function $\Pi_0(\omega)$ is diagonal in the quasiparticle basis, it can be easily obtained from Eq. (65) as

$$\begin{aligned} \delta R^0(\omega) &= \sum_{i,j} \left\{ \frac{\Psi_i^0 V_{ij}^{(+-)} \tilde{\Psi}_j^{0\dagger}}{\omega - E_i - E_j} + \frac{\tilde{\Psi}_i^0 V_{ij}^{(-+)} \Psi_j^{0\dagger}}{-\omega - E_i - E_j} \right\} \\ &= \sum_{i,j} \left\{ \frac{\Psi_i^0 \Psi_i^{0\dagger} V \tilde{\Psi}_j^0 \tilde{\Psi}_j^{0\dagger}}{\omega - E_i - E_j} + \frac{\tilde{\Psi}_i^0 \tilde{\Psi}_i^{0\dagger} V \Psi_j^0 \Psi_j^{0\dagger}}{-\omega - E_i - E_j} \right\}, \end{aligned} \tag{B1}$$

which has poles at the two-quasiparticle energies $\omega = \pm(E_i + E_j)$. Note that we have converted the quasiparticle representation to a general form [cf. the transition densities of Eq. (60)]. Adding the following zero to the right-hand side,

$$\sum_{i,j} \left\{ \frac{\tilde{\Psi}_i^0 \tilde{\Psi}_i^{0\dagger} V(\omega) \tilde{\Psi}_j^0 \tilde{\Psi}_j^{0\dagger}}{\omega + E_i - E_j} + \frac{\tilde{\Psi}_i^0 \tilde{\Psi}_i^{0\dagger} V(\omega) \tilde{\Psi}_j^0 \tilde{\Psi}_j^{0\dagger}}{-\omega - E_i + E_j} \right\} = 0,$$

leads to

$$\begin{aligned} \delta R^0(\omega) = \sum_i \{ &\mathcal{G}_0(\omega - E_i) V(\omega) \tilde{\Psi}_i^0 \tilde{\Psi}_i^{0\dagger} \\ &+ \tilde{\Psi}_i^0 \tilde{\Psi}_i^{0\dagger} V(\omega) \mathcal{G}_0(-\omega - E_i) \}. \end{aligned} \tag{B2}$$

Here the Green's function $\mathcal{G}_0(E)$ is given by

$$\mathcal{G}_0(E) = (E - H_s[R_0])^{-1} = \sum_i \left\{ \frac{\Psi_i^0 \Psi_i^{0\dagger}}{E - E_i} + \frac{\tilde{\Psi}_i^0 \tilde{\Psi}_i^{0\dagger}}{E + E_i} \right\}. \quad \text{(B3)}$$

This Green's function contains both normal and abnormal Green's functions $G_0(E)$ and $F_0(E)$ in the 2×2 matrix form. Equation (B2) can also be derived by the Fourier transform of Eq. (48):

$$\delta R^0(\omega) = \sum_i \{ \delta\tilde{\Psi}_i(\omega) \tilde{\Psi}_i^{0\dagger} + \tilde{\Psi}_i^0 \delta\tilde{\Psi}_i^\dagger(-\omega) \}$$

and $\delta\tilde{\Psi}_i(\omega) = \mathcal{G}_0(\omega - E_i) V(\omega) \tilde{\Psi}_i^0$.

Now let us adopt a single-particle representation $\{\alpha\}$. It should be noted that, since the quasiparticle state has upper and lower components $U(\alpha)$ and $V(\alpha)$, the quantities with two single-particle indices, such as $V(\omega)$, $\delta R^0(\omega)$, and $\mathcal{G}_0(E)$, are expressed in 2×2 matrix form. The response functions $\Pi_0(\omega)$ and $\Pi(\omega)$ with four indices should be expressed in the $(2 \times 2) \otimes (2 \times 2)$ form. In order to avoid these complications, we adopt the primed indices $\alpha', \beta', \ldots$, which are given after Eq. (16).

Equation (B2) is represented as

$$\begin{aligned} \delta R^0(\alpha'\beta'; \omega) &= \sum_{\mu'\nu'} \Pi_0(\alpha'\beta', \mu'\nu'; \omega) V(\mu'\nu'; \omega), \\ \Pi_0(\alpha'\beta', \mu'\nu'; \omega) &= \sum_i \{ \mathcal{G}_0(\alpha'\mu'; \omega - E_i) \tilde{\Psi}_i^0(\nu') \tilde{\Psi}_i^{0\dagger}(\beta') \\ &\quad + \tilde{\Psi}_i^0(\alpha') \tilde{\Psi}_i^{0\dagger}(\mu') \mathcal{G}_0(\nu'\beta'; -\omega - E_i) \}. \end{aligned} \quad \text{(B4)}$$

Similarly, the residual kernel $\mathcal{W}$ is represented by four indices. In principle, according to Eq. (66), we may obtain the QRPA response function $\Pi(\omega)$ and the density response $\delta R(\omega)$.

Here we distinguish the upper $\Psi_i^{0(1)} = U_i$ and lower components $\Psi_i^{0(2)} = V_i$ of the quasiparticle Ψ_i^0, and introduce the 2×2 matrix form for the density $\delta R^{(mn)}$ and the external potential $V^{(mn)}$, and the $(2 \times 2) \otimes (2 \times 2)$ form for the response function $\Pi^{(mn,pq)}$ and the residual kernels $\mathcal{W}^{(mn,pq)}$, with the indices $m, n, p, q = 1$ and 2. If the potential and residual kernels have the diagonal character $V^{(mn)}(\alpha\beta) = V^{(mn)}(\alpha)\delta_{\alpha\beta}$, $\mathcal{W}^{(mn,pq)}(\alpha\beta, \mu\nu) = \mathcal{W}^{(mn,pq)}(\alpha, \mu)\delta_{\alpha\beta}\delta_{\mu\nu}$, we may simplify Eq. (B4) to its diagonal representation

$$\begin{aligned} \Pi_0^{(mn,pq)}(\alpha, \beta; \omega) &= \sum_i \{ \mathcal{G}_0^{(mp)}(\alpha\beta; \omega - E_i) \tilde{\Psi}_i^{0(q)}(\beta) \tilde{\Psi}_i^{0(n)\dagger}(\alpha) \\ &\quad + \tilde{\Psi}_i^{0(m)}(\alpha) \tilde{\Psi}_i^{0(p)\dagger}(\beta) \mathcal{G}_0^{(qn)}(\beta\alpha; -\omega - E_i) \}, \end{aligned} \quad \text{(B5)}$$

and the unperturbed density response is given by

$$\delta R_0^{(mn)}(\alpha\alpha) = \sum_{p,q=1,2} \sum_\beta \Pi_0^{(mn,pq)}(\alpha, \beta) V^{(pq)}(\beta).$$

REFERENCES

Abe, Y., and T. Suzuki, 1983, Eds., Microscopic theories of nuclear collective motions, Prog. Theor. Phys. Suppl. **74–75**.

Åberg, S., H. Flocard, and W. Nazarewicz, 1990, Annu. Rev. Nucl. Part. Sci. **40**, 439.

Aichelin, J., 1991, Phys. Rep. **202**, 233.

Alder, K., A. Bohr, T. Huus, B. Mottelson, and A. Winther, 1956, Rev. Mod. Phys. **28**, 432.

Almehed, D., and N. R. Walet, 2004, Phys. Rev. C **69**, 024302.

Anderson, P. W., 1958, Phys. Rev. **110**, 827.

Anderson, P. W., 1963, Phys. Rev. **130**, 439.

Andrade, X., *et al.*, 2012, J. Phys. Condens. Matter **24**, 233202.

Anguiano, M., J. Egido, and L. Robledo, 2001, Nucl. Phys. A **696**, 467.

Aoyama, S., T. Myo, K. Katō, and K. Ikeda, 2006, Prog. Theor. Phys. **116**, 1.

Arnold, V. I., 1989, *Mathematical methods of classical mechanics* (Springer-Verlag, New York).

Arteaga, D. P., E. Khan, and P. Ring, 2009, Phys. Rev. C **79**, 034311.

Avez, B., C. Simenel, and P. Chomaz, 2008, Phys. Rev. C **78**, 044318.

Avogadro, P., and T. Nakatsukasa, 2011, Phys. Rev. C **84**, 014314.

Avogadro, P., and T. Nakatsukasa, 2013, Phys. Rev. C **87**, 014331.

Ayik, S., 2008, Phys. Lett. B **658**, 174.

Baldo, M., L. M. Robledo, P. Schuck, and X. Viñas, 2013, Phys. Rev. C **87**, 064305.

Baldo, M., P. Schuck, and X. Viñas, 2008, Phys. Lett. B **663**, 390.

Balian, R., and M. Vénéroni, 1985, Ann. Phys. (N.Y.) **164**, 334.

Baran, A., J. A. Sheikh, J. Dobaczewski, W. Nazarewicz, and A. Staszczak, 2011, Phys. Rev. C **84**, 054321.

Baranger, M., and K. Kumar, 1965, Nucl. Phys. **62**, 113.

Baranger, M., M. Strayer, and J.-S. Wu, 2003, Phys. Rev. C **67**, 014318.

Baranger, M., and M. Vénéroni, 1978, Ann. Phys. (N.Y.) **114**, 123.

Barnea, N., 2007, Phys. Rev. C **76**, 067302.

Barranco, F., G. F. Bertsch, R. A. Broglia, and E. Vigezzi, 1990, Nucl. Phys. A **512**, 253.

Belyaev, S. T., 1965, Nucl. Phys. **64**, 17.

Belyaev, S. T., A. V. Smirnov, S. V. Tolokonnikov, and S. A. Fayans, 1987, Sov. J. Nucl. Phys. **45**, 783.

Bender, M., 2008, Eur. Phys. J. Spec. Top. **156**, 217.

Bender, M., G. F. Bertsch, and P.-H. Heenen, 2006, Phys. Rev. C **73**, 034322.

Bender, M., J. Dobaczewski, J. Engel, and W. Nazarewicz, 2002, Phys. Rev. C **65**, 054322.

Bender, M., and P.-H. Heenen, 2008, Phys. Rev. C **78**, 024309.

Bender, M., P.-H. Heenen, and P.-G. Reinhard, 2003, Rev. Mod. Phys. **75**, 121.

Berland, K., V. R. Cooper, K. Lee, E. Schröder, T. Thonhauser, P. Hyldgaard, and B. I. Lundqvist, 2015, Rep. Prog. Phys. **78**, 066501.

Bertsch, G. F., M. Girod, S. Hilaire, J.-P. Delaroche, H. Goutte, and S. Péru, 2007, Phys. Rev. Lett. **99**, 032502.

Bes, D. R., and R. A. Sorensen, 1969, in *Advances in Nuclear Physics*, Vol. 2, edited by J. Negele and E. Vogt (Plenum Press, New York), p. 129.

Bethe, H. A., and R. F. Bacher, 1936, Rev. Mod. Phys. **8**, 82.

Blaizot, J.-P., and G. Ripka, 1986, *Quantum Theory of Finite Systems* (MIT Press, Cambridge).

Błocki, J., and H. Flocard, 1976, Nucl. Phys. A **273**, 45.

Błocki, J., and H. Flocard, 1979, Phys. Lett. B **85**, 163.

Bohr, A., 1976, Rev. Mod. Phys. **48**, 365.

Bohr, A., and B. R. Mottelson, 1969, *Nuclear Structure* (W. A. Benjamin, New York), Vol. I.

Bohr, A., and B. R. Mottelson, 1975, *Nuclear Structure* (W. A. Benjamin, New York), Vol. II.

Bonche, P., J. Dobaczewski, H. Flocard, P.-H. Heenen, and J. Meyer, 1990, Nucl. Phys. A **510**, 466.

Bonche, P., S. Koonin, and J. W. Negele, 1976, Phys. Rev. C **13**, 1226.

Brabec, T., and F. Krausz, 2000, Rev. Mod. Phys. **72**, 545.

Brack, M., J. Damgaard, A. S. Jensen, H. C. Pauli, V. M. Strutinsky, and C. Y. Wong, 1972, Rev. Mod. Phys. **44**, 320.

Brenna, M., G. Colò, and P. F. Bortignon, 2012, Phys. Rev. C **85**, 014305.

Brenna, M., G. Colò, and X. Roca-Maza, 2014, Phys. Rev. C **90**, 044316.

Brink, D., and R. A. Broglia, 2005, *Nuclear Superfluidity, Pairing in Finite Systems* (Cambridge University Press, Cambridge, England).

Brink, D. M., M. J. Giannoni, and M. Veneroni, 1976, Nucl. Phys. A **258**, 237.

Brink, D. M., and F. Stancu, 1981, Phys. Rev. C **24**, 144.

Bubin, S., B. Wang, S. Pantelides, and K. Varga, 2012, Phys. Rev. B **85**, 235435.

Bulgac, A., 2013, Annu. Rev. Nucl. Part. Sci. **63**, 97.

Butler, P. A., and W. Nazarewicz, 1996, Rev. Mod. Phys. **68**, 349.

Caillat, J., J. Zanghellini, M. Kitzler, O. Koch, W. Kreuzer, and A. Scrinzi, 2005, Phys. Rev. A **71**, 012712.

Calvayrac, F., P.-G. Reinhard, E. Suraud, and C. Ullrich, 2000, Phys. Rep. **337**, 493.

Cao, L.-G., G. Colò, H. Sagawa, and P. F. Bortignon, 2014, Phys. Rev. C **89**, 044314.

Car, R., and M. Parrinello, 1985, Phys. Rev. Lett. **55**, 2471.

Carlos, P., H. Beil, R. Bergere, A. Lepretre, and A. Veyssiere, 1971, Nucl. Phys. A **172**, 437.

Carlos, P., H. Beil, R. Bergère, A. Leprêtre, A. D. Miniac, and A. Veyssière, 1974, Nucl. Phys. A **225**, 171.

Carlsson, B. G., and J. Dobaczewski, 2010, Phys. Rev. Lett. **105**, 122501.

Carlsson, B. G., J. Dobaczewski, and M. Kortelainen, 2008, Phys. Rev. C **78**, 044326.

Carlsson, B. G., J. Toivanen, and A. Pastore, 2012, Phys. Rev. C **86**, 014307.

Casida, M. E., C. Jamorski, K. C. Casida, and D. R. Salahub, 1998, J. Chem. Phys. **108**, 4439.

Ceperley, D. M., and B. J. Alder, 1980, Phys. Rev. Lett. **45**, 566.

Chappert, F., M. Girod, and S. Hilaire, 2008, Phys. Lett. B **668**, 420.

Chappert, F., N. Pillet, M. Girod, and J.-F. Berger, 2015, Phys. Rev. C **91**, 034312.

Chu, S. I., and D. A. Telnov, 2004, Phys. Rep. **390**, 1, invited review article.

Clément, E., *et al.*, 2007, Phys. Rev. C **75**, 054313.

Colò, G., H. Sagawa, and P. F. Bortignon, 2010, Phys. Rev. C **82**, 064307.

Corradi, L., A. M. Stefanini, J. H. He, S. Beghini, G. Montagnoli, F. Scarlassara, G. F. Segato, G. Pollarolo, and C. H. Dasso, 1997, Phys. Rev. C **56**, 938.

Cusson, R., P.-G. Reinhard, M. Strayer, J. Maruhn, and W. Greiner, 1985, Z. Phys. A **320**, 475.

Dang, G. D., A. Klein, and N. R. Walet, 2000, Phys. Rep. **335**, 93.

Daoutidis, I., and P. Ring, 2011, Phys. Rev. C **83**, 044303.

Dapo, H., and N. Paar, 2012, Phys. Rev. C **86**, 035804.

De Donno, V., G. Co', M. Anguiano, and A. M. Lallena, 2011, Phys. Rev. C **83**, 044324.

Delaroche, J. P., M. Girod, J. Libert, H. Goutte, S. Hilaire, S. Péru, N. Pillet, and G. F. Bertsch, 2010, Phys. Rev. C **81**, 014303.

Descouvemont, P., and D. Baye, 2010, Rep. Prog. Phys. **73**, 036301.

Di Piazza, A., C. Müller, K. Z. Hatsagortsyan, and C. H. Keitel, 2012, Rev. Mod. Phys. **84**, 1177.

Dobaczewski, J., and J. Dudek, 1995, Phys. Rev. C **52**, 1827.

Dobaczewski, J., W. Nazarewicz, and P.-G. Reinhard, 2014, J. Phys. G **41**, 074001.

Dobaczewski, J., and J. Skalski, 1981, Nucl. Phys. A **369**, 123.

Dobaczewski, J., M. V. Stoitsov, W. Nazarewicz, and P.-G. Reinhard, 2007, Phys. Rev. C **76**, 054315.

Dobson, J. F., 1994, Phys. Rev. Lett. **73**, 2244.

Dreizler, R. M., and E. K. U. Gross, 1990, *Density Functional Theory: An Approach to the Quantum Many-Body Problem* (Springer, Berlin).

Drozdz, S., S. Nishizaki, J. Speth, and J. Wambach, 1990, Phys. Rep. **197**, 1.

Duguet, T., M. Bender, K. Bennaceur, D. Lacroix, and T. Lesinski, 2009, Phys. Rev. C **79**, 044320.

Ebata, S., and T. Nakatsukasa, 2014, JPS Conf. Proc. **1**, 013038.

Ebata, S., and T. Nakatsukasa, 2015, JPS Conf. Proc. **6**, 020056.

Ebata, S., T. Nakatsukasa, and T. Inakura, 2014, Phys. Rev. C **90**, 024303.

Ebata, S., T. Nakatsukasa, T. Inakura, K. Yoshida, Y. Hashimoto, and K. Yabana, 2010, Phys. Rev. C **82**, 034306.

Egido, J., and L. Robledo, 2004, in *Extended Density Functionals in Nuclear Structure Physics*, Lecture Notes in Physics, Vol. 641, edited by G. Lalazissis, P. Ring, and D. Vretenar (Springer, Berlin), pp. 269–302.

Ekardt, W., 1984, Phys. Rev. Lett. **52**, 1925.

Engel, J., 2007, Phys. Rev. C **75**, 014306.

Engel, J., M. Bender, J. Dobaczewski, W. Nazarewicz, and R. Surman, 1999, Phys. Rev. C **60**, 014302.

Engel, Y. M., D. M. Brink, K. Goeke, S. J. Krieger, and D. Vautherin, 1975, Nucl. Phys. A **249**, 215.

Enkovaara, J., *et al.*, 2010, J. Phys. Condens. Matter **22**, 253202.

Erler, J., N. Birge, M. Kortelainen, W. Nazarewicz, E. Olsen, A. M. Perhac, and M. Stoitsov, 2012, Nature (London) **486**, 509.

Erler, J., P. Klüpfel, and P.-G. Reinhard, 2010, J. Phys. G **37**, 064001.

Fattoyev, F. J., C. J. Horowitz, J. Piekarewicz, and G. Shen, 2010, Phys. Rev. C **82**, 055803.

Fracasso, S., and G. Colò, 2005, Phys. Rev. C **72**, 064310.

Fracasso, S., E. B. Suckling, and P. D. Stevenson, 2012, Phys. Rev. C **86**, 044303.

Frauendorf, S., 2001, Rev. Mod. Phys. **73**, 463.

Frauendorf, S., and F. Dönau, 2014, Phys. Rev. C **89**, 014322.

Fu, Y., H. Mei, J. Xiang, Z. P. Li, J. M. Yao, and J. Meng, 2013, Phys. Rev. C **87**, 054305.

Fujikawa, K., and H. Ui, 1986, Prog. Theor. Phys. **75**, 997.

Fukuoka, Y., S. Shinohara, Y. Funaki, T. Nakatsukasa, and K. Yabana, 2013, Phys. Rev. C **88**, 014321.

Gambacurta, D., M. Grasso, and F. Catara, 2011, Phys. Rev. C **84**, 034301.

Gambacurta, D., M. Grasso, V. De Donno, G. Co', and F. Catara, 2012, Phys. Rev. C **86**, 021304.

Gambacurta, D., M. Grasso, and J. Engel, 2015, Phys. Rev. C **92**, 034303.

Giannoni, M. J., and P. Quentin, 1980a, Phys. Rev. C **21**, 2060.

Giannoni, M. J., and P. Quentin, 1980b, Phys. Rev. C **21**, 2076.

Giraud, B. G., 2008, Phys. Rev. C **77**, 014311.

Giraud, B. G., 2010, J. Phys. G **37**, 064002.

Giraud, B. G., B. K. Jennings, and B. R. Barrett, 2008, Phys. Rev. A **78**, 032507.

Goeke, K., R. Y. Cusson, F. Grümmer, P.-G. Reinhard, and H. Reinhardt, 1983, Prog. Theor. Phys. Suppl. **74–75**, 33.

Goeke, K., F. Grümmer, and P.-G. Reinhard, 1983, Ann. Phys. (N.Y.) **150**, 504.

Goeke, K., and P.-G. Reinhard, 1978, Ann. Phys. (N.Y.) **112**, 328.

Goldstone, J., 1961, Nuovo Cimento **19**, 154.

Gonze, X., and C. Lee, 1997, Phys. Rev. B **55**, 10355.

Goriely, S., N. Chamel, and J. M. Pearson, 2013, Phys. Rev. C **88**, 061302.

Goriely, S., S. Hilaire, M. Girod, and S. Péru, 2009, Phys. Rev. Lett. **102**, 242501.

Griffin, J. J., and J. A. Wheeler, 1957, Phys. Rev. **108**, 311.

Grimme, S., 2006, J. Comput. Chem. **27**, 1787.

Gross, E. K. U., and N. T. Maitra, 2012, "Introduction to TDDFT," in *Fundamentals of Time-Dependent Density Functional Theory* (Springer, Berlin), pp. 53–99.

Guo, L., and T. Nakatsukasa, 2012, Eur. Phys. J. Web Conf. **38**, 09003.

Hamamoto, I., 2012, Phys. Rev. C **85**, 064329.

Hamamoto, I., and G. B. Hagemann, 2003, Phys. Rev. C **67**, 014319.

Hansen, P. G., and B. Jonson, 1987, Europhys. Lett. **4**, 409.

Harakeh, M. N., and A. van der Woude, 2001, *Giant Resonances*, Oxford Studies in Nuclear Physics Vol. 24 (Oxford University Press, Oxford).

Hashimoto, Y., 2012, Eur. Phys. J. A **48**, 55.

Hashimoto, Y., and K. Nodeki, 2007, "A numerical method of solving time-dependent hartree-fock-bogoliubov equation with gogny interaction," arXiv:0707.3083.

Heyd, J., G. E. Scuseria, and M. Ernzerhof, 2003, J. Chem. Phys. **118**, 8207.

Heyde, K., and J. L. Wood, 2011, Rev. Mod. Phys. **83**, 1467.

Hinohara, N., 2015, Phys. Rev. C **92**, 034321.

Hinohara, N., M. Kortelainen, and W. Nazarewicz, 2013, Phys. Rev. C **87**, 064309.

Hinohara, N., M. Kortelainen, W. Nazarewicz, and E. Olsen, 2015, Phys. Rev. C **91**, 044323.

Hinohara, N., Z. P. Li, T. Nakatsukasa, T. Nikšić, and D. Vretenar, 2012, Phys. Rev. C **85**, 024323.

Hinohara, N., T. Nakatsukasa, M. Matsuo, and K. Matsuyanagi, 2007, Prog. Theor. Phys. **117**, 451.

Hinohara, N., T. Nakatsukasa, M. Matsuo, and K. Matsuyanagi, 2009, Phys. Rev. C **80**, 014305.

Hinohara, N., K. Sato, T. Nakatsukasa, M. Matsuo, and K. Matsuyanagi, 2010, Phys. Rev. C **82**, 064313.

Hohenberg, P., and W. Kohn, 1964, Phys. Rev. **136**, B864.

Holzwarth, G., and T. Yukawa, 1974, Nucl. Phys. A **219**, 125.

Ichikawa, T., K. Matsuyanagi, J. A. Maruhn, and N. Itagaki, 2014, Phys. Rev. C **90**, 034314.

Id Betan, R., R. J. Liotta, N. Sandulescu, and T. Vertse, 2002, Phys. Rev. Lett. **89**, 042501.

Ieki, K., *et al.*, 1993, Phys. Rev. Lett. **70**, 730.

Ikeda, K., 1992, Nucl. Phys. A **538**, 355.

Ikeda, K., S. Yoshida, and S. Yamaji, 1986, Z. Phys. A **323**, 285.

Imagawa, H., and Y. Hashimoto, 2003, Phys. Rev. C **67**, 037302.

Inakura, T., W. Horiuchi, Y. Suzuki, and T. Nakatsukasa, 2014, Phys. Rev. C **89**, 064316.

Inakura, T., H. Imagawa, Y. Hashimoto, S. Mizutori, M. Yamagami, and K. Matsuyanagi, 2006, Nucl. Phys. A **768**, 61.

Inakura, T., H. Imagawa, Y. Hashimoto, M. Yamagami, S. Mizutori, and K. Matsuyanagi, 2005, Eur. Phys. J. A **25**, 545.

Inakura, T., T. Nakatsukasa, and K. Yabana, 2009a, Phys. Rev. C **80**, 044301.

Inakura, T., T. Nakatsukasa, and K. Yabana, 2009b, Eur. Phys. J. A **42**, 591.

Inakura, T., T. Nakatsukasa, and K. Yabana, 2011, Phys. Rev. C **84**, 021302.

Inakura, T., T. Nakatsukasa, and K. Yabana, 2013, Phys. Rev. C **88**, 051305.

Inglis, D. R., 1954, Phys. Rev. **96**, 1059.

Inglis, D. R., 1956, Phys. Rev. **103**, 1786.

Itoh, M., *et al.*, 2003, Phys. Rev. C **68**, 064602.

Iwata, Y., T. Otsuka, J. A. Maruhn, and N. Itagaki, 2010a, Nucl. Phys. A **836**, 108.

Iwata, Y., T. Otsuka, J. A. Maruhn, and N. Itagaki, 2010b, Phys. Rev. Lett. **104**, 252501.

Jancovici, B., and D. Schiff, 1964, Nucl. Phys. **58**, 678.

Johnson, C. W., G. F. Bertsch, and W. D. Hazelton, 1999, Comput. Phys. Commun. **120**, 155.

Kanesaki, N., T. Marumori, F. Sakata, and K. Takada, 1973a, Prog. Theor. Phys. **49**, 181.

Kanesaki, N., T. Marumori, F. Sakata, and K. Takada, 1973b, Prog. Theor. Phys. **50**, 867.

Kim, K.-H., T. Otsuka, and P. Bonche, 1997, J. Phys. G **23**, 1267.

Kishimoto, T., J. M. Moss, D. H. Youngblood, J. D. Bronson, C. M. Rozsa, D. R. Brown, and A. D. Bacher, 1975, Phys. Rev. Lett. **35**, 552.

Klein, A., and E. R. Marshalek, 1991, Rev. Mod. Phys. **63**, 375.

Klein, A., N. R. Walet, and G. D. Dang, 1991, Ann. Phys. (N.Y.) **208**, 90.

Koch, W., and M. C. Holthausen, 2001, *A Chemist's Guide to Density Functional Theory* (Wiley-VCH, Weinheim).

Kohn, W., and L. J. Sham, 1965, Phys. Rev. **140**, A1133.

Koonin, S. E., K. T. R. Davies, V. Maruhn-Rezwani, H. Feldmeier, S. J. Krieger, and J. W. Negele, 1977, Phys. Rev. C **15**, 1359.

Kortelainen, M., T. Lesinski, J. Moré, W. Nazarewicz, J. Sarich, N. Schunck, M. V. Stoitsov, and S. Wild, 2010, Phys. Rev. C **82**, 024313.

Kortelainen, M., J. McDonnell, W. Nazarewicz, P.-G. Reinhard, J. Sarich, N. Schunck, M. V. Stoitsov, and S. M. Wild, 2012, Phys. Rev. C **85**, 024304.

Kortelainen, M., *et al.*, 2014, Phys. Rev. C **89**, 054314.

Krausz, F., and M. Ivanov, 2009, Rev. Mod. Phys. **81**, 163.

Kuriyama, A., K. Matsuyanagi, F. Sakata, K. Takada, and M. Yamamura, 2001, Prog. Theor. Phys. Suppl. **141**, 1.

Lacroix, D., and S. Ayik, 2014, Eur. Phys. J. A **50**, 95.

Laurent, A. D., and D. Jacquemin, 2013, Int. J. Quantum Chem. **113**, 2019.

Levine, Z. H., 1984, Phys. Rev. A **30**, 1120.

Levine, Z. H., and P. Soven, 1983, Phys. Rev. Lett. **50**, 2074.

Levine, Z. H., and P. Soven, 1984, Phys. Rev. A **29**, 625.

Levy, M., 1979, Proc. Natl. Acad. Sci. U.S.A. **76**, 6062.

Li, Z. P., T. Nikšić, P. Ring, D. Vretenar, J. M. Yao, and J. Meng, 2012, Phys. Rev. C **86**, 034334.

Li, Z. P., T. Nikšić, D. Vretenar, and J. Meng, 2010, Phys. Rev. C **81**, 034316.

Li, Z. P., T. Nikšić, D. Vretenar, J. Meng, G. A. Lalazissis, and P. Ring, 2009, Phys. Rev. C **79**, 054301.

Li, Z. P., T. Nikšić, D. Vretenar, P. Ring, and J. Meng, 2010, Phys. Rev. C **81**, 064321.

Li, Z. P., J. M. Yao, D. Vretenar, T. Nikšić, H. Chen, and J. Meng, 2011, Phys. Rev. C **84**, 054304.

Liang, H., T. Nakatsukasa, Z. Niu, and J. Meng, 2013, Phys. Rev. C **87**, 054310.

Liang, H., T. Nakatsukasa, Z. Niu, and J. Meng, 2014, Phys. Scr. **89**, 054018.

Liang, H., N. Van Giai, and J. Meng, 2008, Phys. Rev. Lett. **101**, 122502.

Libert, J., M. Girod, and J.-P. Delaroche, 1999, Phys. Rev. C **60**, 054301.

Litvinova, E., 2012, Phys. Rev. C **85**, 021303.

Litvinova, E., and P. Ring, 2006, Phys. Rev. C **73**, 044328.

Litvinova, E., P. Ring, and V. Tselyaev, 2008, Phys. Rev. C **78**, 014312.

Litvinova, E., P. Ring, and V. Tselyaev, 2010, Phys. Rev. Lett. **105**, 022502.

Litvinova, E. V., and A. V. Afanasjev, 2011, Phys. Rev. C **84**, 014305.

Long, W., H. Sagawa, N. V. Giai, and J. Meng, 2007, Phys. Rev. C **76**, 034314.

Losa, C., A. Pastore, T. Døssing, E. Vigezzi, and R. A. Broglia, 2010, Phys. Rev. C **81**, 064307.

Ludde, H. J., and R. M. Dreizler, 1983, J. Phys. B **16**, 3973.

Lunney, D., J. M. Pearson, and C. Thibault, 2003, Rev. Mod. Phys. **75**, 1021.

Mahaux, C., P. F. Bortignon, R. A. Broglia, and C. H. Dasso, 1985, Phys. Rep. **120**, 1.

Margueron, J., H. Sagawa, and K. Hagino, 2008, Phys. Rev. C **77**, 054309.

Marques, M., and E. Gross, 2004, Annu. Rev. Phys. Chem. **55**, 427.

Martin, R. M., 2004, *Electronic Structure: Basic Theory and Practical Methods* (Cambridge University Press, Cambridge, England).

Martini, M., S. Péru, and S. Goriely, 2014, Phys. Rev. C **89**, 044306.

Maruhn, J. A., P.-G. Reinhard, P. D. Stevenson, J. R. Stone, and M. R. Strayer, 2005, Phys. Rev. C **71**, 064328.

Maruhn, J. A., P.-G. Reinhard, P. D. Stevenson, and A. S. Umar, 2014, Comput. Phys. Commun. **185**, 2195.

Marumori, T., 1977, Prog. Theor. Phys. **57**, 112.

Marumori, T., T. Maskawa, F. Sakata, and A. Kuriyama, 1980, Prog. Theor. Phys. **64**, 1294.

Matsuo, M., 1986, Prog. Theor. Phys. **76**, 372.

Matsuo, M., 2001, Nucl. Phys. A **696**, 371.

Matsuo, M., 2015, Phys. Rev. C **91**, 034604.

Matsuo, M., and K. Matsuyanagi, 1985a, Prog. Theor. Phys. **74**, 288.

Matsuo, M., and K. Matsuyanagi, 1985b, Prog. Theor. Phys. **74**, 1227.

Matsuo, M., T. Nakatsukasa, and K. Matsuyanagi, 2000, Prog. Theor. Phys. **103**, 959.

Matsuo, M., Y. R. Shimizu, and K. Matsuyanagai, 1985, in *Proceedings of The Niels Bohr Centennial Conference on Nuclear Structure*, edited by R. Broglia, G. Hagemann, and B. Herskind (North-Holland, Amsterdam), p. 161.

Matsuyanagi, K., N. Hinohara, and K. Sato, 2013, "BCS-pairing and nuclear vibrations," in *Fifty Years of Nuclear BCS*, edited by R. A. Broglia and V. Zelevinsky (World Scientific, Singapore), Chap. 9, pp. 111–124.

Matsuyanagi, K., M. Matsuo, T. Nakatsukasa, N. Hinohara, and K. Sato, 2010, J. Phys. G **37**, 064018.

Matsuyanagi, K., M. Matsuo, T. Nakatsukasa, K. Yoshida, N. Hinohara, and K. Sato, 2016, J. Phys. G **43**, 024006.

Mayer, M. G., and J. H. D. Jensen, 1955, *Elementary theory of nuclear shell structure* (John Wiley & Sons, New York).

Messud, J., M. Bender, and E. Suraud, 2009, Phys. Rev. C **80**, 054314.

Michel, N., K. Matsuyanagi, and M. Stoitsov, 2008, Phys. Rev. C **78**, 044319.

Michel, N., W. Nazarewicz, M. Płoszajczak, and K. Bennaceur, 2002, Phys. Rev. Lett. **89**, 042502.

Mizuyama, K., G. Colò, and E. Vigezzi, 2012, Phys. Rev. C **86**, 034318.

Mizuyama, K., M. Matsuo, and Y. Serizawa, 2009, Phys. Rev. C **79**, 024313.

Moghrabi, K., M. Grasso, X. Roca-Maza, and G. Colò, 2012, Phys. Rev. C **85**, 044323.

Mottelson, B., 1976, Rev. Mod. Phys. **48**, 375.

Muga, J. G., J. P. Palao, B. Navarro, and I. L. Egusquiza, 2004, Phys. Rep. **395**, 357.

Mukherjee, A., and M. Pal, 1982, Nucl. Phys. A **373**, 289.

Mustonen, M. T., and J. Engel, 2013, Phys. Rev. C **87**, 064302.

Mustonen, M. T., T. Shafer, Z. Zenginerler, and J. Engel, 2014, Phys. Rev. C **90**, 024308.

Nagano, R., K. Yabana, T. Tazawa, and Y. Abe, 2000, Phys. Rev. A **62**, 062721.

Nakada, H., 2013, Phys. Rev. C **87**, 014336.

Nakada, H., and T. Inakura, 2015, Phys. Rev. C **91**, 021302.

Nakamura, T., *et al.*, 1994, Phys. Lett. B **331**, 296.

Nakamura, T., *et al.*, 2006, Phys. Rev. Lett. **96**, 252502.

Nakatsukasa, T., 2012, Prog. Theor. Exp. Phys. **2012**, 01A207.

Nakatsukasa, T., 2014, J. Phys. Conf. Ser. **533**, 012054.

Nakatsukasa, T., P. Avogadro, S. Ebata, T. Inakura, and K. Yoshida, 2011, Acta Phys. Pol. B **42**, 609.

Nakatsukasa, T., T. Inakura, and K. Yabana, 2007, Phys. Rev. C **76**, 024318.

Nakatsukasa, T., K. Matsuyanagi, S. Mizutori, and Y. R. Shimizu, 1996, Phys. Rev. C **53**, 2213.

Nakatsukasa, T., N. Walet, and G. D. Dang, 1999, Phys. Rev. C **61**, 014302.

Nakatsukasa, T., and K. Yabana, 2001, J. Chem. Phys. **114**, 2550.

Nakatsukasa, T., and K. Yabana, 2002, Prog. Theor. Phys. Suppl. **146**, 447.

Nakatsukasa, T., and K. Yabana, 2003a, Chem. Phys. Lett. **374**, 613.

Nakatsukasa, T., and K. Yabana, 2003b, Eur. Phys. J. A **20**, 163.

Nakatsukasa, T., and K. Yabana, 2005, Phys. Rev. C **71**, 024301.

Nambu, Y., 1960, Phys. Rev. **117**, 648.

Negele, J. W., 1970, Phys. Rev. C **1**, 1260.

Negele, J. W., 1982, Rev. Mod. Phys. **54**, 913.

Negele, J. W., and D. Vautherin, 1972, Phys. Rev. C **5**, 1472.

Nesterenko, V. O., W. Kleinig, J. Kvasil, P. Vesely, P.-G. Reinhard, and D. S. Dolci, 2006, Phys. Rev. C **74**, 064306.

Nesterenko, V. O., J. Kvasil, and P.-G. Reinhard, 2002, Phys. Rev. C **66**, 044307.

Nikšić, T., N. Kralj, T. Tutiš, D. Vretenar, and P. Ring, 2013, Phys. Rev. C **88**, 044327.

Nikšić, T., Z. P. Li, D. Vretenar, L. Próchniak, J. Meng, and P. Ring, 2009, Phys. Rev. C **79**, 034303.

Nikšić, T., D. Vretenar, and P. Ring, 2008, Phys. Rev. C **78**, 034318.

Nikšić, T., D. Vretenar, and P. Ring, 2011, Prog. Part. Nucl. Phys. **66**, 519.

Niu, Y. F., G. Colò, and E. Vigezzi, 2014, Phys. Rev. C **90**, 054328.

Niu, Z. M., Y. F. Niu, H. Z. Liang, W. H. Long, T. Nikšić, D. Vretenar, and J. Meng, 2013, Phys. Lett. B **723**, 172.

Oba, H., and M. Matsuo, 2009, Phys. Rev. C **80**, 024301.

Oberacker, V. E., and A. S. Umar, 2013, Phys. Rev. C **87**, 034611.

Oberacker, V. E., A. S. Umar, J. A. Maruhn, and P.-G. Reinhard, 2010, Phys. Rev. C **82**, 034603.

Oberacker, V. E., A. S. Umar, and C. Simenel, 2014, Phys. Rev. C **90**, 054605.

Okołowicz, J., M. Płoszajczak, and I. Rotter, 2003, Phys. Rep. **374**, 271.

Oliveira, L. N., E. K. U. Gross, and W. Kohn, 1988, Phys. Rev. Lett. **60**, 2430.

Olsen, J., H. J. A. Jensen, and P. Jørgensen, 1988, J. Comput. Phys. **74**, 265.

Onida, G., L. Reining, and A. Rubio, 2002, Rev. Mod. Phys. **74**, 601.

Onishi, N., and T. Une, 1975, Prog. Theor. Phys. **53**, 504.

Paar, N., T. Nikšić, D. Vretenar, and P. Ring, 2004, Phys. Rev. C **69**, 054303.

Paar, N., P. Ring, T. Nikšić, and D. Vretenar, 2003, Phys. Rev. C **67**, 034312.

Paar, N., D. Vretenar, E. Khan, and G. Colò, 2007, Rep. Prog. Phys. **70**, 691.

Pardi, C. I., and P. D. Stevenson, 2013, Phys. Rev. C **87**, 014330.

Parr, R. G., and W. Yang, 1989, *Density-Functional Theory of Atoms and Molecules* (Oxford University Press, New York).

Pei, J. C., M. Kortelainen, Y. N. Zhang, and F. R. Xu, 2014, Phys. Rev. C **90**, 051304.

Peierls, R. E., and D. J. Thouless, 1962, Nucl. Phys. **38**, 154.

Pekker, D., and C. Varma, 2015, Annu. Rev. Condens. Matter Phys. **6**, 269.

Perdew, J. P., A. Ruzsinszky, J. Tao, V. N. Staroverov, G. E. Scuseria, and G. I. Csonka, 2005, J. Chem. Phys. **123**, 062201.

Perdew, J. P., and A. Zunger, 1981, Phys. Rev. B **23**, 5048.

Persico, M., and G. Granucci, 2014, Theor. Chem. Acc. **133**, 1526.

Péru, S., G. Gosselin, M. Martini, M. Dupuis, S. Hilaire, and J.-C. Devaux, 2011, Phys. Rev. C **83**, 014314.

Péru, S., and H. Goutte, 2008, Phys. Rev. C **77**, 044313.

Próchniak, L., P. Quentin, D. Samsoen, and J. Libert, 2004, Nucl. Phys. A **730**, 59.

Próchniak, L., and S. G. Rohoziński, 2009, J. Phys. G **36**, 123101.

Reinhard, P.-G., and K. Goeke, 1979, Phys. Rev. C **20**, 1546.

Reinhard, P.-G., and K. Goeke, 1987, Rep. Prog. Phys. **50**, 1.

Reinhard, P.-G., P. D. Stevenson, D. Almehed, J. A. Maruhn, and M. R. Strayer, 2006, Phys. Rev. E **73**, 036709.

Reinhard, P.-G., A. S. Umar, K. T. R. Davies, M. R. Strayer, and S.-J. Lee, 1988, Phys. Rev. C **37**, 1026.

Ring, P., and P. Schuck, 1980, *The Nuclear Many-Body Problems*, Texts and Monographs in Physics (Springer-Verlag, New York).

Robledo, L. M., and G. F. Bertsch, 2011, Phys. Rev. C **84**, 054302.

Roca-Maza, X., X. Viñas, M. Centelles, P. Ring, and P. Schuck, 2011, Phys. Rev. C **84**, 054309.

Rodríguez, T. R., 2014, Phys. Rev. C **90**, 034306.

Rodríguez, T. R., and J. L. Egido, 2010, Phys. Rev. C **81**, 064323.

Rodríguez, T. R., and J. L. Egido, 2011, Phys. Lett. B **705**, 255.

Rohlfing, M., and S. G. Louie, 2000, Phys. Rev. B **62**, 4927.

Rohoziński, S. G., 2012, J. Phys. G **39**, 095104.

Rowe, D. J., 1982, Nucl. Phys. A **391**, 307.

Rowe, D. J., and R. Bassermann, 1976, Can. J. Phys. **54**, 1941.

Rowe, D. J., and J. Wood, 2010, *Fundamentals of Nuclear Models, Foundational Models* (World Scientific, Singapore).

Roynette, J. C., H. Doubre, N. Frascaria, J. C. Jacmart, N. Poffe, and M. Riou, 1977, Phys. Lett. B **67**, 395.

Runge, E., and E. K. U. Gross, 1984, Phys. Rev. Lett. **52**, 997.

Sabbey, B., M. Bender, G. F. Bertsch, and P.-H. Heenen, 2007, Phys. Rev. C **75**, 044305.

Sagawa, H., 2001, Prog. Theor. Phys. Suppl. **142**, 1.

Sahm, C. C., H. G. Clerc, K.-H. Schmidt, W. Reisdorf, P. Armbruster, F. P. Hessberger, J. G. Keller, G. Münzenberg, and D. Vermeulen, 1985, Nucl. Phys. A **441**, 316.

Sakamoto, H., and T. Kishimoto, 1988, Nucl. Phys. A **486**, 1.

Sakata, F., T. Marumori, and K. Takada, 1981, Prog. Theor. Phys. Suppl. **71**, 48.

Sarriguren, P., 2012, Phys. Rev. C **86**, 034335.

Sarriguren, P., E. M. de Guerra, and A. Escuderos, 2001, Nucl. Phys. A **691**, 631.

Sato, K., 2015, Prog. Theor. Exp. Phys. **2015**, 123D01.

Sato, K., and N. Hinohara, 2011, Nucl. Phys. A **849**, 53.

Sato, K., N. Hinohara, K. Yoshida, T. Nakatsukasa, M. Matsuo, and K. Matsuyanagi, 2012, Phys. Rev. C **86**, 024316.

Satuła, W., and R. A. Wyss, 2005, Rep. Prog. Phys. **68**, 131.

Scamps, G., and D. Lacroix, 2013a, Phys. Rev. C **87**, 014605.

Scamps, G., and D. Lacroix, 2013b, Phys. Rev. C **88**, 044310.

Scamps, G., and D. Lacroix, 2014, Phys. Rev. C **89**, 034314.

Scamps, G., D. Lacroix, G. F. Bertsch, and K. Washiyama, 2012, Phys. Rev. C **85**, 034328.

Scamps, G., C. Simenel, and D. Lacroix, 2015, Phys. Rev. C **92**, 011602.

Schmid, K., and P.-G. Reinhard, 1991, Nucl. Phys. A **530**, 283.

Sekizawa, K., and K. Yabana, 2013, Phys. Rev. C **88**, 014614.

Sekizawa, K., and K. Yabana, 2014, Phys. Rev. C **90**, 064614.

Sekizawa, K., and K. Yabana, 2015, Eur. Phys. J. Web Conf. **86**, 00043.

Serizawa, Y., and M. Matsuo, 2009, Prog. Theor. Phys. **121**, 97.

Shimada, M., S. Tagami, and Y. R. Shimizu, 2015, Prog. Theor. Exp. Phys. **2015**, 063D02.

Shimizu, Y. R., and K. Matsuyanagi, 2001, Prog. Theor. Phys. Suppl. **141**, 285.

Shimoura, S., T. Nakamura, M. Ishihara, N. Inabe, T. Kobayashi, T. Kubo, R. H. Siemssen, I. Tanihata, and Y. Watanabe, 1995, Phys. Lett. B **348**, 29.

Shinohara, S., H. Ohta, T. Nakatsukasa, and K. Yabana, 2006, Phys. Rev. C **74**, 054315.

Shinohara, Y., K. Yabana, Y. Kawashita, J.-I. Iwata, T. Otobe, and G. F. Bertsch, 2010, Phys. Rev. B **82**, 155110.

Shlomo, S., and G. Bertsch, 1975, Nucl. Phys. A **243**, 507.

Shoji, T., and Y. R. Shimizu, 2009, Prog. Theor. Phys. **121**, 319.

Sholl, D., and J. A. Steckel, 2009, *Density Functional Theory: A Practical Introduction* (Wiley-Interscience, Hoboken).

Shoppa, T. D., S. E. Koonin, K. Langanke, and R. Seki, 1993, Phys. Rev. C **48**, 837.

Shun-jin, W., and W. Cassing, 1985, Ann. Phys. (N.Y.) **159**, 328.

Simenel, C., 2010, Phys. Rev. Lett. **105**, 192701.

Simenel, C., 2011, Phys. Rev. Lett. **106**, 112502.

Simenel, C., 2012, Eur. Phys. J. A **48**, 152.

Simenel, C., and P. Chomaz, 2003, Phys. Rev. C **68**, 024302.

Simenel, C., and P. Chomaz, 2009, Phys. Rev. C **80**, 064309.

Simenel, C., P. Chomaz, and G. de France, 2001, Phys. Rev. Lett. **86**, 2971.

Simenel, C., P. Chomaz, and G. de France, 2007, Phys. Rev. C **76**, 024609.

Simenel, C., R. Keser, A. S. Umar, and V. E. Oberacker, 2013, Phys. Rev. C **88**, 024617.

Sonika, *et al.*, 2015, Phys. Rev. C **92**, 024603.

Sousa, S. F., P. A. Fernandes, and M. J. Ramos, 2007, J. Phys. Chem. A **111**, 10439.

Stephens, P. J., F. J. Devlin, C. F. Chabalowski, and M. J. Frisch, 1994, J. Phys. Chem. **98**, 11623.

Stetcu, I., C. A. Bertulani, A. Bulgac, P. Magierski, and K. J. Roche, 2015, Phys. Rev. Lett. **114**, 012701.

Stetcu, I., A. Bulgac, P. Magierski, and K. J. Roche, 2011, Phys. Rev. C **84**, 051309.

Stoitsov, M., M. Kortelainen, S. K. Bogner, T. Duguet, R. J. Furnstahl, B. Gebremariam, and N. Schunck, 2010, Phys. Rev. C **82**, 054307.

Stoitsov, M., M. Kortelainen, T. Nakatsukasa, C. Losa, and W. Nazarewicz, 2011, Phys. Rev. C **84**, 041305.

Stringari, S., 1979, Nucl. Phys. A **325**, 199.

Swiatecki, W. J., 1982, Nucl. Phys. A **376**, 275.

Tamura, T., and T. Udagawa, 1964, Nucl. Phys. **53**, 33.

Tao, J., J. P. Perdew, V. N. Staroverov, and G. E. Scuseria, 2003, Phys. Rev. Lett. **91**, 146401.
Tavernelli, I., 2015, Acc. Chem. Res. **48**, 792.
Terasaki, J., and J. Engel, 2006, Phys. Rev. C **74**, 044301.
Terasaki, J., and J. Engel, 2010, Phys. Rev. C **82**, 034326.
Terasaki, J., and J. Engel, 2011, Phys. Rev. C **84**, 014332.
Terasaki, J., J. Engel, and G. F. Bertsch, 2008, Phys. Rev. C **78**, 044311.
Thouless, D. J., and J. G. Valatin, 1962, Nucl. Phys. **31**, 211.
Tian, Y., Z. Y. Ma, and P. Ring, 2009, Phys. Lett. B **676**, 44.
Tohyama, M., 2001, Phys. Rev. C **64**, 067304.
Tohyama, M., and M. Gong, 1989, Z. Phys. A **332**, 269.
Tohyama, M., and T. Nakatsukasa, 2012, Phys. Rev. C **85**, 031302.
Tohyama, M., and P. Schuck, 2007, Eur. Phys. J. A **32**, 139.
Tohyama, M., and A. Umar, 2002, Phys. Lett. B **549**, 72.
Toivanen, J., B. G. Carlsson, J. Dobaczewski, K. Mizuyama, R. R. Rodríguez-Guzmán, P. Toivanen, and P. Veselý, 2010, Phys. Rev. C **81**, 034312.
Tomonaga, S.-I., 1955, Prog. Theor. Phys. **13**, 467.
Tran, F., and P. Blaha, 2009, Phys. Rev. Lett. **102**, 226401.
Tretiak, S., C. M. Isborn, A. M. N. Niklasson, and M. Challacombe, 2009, J. Chem. Phys. **130**, 054111.
Tselyaev, V. I., 2007, Phys. Rev. C **75**, 024306.
Tselyaev, V. I., 2013, Phys. Rev. C **88**, 054301.
Ullrich, C. A., 2012, *Time-Dependent Density Functional Theory: Concepts and Applications* (Oxford University Press, New York).
Umar, A. S., J. A. Maruhn, N. Itagaki, and V. E. Oberacker, 2010, Phys. Rev. Lett. **104**, 212503.
Umar, A. S., and V. E. Oberacker, 2005, Phys. Rev. C **71**, 034314.
Umar, A. S., and V. E. Oberacker, 2006a, Phys. Rev. C **74**, 061601.
Umar, A. S., and V. E. Oberacker, 2006b, Phys. Rev. C **74**, 021601.
Umar, A. S., and V. E. Oberacker, 2006c, Phys. Rev. C **73**, 054607.
Umar, A. S., and V. E. Oberacker, 2007, Phys. Rev. C **76**, 014614.
Umar, A. S., and V. E. Oberacker, 2008, Phys. Rev. C **77**, 064605.
Umar, A. S., V. E. Oberacker, and C. J. Horowitz, 2012, Phys. Rev. C **85**, 055801.
Umar, A. S., V. E. Oberacker, J. A. Maruhn, and P.-G. Reinhard, 2009, Phys. Rev. C **80**, 041601.
Umar, A. S., V. E. Oberacker, J. A. Maruhn, and P.-G. Reinhard, 2012, Phys. Rev. C **85**, 017602.
Umar, A. S., V. E. Oberacker, and C. Simenel, 2015, Phys. Rev. C **92**, 024621.
Umar, A. S., M. R. Strayer, and P.-G. Reinhard, 1986, Phys. Rev. Lett. **56**, 2793.
van Leeuwen, R., 1999, Phys. Rev. Lett. **82**, 3863.
van Leeuwen, R., and E. J. Baerends, 1994, Phys. Rev. A **49**, 2421.
Vignale, G., 1995, Phys. Rev. Lett. **74**, 3233.
Vignale, G., and W. Kohn, 1996, Phys. Rev. Lett. **77**, 2037.
Villars, F., 1977, Nucl. Phys. A **285**, 269.
Villars, F. M. H., 1983, Prog. Theor. Phys. Suppl. **74–75**, 184.
Vretenar, D., A. V. Afanasjev, G. A. Lalazissis, and P. Ring, 2005, Phys. Rep. **409**, 101.
Wachter, G., C. Lemell, J. Burgdörfer, S. A. Sato, X.-M. Tong, and K. Yabana, 2014, Phys. Rev. Lett. **113**, 087401.
Wacker, O. J., R. Kümmel, and E. K. U. Gross, 1994, Phys. Rev. Lett. **73**, 2915.
Washiyama, K., 2015, Phys. Rev. C **91**, 064607.
Washiyama, K., and D. Lacroix, 2008, Phys. Rev. C **78**, 024610.
Weisskopf, V. F., 1957, Nucl. Phys. **3**, 423.
Weizsäcker, C., 1935, Z. Phys. **96**, 431.
Wilets, L., and M. Jean, 1956, Phys. Rev. **102**, 788.
Winther, A., 1994, Nucl. Phys. A **572**, 191.
Wopperer, P., P. Dinh, P.-G. Reinhard, and E. Suraud, 2015, Phys. Rep. **562**, 1.
Yabana, K., and G. F. Bertsch, 1996, Phys. Rev. B **54**, 4484.
Yabana, K., Y. Kawashita, T. Nakatsukasa, and J.-I. Iwata, 2011, in *Charged Particle and Photon Interactions with Matter: Recent Advances, Applications, and Interfaces* (CRC Press, Boca Raton), pp. 65–86.
Yabana, K., T. Nakatsukasa, J.-I. Iwata, and G. F. Bertsch, 2006, Phys. Status Solidi (b) **243**, 1121.
Yabana, K., T. Sugiyama, Y. Shinohara, T. Otobe, and G. F. Bertsch, 2012, Phys. Rev. B **85**, 045134.
Yamada, K., 1993, Prog. Theor. Phys. **89**, 995.
Yamagami, M., J. Margueron, H. Sagawa, and K. Hagino, 2012, Phys. Rev. C **86**, 034333.
Yamagami, M., Y. R. Shimizu, and T. Nakatsukasa, 2009, Phys. Rev. C **80**, 064301.
Yamamura, M., and A. Kuriyama, 1987, Prog. Theor. Phys. Suppl. **93**, 1.
Yannouleas, C., and U. Landman, 2007, Rep. Prog. Phys. **70**, 2067.
Yao, J. M., K. Hagino, Z. P. Li, J. Meng, and P. Ring, 2014, Phys. Rev. C **89**, 054306.
Yao, J. M., H. Mei, H. Chen, J. Meng, P. Ring, and D. Vretenar, 2011, Phys. Rev. C **83**, 014308.
Yao, J. M., J. Meng, P. Ring, and D. Vretenar, 2010, Phys. Rev. C **81**, 044311.
Yoshida, K., 2009, Phys. Rev. C **79**, 054303.
Yoshida, K., 2013, Prog. Theor. Exp. Phys. **2013**, 113D02.
Yoshida, K., and T. Nakatsukasa, 2011, Phys. Rev. C **83**, 021304.
Yoshida, K., and T. Nakatsukasa, 2013, Phys. Rev. C **88**, 034309.
Yoshida, K., and N. Van Giai, 2008, Phys. Rev. C **78**, 014305.
Yu, Y., and A. Bulgac, 2003, Phys. Rev. Lett. **90**, 222501.
Yuldashbaeva, E. K., J. Libert, P. Quentin, and M. Girod, 1999, Phys. Lett. B **461**, 1.
Zangwill, A., and P. Soven, 1980, Phys. Rev. A **21**, 1561.
Zhang, H., Y. Miyamoto, and A. Rubio, 2012, Phys. Rev. Lett. **109**, 265505.
Zhao, P. W., Z. P. Li, J. M. Yao, and J. Meng, 2010, Phys. Rev. C **82**, 054319.
Zinser, M., *et al.*, 1997, Nucl. Phys. A **619**, 151.